2016

# MECHANISMS AND CONSIQENCES OF LYSOSOMAL MEMBRANE PERMEABILIZATION FOLLOWING EXPOSURE TO BIOACTIVE PARTICLES

Forrest Connell Jessop

# MECHANISMS AND CONSIQENCES OF LYSOSOMAL MEMBRANE PERMEABILIZATION FOLLOWING EXPOSURE TO BIOACTIVE PARTICLES

By

FORREST CONNELL JESSOP

B.S., UNIVERSITY OF UTAH, SALT LAKE CITY, UTAH, U.S.A . 2011

Dissertation

presented in partial fulfillment of the requirements

for the degree of

Doctor of Philosophy

in Toxicology

The University of Montana

Missoula, MT

Official Graduation Date (May 2016)

Approved by:

Scott Whittenburg, Dean of The Graduate School

Graduate School

Andrij Holian, Director

Center for Environmental Health Sciences

Elizabeth Putnam, Chair

Department of Biomedical and Pharmaceutical Sciences

Keven Roberts, Associate Professor

Center for Environmental Health Sciences

Christopher Migliaccio, Assistant Professor

Center for Environmental Health Science

John Hoidal, M.D. Chair

Department of Internal Medicine, University of Utah

Jessop, Forrest, Ph.D., May 2016 *Toxicology*

MECHANISMS AND CONSEQUENCES OF LYSOSOMAL MEMBRANE PERMEABILIZATION FOLLOWING EXPOSURE TO BIOACTIVE PARTICLES

Committee Chair: Andrij Holian

## Abstract

Exposure to bioactive environmental particles and engineered nanoparticles are a significant public health concern. Inhalation of bioactive particles can result in chronic inflammation, which drives tissue remodeling and fibrosis. Furthermore, chronic inflammation can increase individual susceptibility to other diseases including cancer and autoimmune diseases. The macrophage is the critical cell in particle clearance following exposure, and is central to the inflammatory responses and tissue remodeling. Phagocytosed bioactive particles within macrophages cause cytotoxicity and activation of the NLRP3 inflammasome, outcomes that are both essential to inflammation and disease development. However, mechanisms that regulate NLRP3 inflammasome activity and cytotoxicity have not fully been elucidated. The objective of this body of work was to further define common yet critical mechanisms that cause and/or mediate NLRP3 inflammasome activity following exposure to bioactive particles. In these studies we demonstrate that bioactive particles including silica and engineered nanomaterials cause lysosome membrane permeabilization (LMP) and the

release of lysosomal proteases, which precedes and facilitates NLRP3 inflammasome activation. Bioactive particles cause LMP through a mechanism that requires phagolysosome acidification. LMP and the activation of the NLRP3 inflammasome are required for secretion of pro-inflammatory cytokines and the alarmin High Mobility Group Box 1 (HMGB1). Once secreted, HMGB1 can further drive NLRP3 inflammasome activity through sterile priming, similar to the non-sterile mechanism utilized by endotoxin. A second critical pathway for regulation of the NLRP3 inflammasome was autophagy. Mice with macrophages deficient in autophagy had greater inflammation and chronic disease following silica exposure, supporting a protective anti-inflammatory role for autophagic activity. Together, these data reveal novel critical mechanisms in the regulation of NLRP3 inflammasome activity following bioactive particle exposure, and provide multiple potential therapeutic targets for the suppression of inflammation and disease.

TABLE OF CONTENTS

Page

List of Tables Page

List of Figures

# CHAPTER 1: BACKGROUND AND SIGNIFICANCE

## *1.0. Inflammation and Chronic Disease*

Interstitial lung disease (ILD) is a general term that encompasses 300+ disorders that affect the tissue surrounding the alveoli of the lung. Sarcoidosis, idiopathic pulmonary fibrosis, extrinsic allergic alveolitis, drug-induced (such as bleomycin) ILD, and pneumoconiosis are some of the most prevalent ILD [1]. Chronic inflammation is a critical factor in the development of most ILD. Anti-inflammatory and anti-fibrotic drugs are often used to slow disease progression, but unfortunately, there are no cures for ILD once it has progressed to fibrosis. Poor understanding of the mechanisms of chronic inflammation contributes to the inability to find a cure.

Pneumoconiosis and bleomycin-induced ILD involve chronic inflammation resulting from particle-induced sterile injury. Crystalline silica is the primary exposure in pneumoconiosis, while endogenous formed uric acid crystals causes sterile injury and inflammation with bleomycin treatment [2, 3]. Similarly, exposure to bioactive-engineered nanomaterial (ENM) including Multi-walled Carbon Nanotubes (MWCNT) and Titanium Nanobelts (TNB) results in significant sterile injury and ILD *in vivo* [4-7]. Since chronic inflammation is a primary driver of disease, we hypothesize that particle exposure models may be used to identify mechanisms and therapeutic targets common to multiple ILDs. An increasing number of reports demonstrate that the active NLRP3 inflammasome, which is involved in sensing sterile injury, is a point of convergence in chronic inflammatory signaling [8]. However, this knowledge has not been translated into effective therapies. Although there is extensive information *in*

*vitro* regarding how the NLRP3 inflammasome becomes activated, the more relevant challenge arises in elucidating why the NLRP3 inflammasome remains active *in vivo* in sterile chronic inflammatory diseases. This introduction reviews essential information currently understood regarding the NRLP3 inflammasome, its activation and regulation. Furthermore, it will outline important gaps of knowledge vital to the aims of this research.

### *1.1. NLRP3 Inflammasome Sensing of Sterile Injury*

NLRP3 (**N**od-**l**ike **R**eceptor containing a **P**yrin domain **3**) is one member of a larger family of pattern recognition receptors (See Table 1). NLRP3 is considered the most promiscuous receptor of the family, a property necessary for sensing a broad range of exogenous and endogenous agonists following sterile injury. The receptor is constitutively expressed in a non-oligomerized state in healthy cells, but oligomerizes following sterile injury into the NLRP3 inflammasome complex [9]. The molecular oligomerization event is reminiscent of the mechanisms resulting in the formation of the apoptosome. Associated with the NLRP3 inflammasome complex is the adapter protein ASC (Apoptosis-associated speck-like protein, also known as Caspase-recruitment domain or PYCARD), which facilitates the recruitment of pro-caspase-1. Assembly of the NLRP3 inflammasome complex results in auto-proteolytic processing of pro-caspase-1 to its active form. Active caspase-1 facilitates multiple downstream events, including the processing of cytokines IL-1$\beta$ and IL-18 to their active forms. Once secreted, IL-1$\beta$ has been reported to play a critical role in the pyrogenic and neutrophilic response following sterile injury, and is important in the

development of chronic disease [10]. The active NLRP3 inflammasome is also involved in a caspase-1 mediated, pro-inflammatory cell death pathway termed pyroptosis. Finally, through an undefined mechanism, the active NLRP3 inflammasome has been reported to regulate unconventional secretion of IL-1β [11].

**Table 1: The Inflammasome and Mechanisms of Activation**

| Receptor | Activating Agents | Mechanisms for Activation |
|---|---|---|
| NLRP3 | Pore-forming toxins<br><br>UV radiation<br><br>Endogenous Crystal Particles (Uric Acid, Cholesterol, Amyloid Plaques)<br><br>Exogenous Crystals (Silica, Asbestos, Engineered Nanomaterials, Alum)<br><br>Extracellular ATP | K+ efflux<br><br>Cytosolic lysosomal cathepsins<br><br>Mitochondrial Re-localization and ROS<br><br>Cytosolic mtDNA<br><br>Mitochondrial cardiolipin release |
| NLRP1B | *B. anthracis* lethal toxin<br><br>MDP | NLRP1B cleavage |
| NLRC4 | Gram-negative bacteria with type III or IV secretion systems:<br><br>Cytosolic flagella | Bacterial Component + NLRC4 Phosphorylation |
| AIM2 | dsDNA<br><br>*F. tularenis*<br><br>*L. monocytogenes* | dsDNA detection and binding |

### *1.2. NLRP3 Inflammasome Activation in Macrophage*

The pulmonary macrophage is a central cell in maintaining the immune balance and sterility of the lung. Macrophage populations in the lungs are heterogeneous and

present in multiple-compartments, including the alveolar and interstitial spaces. The alveolar macrophage (AM) is a critical cell in phagocytosis and clearance of particles following inhalation exposure. We have previously reported that innate immune function, with a specific emphasis on macrophage activity, was sufficient to cause inflammation and disease in a murine model of silicosis [12]. Others have reported critical roles for the macrophage in other NLRP3 inflammasome mediated diseases including atherosclerosis, which involves cholesterol crystal exposure [13]. Together, these studies provide evidence that macrophages are the critical cell regulating the inflammatory and fibrotic response following exposure to particles, whether environmental or endogenously formed. Therefore, the studies in this dissertation are primarily oriented around mechanisms of NLRP3 inflammasome persistence and regulation *in vivo*.

### *1.3. Mechanisms of NLRP3 inflammasome activation*

Activation of the NLRP3 inflammasome in macrophages requires two signals: 1) an extracellular priming signal that activates NF-κB resulting in transcription/translation of NLRP3 inflammasome components and cytokines, and 2) an agonist that interacts with the NLR binding domain facilitating the oligomerization of the NLRP3 inflammasome. In macrophages exposed to particles *in vitro*, bacterial endotoxin (LPS) is used as the priming agent. In sterile injury, priming is likely caused by other host derived alarmins or Danger Associated Molecular Patterns (DAMPs). Under basal conditions, NLRP3 and other inflammasome components are hyper-ubiquitinated to prevent activation and to provide targeting for degradation [14, 15].

TLR signaling and activation of NF-κB has been reported to play an important role in the de-ubiquitination of NLRP3 inflammasome components allowing for oligomerization [14, 15].

Specific agonists that bind the NLRP3 receptor (Signal 2) facilitating oligomerization have not been determined, though critical upstream events have been identified. Phagocytosed silica and alum particles can cause lysosome membrane permeabilization (LMP), resulting in leak of lysosomal contents into the cytosol resulting in NLRP3 assembly and cytotoxicity [16]. Engineered nanomaterials have also been reported to cause NLRP3 inflammasome activation via LMP [4, 5]. The lysosomal protease cathepsin B has specifically been implicated in activation of the NLRP3 inflammasome [16], though the mechanism by which this occurs has not been determined. Other, but perhaps less critical pathways of NLRP3 inflammasome activation for bioactive particle exposures includes mitochondrial destabilization and ROS, cytosolic mtDNA or Cardiolipin, and potassium efflux [9]. Mechanisms resulting in NLRP3 inflammasome assembly are summarized in Table 1.

### *1.4. Signal 1: DAMPs and NLRP3 inflammasome priming*

Danger Associated Molecular Patterns (DAMPs) are associated with cellular injury and death, and include a broad class of endogenous proteins, lipids, particles, and nucleic acids (See Table 2). DAMPs also include endogenously formed uric acid and cholesterol crystals resulting from impaired metabolic processes, both of which are capable of activating signal 2 (facilitating NLRP3 inflammasome assembly) [13, 2]. Most DAMPs do not act as signal 2, but are important in stimulating NF-κB activity

(signal 1). DAMPs in this class are often termed alarmins, due to their inability to directly cause cellular injury. DAMPs responsible for priming the NLRP3 inflammasome following bioactive particle exposure have not been fully elucidated *in vivo*.

HMGB1 is a nuclear architectural protein that can be released from necrotic cells, and actively secreted from macrophages via an unconventional secretion pathway [17-20]. During stress, HMGB1 translocates from the nucleus into the cytosol. Cytosolic HMGB1 has been reported to induce autophagy via binding to Beclin-1 in fibroblasts [21]. Autophagy induction may act as a platform for packaging of HMGB1 prior to unconventional secretion [11]. Macrophages have been shown to actively secrete HMGB1 through an NLRP3 inflammasome and caspase-1-mediated pathway following nigericin treatment and starvation, and with endotoxemia/infection [11, 20]. Whether NLRP3 inflammasome activity is required for HMGB1 secretion in particle-exposed macrophages has not been determined. Cellular necrosis, apoptosis, and NLRP3 activation in macrophages are all observed with bioactive particle exposure, which could potentially result in HMGB1 release. Secretion of HMGB1 with particle exposure *in vitro* and *vivo* has not been assessed.

Once outside the cell, HMGB1 has been shown to bind TLRs (primarily TLR4, but TLR2 and TLR9 when associated with other DAMPs, See Table 2) and the Receptor for Advanced Glycation End Products (RAGE). Extracellular HMGB1 has been reported to have either chemotactic or NF-κB-inducing activity depending upon its redox state [22]. HMGB1 neutralization studies in a murine model of bleomycin-induced lung injury demonstrated a critical role for HMGB1 in driving chronic disease

[23]. Others have reported a role for HMGB1-nucleic acid complexes in inflammation during autoimmune diseases, including Systemic Lupus Erythematous, which has increased prevalence in individuals with pneumoconiosis [24, 10, 3, 25]. Together, these reports support investigating HMGB1 and its role in particle-induced inflammation and disease.

**Table 2: DAMPs and Reported Activity in models of sterile injury**

| DAMP/Alarmin | Receptor | Associated Activity | Ref |
|---|---|---|---|
| HMGB1 | TLR2*, TLR4, TLR9*, RAGE, CD24 | NF-kB (TLRs)<br>MAPK and NF-kB (RAGE)<br>Chemotaxis | [26, 22, 27-30] |
| Histones | TLR9 | NF-κB | [31] |
| IL-1α | IL-1R | NF-κB | [32] |
| Cholesterol Crystals | NLRP3 | Caspase-1 | [13] |
| Uric Acid Crystals | NLRP3 | Caspase-1 | [2] |
| Hyaluronin | TLR2, TLR4 | NF-κB | [33, 34] |
| ATP | NLRP3, P2X4 | Caspase-1 | [35, 36] |
| S100/Calgranulin | RAGE | NF-κB and generation of ROS | [37, 38] |
| mtDNA | TLR9, TLR4 | NF-κB | [39, 40] |
| B-amyloid | RAGE, NLRP3 | Caspase-1<br>NF-κB and ROS | [41, 42] |
| Nucleic Acids (RNA/DNA) | TLR9, TLR3 | NF-κB | [43, 29, 44] |
| IL-33 | IL-33R | TH2 signaling | [45] |
| Heparin sulfate | TLR4 | NF-κB | [46] |

Table 2: This is a non-comprehensive list of DAMPs that have been shown to be involved in sterile injury. While not all DAMPs are involved in sterile injury following exposure to bioactive particles, common pathways are activated, including priming of the NLRP3 inflammasome through NF-κB.

*HMGB1 specificity to these receptors has been shown when complexed to other DAMPs, including nucleic acids or endosomes.

### *1.5. Signal 2: NLRP3 Inflammasome activation following LMP*

Phagocytosed particles can cause LMP (Signal 2), resulting in an intermediate signal that facilitates the assembly of the NLRP3 inflammasome and the activation of cell death pathways [47]. LMP is observed *in vitro* with particles known to cause inflammation and disease *in vivo*, including silica, alum, and cholesterol crystals [13, 16]. This is also reported to be the case following exposure to various ENM as well [4, 5]. Following particle phagocytosis, lysosomes fuse with the phagosome in order to degrade the particle(s) and neutralize the threat, similar to mechanisms responsible for elimination of pathogens. However, many particles are resistant to lysosomal degradation, and consequently, the intracellular fate of particles within the phagolysosome is not clear. While bioactive particles may cause LMP, mechanisms responsible for permeabilization of the membrane have not been elucidated. Downstream consequences of LMP include translocation of lysosomal hydrolases and cathepsins into the cytosol, mitochondrial damage, and ROS. Cytosolic cathepsin B has been reported to be critical for activation of NLRP3 inflammasome [16], however other cathepsins could be involved in both NLRP3 inflammasome activation and the cytotoxic response. Multiple mechanisms have been proposed for how particles cause LMP. The most critical of these mechanisms are highlighted below and illustrated in Figure 1:

*1.5.1. Reactive Oxygen Species (ROS)*- ROS damage to the inner and/or outer leaflet of the phagolysosome could lead to lipid peroxidation. This has been proposed as a mechanism of LMP for ischemia/reperfusion and radiation-induced injury [48,

49]. Within the lysosome, hydrogen peroxide produced from NADPH Oxidases could potentially react with inter-lysosomal iron to generate ROS via Fenton reactions [50]. Utilization of iron chelators and antioxidants prevents LMP during oxidative stress [48-50]. Direct injury to mitochondria (in the case of radiation) or mitochondrial injury by cytosolic cathepsins following particle-induced LMP could potentially be a source of ROS that enhance LMP. Direct evidence showing intra-lysosomal ROS-induced LMP following particle exposure is non-existent, though the potential for this mechanism remains plausible.

*1.5.2. Direct particle-membrane interactions*- A second potential mechanism of particle-LMP is membrane perturbation via particle-membrane interactions. Directly assessing particle-membrane interactions within macrophages has significant technical challenges. Consequently, there is limited evidence of what changes take place when particles directly interact with lysosomal membranes to cause LMP.

Silica nanoparticles have been reported to alter membrane fluidity and integrity *in situ* [51]. Furthermore, silica particles have been reported to cause RBC lysis [52], suggesting that particles can directly interact with membranes resulting in permeabilization. Specific physiochemical characteristics of nanoparticles are important in determining their pro-inflammatory potential [4-6, 53, 7], which would support the notion that physiochemical characteristics of particles could also define their LMP-inducing potential. We hypothesized that inhibiting lysosomal acidification, which would also prevent degradation of the protein corona surrounding the phagocytosed particle, would also prevent particle-induced LMP. These studies are

included in Chapter 3 of this dissertation. While these studies do not directly address mechanisms by which particles interact with the phagolysosome membranes and cause LMP, they do provide supportive evidence for future studies on this subject.

*1.5.3. Lysosomal proteases*- There is a possibility that lysosomal proteases may contribute to LMP by acting on specific proteins inside or on the outer membrane leaflet. There are reports demonstrating a specific role for cathepsin B in facilitating LMP following treatment with membrane detergents [54, 55]. The ability of cathepsins to cause LMP may result from cleavage of lysosomal membrane proteins such as LAMP1 or LAMP2 [56]. Others suggest that cathepsin B, once leaked, may further enhance LMP by targeting lysosomal stabilizing proteins on the outer leaflet such as Sphingosine Kinase 1 [54, 57]. Calpain, another lysosomal protease, has been reported to play a role in LMP following ischemic and hypochlorous acid-induced injury through targeting of the lysosomal stabilizing protein Hsp70 [58]. Nevertheless, the contribution of lysosomal proteases to LMP following bioactive particle exposure is not known. Generally, active cathepsin B is associated with most particle exposures, however only certain particles cause LMP, supporting the notion that cathepsin B would not be the defining factor in LMP. Consequently, we hypothesized that cathepsin B would play a minimal role in particle-induce LMP. We assessed the contribution of cathepsin B to LMP in Chapter 3 of this dissertation.

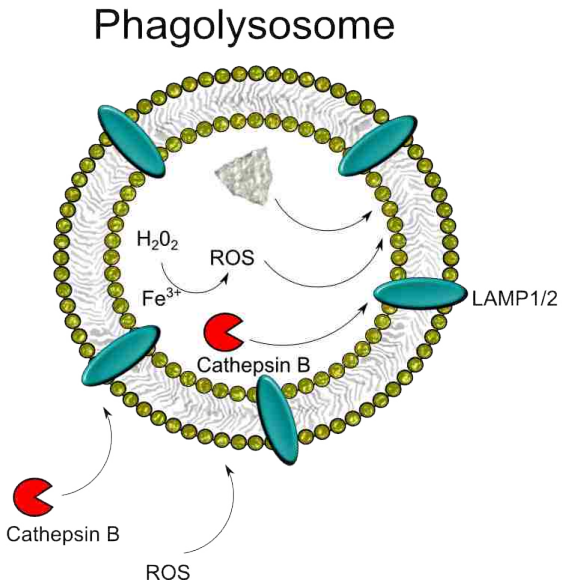


**Figure 1:** *Mechanisms of LMP.* Most notable mechanisms proposed to induce LMP following bioactive particle exposure. ROS has been proposed to cause LMP through lipid peroxidation. Secondly, particles may directly interact with the membrane, and the physiochemical characteristics of the particle would define its membrane-interacting potential. Finally, lysosomal proteases such as cathepsin B have been implicated in LMP through targeting of lysosomal stabilizing proteins including LAMP1/2.

### 1.6. Methods for detection of LMP

Detection of LMP following particle exposure has multiple technical challenges. Often studies report LMP using lysomotropic dyes such as acridine orange or LysoTracker™. These results can be difficult to interpret, since release of lysomotropic dyes from lysosomal compartments into the cytosol or changes in fluorescent profiles can be due to changes in ion pump activity or dye uptake, rather

than perturbations in membrane integrity [59]. Therefore, these assays should not be used as primary evidence of LMP and should be supported with other assays. Others have successfully utilized fluorescent-labeled dextran of varied molecular weights to assess LMP [16]. Effects of dextran on the particle or the lysosome need to be accounted for in these studies. Furthermore, FITC undergoes quenching at low pH, and therefore use of this fluorophore may complicate interpretation. An additional important factor to consider is that the fluorescent-based assays discussed are primarily qualitative or semi-quantitative. With the rapidly growing market of ENM, more robust methods are needed to screen particles for their LMP-inducing potential and downstream NLRP3 inflammasome activity. For these reasons, we adapted methods recently developed by Aits et al [60], which utilize digitonin for selective extraction of the cytosol following LMP. Cathepsin or other lysosomal enzyme activity can then be quantified within the extracted cytosolic fraction.

### *1.7. Impaired lysosome integrity in persistent NLRP3 inflammasome activity*

An increasing numbers of reports associate impaired lysosomal integrity with chronic inflammatory disease [61, 62]. Consequently, the lysosome as a therapeutic target is being explored for multiple disorders including liver fibrosis, neurodegenerative diseases, cardiovascular disease, and lysosome storage disorders. Extracellular lysosomal cysteine proteases have been implicated in inflammation and tissue remodeling in lung disease [63]. Therefore, targeting lysosomal stability or associated activity of lysosomal proteases may have broad therapeutic merit. We hypothesize that LMP is a central mechanism driving persistent

NLRP3 inflammasome activity in the lung *in vivo*. The contribution of LMP to persistent NLRP3 inflammasome activity *in vivo* has not been shown with bioactive particle exposure. These studies are included in Chapter 3.

### *1.8. Autophagy is a primary regulator of the activated NLRP3 inflammasome*

Autophagic dysfunction is an emerging paradigm contributing to the toxicity of ENM [62]. Dysfunction in autophagy is associated with multiple chronic inflammatory diseases including Crohn's Disease, Chronic Obstructive Pulmonary Disease and Idiopathic Pulmonary Fibrosis [64]. Autophagy was initially identified within yeast cells during starvation as a mechanism through which multi-protein structures are sequestered, broken down into their basic amino acids, and recycled for cellular survival. Autophagy is highly conserved across species in most cell types, and is critical in other activities including capturing cytosolic pathogens, sequestering damaged organelles, and unconventional secretion processes [65-67]. The autophagic pathway has an almost limitless degradative capacity, and can break down lipid droplets and nucleic acid complexes in addition to protein structures, thereby providing the cell with new nutrient pools. Multiple cellular stress signals can induce autophagy, the most notable being inhibition of mTORC1 and increases in AMPK [67, 68]. Other autophagy activating signals include growth hormones, hypoxia, and accumulation of misfolded proteins [67]. There are multiple forms of autophagy, including macroautophagy, microautophagy, and chaperone-mediated autophagy. While these other forms of autophagy may play a role in particle-induced inflammation and disease, for the studies in this dissertation macroautophagy is the

primary focus due to its ability to sequestering bulk or large structures resulting from cellular damage. For convenience, macroautophagy will be termed autophagy throughout the rest of the dissertation.

Activation of the autophagic pathway results in nucleation of Beclin-1 (Atg6), Atg14L and PI3Kinase Class III, which generates phosphatidyl-inositol-3-phosphate (PI3P). PI3P facilitates the recruitment of other Atg proteins. An Atg ubiquitination-like conjugation system (that includes Atg12, Atg7, Atg5, and Atg16L1) catalyzes phagophore elongation. During phagophore elongation, Microtubule-associated protein 1A/1B-light chain 3 (LC3-I) is cleaved to LC3-II and incorporated into the expanding membrane. LC3-II is a unique identifier of autophagic vesicles, and is critical for targeting of cellular components to the autophagosome. Autophagy specific chaperones, such as SQSTM1 (p62), bind ubiquitinated protein or organelle surfaces, and with their cargo associate with LC3-II [69]. Once formed, the autophagosome is a double membrane organelle, which makes it possible to visualize using Transition Electron Microscopy [70]. Autophagic vesicles carrying their cargo and chaperones eventually fuse with lysosomes, which are the primary organelle for degradation and recycling. Consequently, impaired lysosome integrity could also influence autophagy.

In addition to degrading damaged multi-protein complexes and organelles, autophagy has been reported to play an important role in sequestration of NLRP3 and AIM inflammasomes, ASC, and pro-IL-1$\beta$ [71, 72]. Therefore, autophagy could be an important regulatory mechanism of chronic inflammation and cytotoxicity following bioactive particle exposures. Lysosome impairment, and or direct

impairment of the autophagic pathway, has been associated with increased cytotoxicity [62]. Rare earth oxide nanoparticles have been reported to disrupt autophagic flux through the lysosome, which contributes to NLRP3 inflammasome persistence [73]. The impact of particle exposure on the autophagic pathway is not clear, and the relative contribution of autophagy to inflammation and disease following particle exposure has not been determined. Autophagy is a relatively new topic in particle toxicology, and Chapter 4 presents studies focused on the contribution of autophagy in macrophages to silica-induced cytotoxicity, inflammation and disease.

### *1.9. Unifying Project Rationale*

The overall objectives of these studies are to further our understanding of mechanisms by which the NLRP3 inflammasome is activated and remains activated contributing to the development of ILD. In this dissertation, we address multiple gaps of knowledge associated with NLRP3 inflammasome activity including 1) defining the endogenous sterile priming signal, 2) determine mechanisms required for particle-induced LMP and the contribution of LMP to NLRP3 inflammasome persistence and HMGB1 release *in vivo*, and 3) determining the contribution of autophagy to particle-induced inflammation and disease. The central hypothesis is that persistent NLRP3 inflammasome activity is dependent upon lysosome membrane permeabilization and sterile priming by the alarmin High Mobility Group Box 1 (HMGB1). Further, we hypothesize that autophagy will be a critical regulatory mechanism for suppressing particle-induced NLRP3 inflammasome activity. The overall rationale is that defining

mechanisms regulating NLRP3 inflammasome activity will provide critical information to reduce inflammation that drives chronic lung disease. The study rationale is summarized in Figure 2.

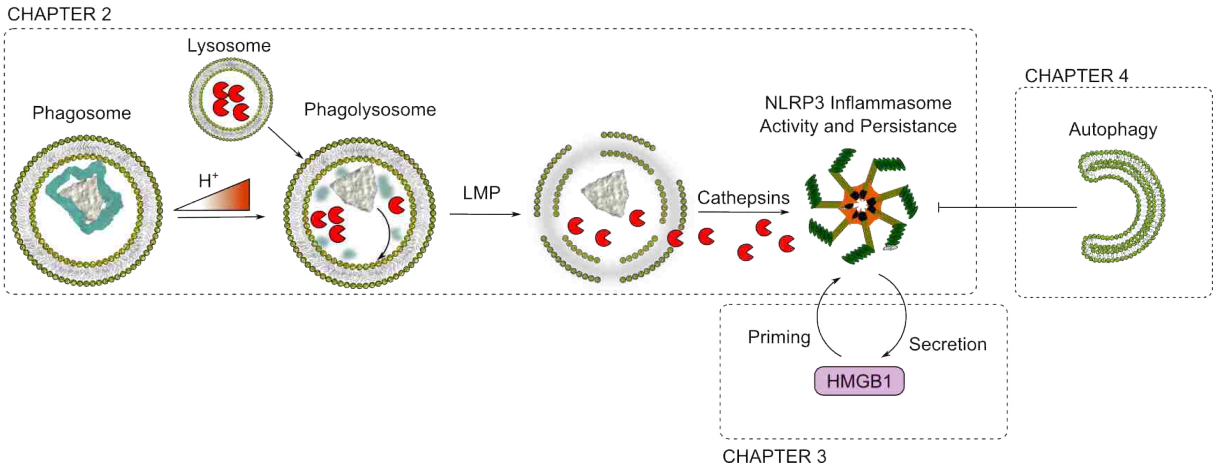


**Figure 2:** *Project Outline.* Chapter 2 of this dissertation explores the hypothesis that HMGB1 is the NLRP3 inflammasome-priming signal during particle-induced sterile injury following MWCNT. Chapter 3 of this dissertation focuses on mechanisms by which bioactive particles cause LMP, and contribution of LMP to persistent NLRP3 activity and HMGB1 release *in vivo*. Finally, Chapter 4 focuses on the contribution of autophagy to regulating NLRP3 inflammasome activity, cytotoxicity, and chronic lung disease following silica exposure.

CHAPTER 1: EXTRACELLULAR HMGB1 REGULATES MULTI-WALLED CARBON NANOTUBE-INDUCED INFLAMMATION *IN VIVO*

## 2.0. Manuscript Information Page

**Authors:** Forrest Jessop and Andrij Holian

**Original citation: J**essop, F. and Holian, A. (2015) Extracellular HMGB1 regulates multi-walled carbon nanotube-induced inflammation *in vivo*. Nanotoxicology 9, 365-72.

**Status of Manuscript:**

___ Prepared for submission to a peer-reviewed journal

___ Officially submitted to a peer-review journal

___ Accepted by a peer-review journal

_X_ Published in a peer review journal

Published by Taylor & Francis, Informa UK Ltd., 2014

## 2.1. Extracellular HMGB1 Regulates Multi-walled Carbon Nanotube-induced Inflammation *in vivo*

Forrest Jessop[1†] and Andrij Holian[1]

[1]University of Montana, Center for Environmental Health Sciences

**Correspondence author[†]**: Forrest Jessop, University of Montana: Center for Environmental Health Sciences, 32 Campus Drive, Missoula, MT 59812, USA; Phone: 406-243-4478, Fax: 406-243-2807, email: forrest.jessop@umontana.edu

## 2.2. Abstract

Endotoxin is often used to activate NF-κB *in vitro* when assessing NLRP3 inflammasome activation by various exogenous particles including nanoparticles. However, the endogenous source of this signal 1 is unknown. High Mobility Group Box 1 (HMGB1) is known to play a critical role in acute lung injury, however the potential contribution of the alarmin HMGB1 to NLRP3 Inflammasome activation has not been determined in response to nanoparticles *in vivo*. In this study, the ability of multi-walled carbon nanotubes (MWCNT) to cause release of HMGB1 *in vitro* and *in vivo,* as well as the potential of HMGB1 to function as signal 1 *in vitro* and *in vivo,* was determined. HMGB1 activity *in vivo* was assessed by administration of HMGB1 neutralization antibodies following MWCNT exposure. *Caspase-1*$^{-/-}$ mice were utilized to elucidate the dependence of HMGB1 secretion on NLRP3 inflammasome activity. MWCNT exposure increased extracellular HMGB1 levels in primary alveolar macrophages from C57Bl/6 mice and C10 mouse epithelial cell culture supernatants, and in C57Bl/6 mouse lung lavage fluid. MWCNT-induced HMGB1 secretion was dependent upon caspase-1. HMGB1 increased MWCNT-induced IL-1β release from macrophages *in vitro*, and neutralization of extracellular HMGB1 reduced MWCNT-induced IL-1β secretion *in vivo*. HMGB1 neutralization was accompanied with overall decreased inflammation. In summary, this study suggests extracellular HMGB1 participates in NLRP3 inflammasome activity and regulates IL-1β associated sterile inflammation induced by MWCNT.

**Key Words:** MWCNT, DAMP, IL-1β, sterile inflammation, caspase-1

## 2.3. Background

MWCNT have remarkable physiochemical properties that will advance the fields of medicine, electronics, and engineering. However, the high demand for these materials, in concert with their toxicity potential, may pose a future health risk for humans. Pulmonary exposure studies in murine models have revealed that MWCNT exposure has negative consequences, including chronic inflammation leading to granuloma formation and fibrosis, along with asthma-like pathology [4, 74, 7, 75-77]. The mechanisms that promote chronic inflammation are not clear, but activation of the NLRP3 inflammasome in macrophages and IL-1β signaling has been shown to be necessary for MWCNT-induced inflammation [4, 78, 79].

The NLRP3 Inflammasome is a multi-protein scaffolding complex that is assembled in macrophages following MWCNT exposure. Assembly of the NLRP3 Inflammasome complex results in activation of caspase-1, which in turn, processes pro-IL-1β and pro-IL-18 to their active, pyrogenic forms [80]. However, assembly of the NLRP3 complex alone does not result in IL-1β secretion *in vitro* [81], for a signal (often described as signal 1) is required for production of pro-IL-1β, usually accomplished by adding low levels of endotoxin. This two hit method is widely used to assess the inflammatory potential of particles *in vitro*. However, in mice kept in SPF facilities treated with MWCNT or in conditions of sterile injury in humans, endotoxin likely plays a minimal role, suggesting some other endogenous signal is involved.

High Mobility Group Box 1 (HMGB1) is a nuclear architectural protein that is secreted from injured/dead cells [82, 19, 83, 84], as well as actively secreted from

cells of monocytic origin [17]. Secreted HMGB1 belongs to a large family of Danger Associated Molecular Patterns (DAMPs) ligands, and has been implicated as an activator of NF-κB in sterile inflammation. It has been reported that HMGB1 is secreted via a non-conventional NLRP3 Inflammasome-mediated mechanism [18, 85]. Once outside the cell, HMGB1 has been shown to bind TLR4 and/or the Receptor for Advanced Glycation End-products (RAGE) [86, 87], and through this mechanism is suggested to mediate sepsis/LPS induced acute lung injury (ALI), hemorrhagic shock, and ventilator-induced ALI [88-92]. HMGB1 has also been identified as a mediator of bleomycin-induced fibrosis, likely through regulating the severity of the acute inflammatory response [23]. Although HMGB1 has been shown to play specific roles in these injury models, the secretory pathway of HMGB1 and extracellular activity in MWCNT-induced inflammation, which has characteristics distinct from other exposure models, is unknown. Additionally, whether HMGB1 contributes to NLRP3 Inflammasome-mediated inflammation following MWCNT exposure, or whether other DAMPs are more critical to this activity, is not known.

The objective of this study was to elucidate the contribution of HMGB1 to MWCNT-induced acute inflammation. Specifically, we hypothesized that HMGB1 has the ability to regulate NLRP3 Inflammasome activity, and therefore, targeting extracellular HMGB1 signaling or pathways that regulate HMGB1 secretion will be mechanisms to decrease NLRP3 Inflammasome activity. In this study we assessed for the presence and activity of HMGB1 following MWCNT exposure *in vivo* and *in vitro*. The MWCNT used in this study has previously been shown to induce a robust inflammatory and pathological response [78, 4]. The potential of extracellular HMGB1

to act on primary AM is of particular focus in this study since previous findings report strong correlations between AM production of IL-1β and pathology score following MWCNT exposure [4]. Furthermore, *caspase-1*$^{-/-}$ mice were used to assess the contribution of NLRP3 Inflammasome activation to HMGB1 secretion. Together, this study describes a critical role for HMGB1 signaling in MWCNT-induced NLRP3 Inflammasome activity and associated inflammation.

## 2.4. Materials and Methods

*2.4.1. MWCNT Preparation:* The MWCNT selected for these studies, designated FA-21 (Sun Innovations, Inc., Fremont, CA, USA; www.nanomaterialstore.com), was selected due to its potent NLRP3 Inflammasome activity, and has been characterized elsewhere [4]. This specific MWCNT is 1 of 24 samples provided by Dr. Nigel Walker and Brad Collins at the National Toxicology Program (NTP) at the National Institute of Environmental Health Sciences (NIEHS). Purity and metal content of the MWCNT were determined using thermal gravimetric analysis (TGA) and x-ray fluorescence spectrometry, respectively. Diameter and agglomeration state of the MWCNT were determined by transmission electron microscopy (TEM) and dynamic light scattering (DLS), respectively. This pro-inflammatory MWCNT has high nickel contamination (approximately 5.54%), and forms agglomerates that range from 122 nm to 469 nm depending on the dispersion media. Additionally, the MWCNT is free from endotoxin contamination, a critical quality for investigating the sterile inflammatory response. Prior to *in vivo* exposure by instillation or dispersion *in vitro*, MWCNT were suspended in dispersion medium (DM, 0.6 mg/ml mouse serum albumin (Sigma-

Aldrich, Saint Louis, MO) and 0.01 mg/ml 1,2-dipalmitoyl-sn-glycero- 3-phosphocholine (Sigma-Aldrich) in PBS) and suspended using sonication for 1 min [93].

*2.4.2. Animals:* C57Bl/6 and *caspase-1*$^{-/-}$ mice (2-month old) were housed in specific pathogen free and controlled environmental conditions (22 ± 2°C; 30-40% humidity, 12 hr light, 12 hr dark cycle) and provided food and water *ad libitum*. All procedures were performed under protocols approved by the IACUC of the University of Montana.

*2.4.3. Alveolar Macrophage isolation and culture:* Mice were euthanized by sodium pentobarbital (Euthasol™ Shering-Plough, Lot # 1JRR11V), and the lungs with the heart were removed. After lavage, AM were isolated by centrifugation (400 x g, 5 min). Retrieved cells were counted using a Coulter Z2 particle counter (Beckman Coulter, Miami, FL). AM were suspended in RPMI media supplemented with 10% fetal bovine serum (FBS), sodium pyruvate, and supplemented with an antimycotic/antibiotic cocktail (Mediatech, Manassas, VA). Cells were suspended at 1 x $10^6$ cells/mL and exposed to MWCNT (25 ug/mL, 2.5 µg/$10^5$ cells) for 24 hr at 37°C in a water-jacketed $CO_2$ incubator (ThermoForma, Houston, TX) in a 96 well culture plate. Recombinant HMGB1 (LPS free) was purchased from HMGBiotech. Cells were exposed to LPS (10 ng/mL) or rHMGB1 (dose response: 0, 0.5, 1, 2 µg/mL) at the same time as the MWCNT. rHMGB1 was formulated by the manufacture to be the disulfide isoform, or cytokine active form [26, 22]. After 24 hours of culture with the

particle and treatment groups, supernatants were collected and assessed for extracellular IL-1β and/or HMGB1.

*2.4.4. C10 Cell Culture and Exposure:* C10 epithelial cells, an immortalized non-transformed type II pneumocytic cell line cultured from BALB/c mice, were generously provided by Dr. Galya Orr (Pacific Northwest National Laboratories, Richland, WA). C10 cells were maintained in media identical to that used for AM. Cells were removed by trypsinization for 5-10 min at 37°C, and plated at 80% density for 3 hours prior to exposure to allow for adherence and acclimation. Cells were treated with MWCNT (25 μg/mL) for 24 hr, after which the cell supernatants were collected, and debri removed by centrifugation in order to assess extracellular HMGB1 levels by Western Blot.

*2.4.5. In vivo experiments:* Mice were exposed to MWCNT (2 mg/Kg or 50 μg/25 g mouse) by oropharyngeal aspiration [94]. Briefly, mice were anaesthetized using isoflurane inhalation and the MWCNT prepared in DM were delivered into the back of the throat while holding the tongue to the side, allowing for aspiration into the lungs. For HMGB1 neutralization studies, mice were instilled with chicken anti-HMGB1 IgY or Control IgY (Shinotest, Japan), or vehicle (PBS) only via oropharyngeal aspiration 1 hour following MWCNT instillations. After 1 day, the lungs were lavaged as described with ice cold PBS (pH 7.4). AM were removed by centrifugation (400 x g, 5 min, 4°C) and cell counts obtained using the Coulter Z2 particle counter. Portions of the cells were stained for differential analysis with Wright's Giemsa stain using a

Hematek 2000 autostainer (Miles-Bayer-Siemens Diagnostics, Deerfield, IL). The acellular lavage was retained for assessment of IL-1β and HMGB1.

*2.4.6. Assessment of endogenous HMGB1 in vitro:* MWCNT or DM were instilled into C57Bl/6 or caspase-$1^{-/-}$ mice as previously described and after 24 hours mice were euthanized and lungs lavaged by instilling and retrieving 1 mL cold PBS repeatedly (3x) to maximize concentration of extracellular HMGB1 in the lavage fluid. HMGB1 was either retained or removed from the lavage fluid by immunoprecipitation. Naïve AM were isolated as described and exposed to MWCNT (25 μg/mL) *in vitro* and the lung lavage fluid from MWCNT- or DM-treated mice with or without HMGB1. Prior to treatment, lavage fluid was supplemented with 1% FCS to prevent AM starvation. After 24 hours, supernatants were collected and assessed for IL-1β production.

*2.4.7. HMGB1 immunoprecipitation and Western Blot Analysis:* Protein A coated magnetic Dynabeads® (Life Technologies) were prepared according to manufacture's instructions, and coated with 5 μg of anti-HMGB1 antibody (C-terminal epitope, Sigma Aldrich). 1.5 mg of the bead/antibody conjugates were added to 1 mL of the lavage fluid and incubated overnight at 4°C with gentle tumbling. HMGB1 was then immunoprecipitated by magnetic separation, and the remaining lavage fluid and immunoprecipitated product were assessed for the presence of HMGB1 by traditional Western Blot analysis to confirm that HMGB1 had been successfully removed. Briefly, 30 μL of sample including: cell supernatant, lavage fluid, or immunoprecipitated HMGB1 was loaded on a 12-4% Bis-Tris polyacrylamide gel and

run for 1 hour at 150 V. Protein was electrophoresed onto a PVDF membrane, and blocked with 5% nonfat dry milk in Tris-buffered saline. After blocking, the membrane was incubated overnight at 4°C with anti-HMGB1 antibody (1:1000), washed 3 times, and then detected using a donkey anti-rabbit horseradish peroxidase-coupled secondary antibody (1:10,000). After washing 3 more times, the blot was developed using Fempto™ chemo-luminescence detection reagents (Pierce, Thermo Scientific, Rockford, IL).

*2.4.8. HMGB1 Assay:* HMGB1 was measured by ELISA using commercially available antibodies (R&D Systems, Minneapolis MN; EMD Millipore, Billerica, MA, Santa-Cruz Biotech, Dallas, TX) and previously validated protocols [95, 96]. Slight adjustments were made to these protocols, including decreased blocking time (2 hours) in 4% BSA in PBS, 2 hours of sample incubation with the primary antibody, followed by a 2 hour detection antibody incubation. ELISA specificity was confirmed by Western Blot. Lavage samples were run immediately on the ELISA in order to remove variability and potential degradation caused by freeze-thaw.

*2.4.9. Cytokine Assays:* IL-1$\beta$ and TNF-$\alpha$ were measured using mouse Duo-Set ELISA (R&D Systems, Minneapolis, MN) following the manufacture's protocol. Total Protein was measured using the BCA assay (Pierce, Thermo Scientific, Rockford, IL).

*2.4.10. Statistical Analysis:* Statistical analyses involved comparison of means using a one or two-way ANOVA followed by Dunnett's test or Bonferroni's test to

compensate for increased type I error. All probabilities were two-tailed unless otherwise stated. Statistical power was greater than 0.8. Statistical significance was defined as a probability of type I error occurring at less than 5% ($P < 0.05$). The minimum number of experimental replications was 3. Graphics and analyses were performed on PRISM 5.0.

## 2.5. Results

*2.5.1. MWCNT exposure increases extracellular HMGB1 levels:* The ability of MWCNT to induce HMGB1 secretion was assessed by instilling C57Bl/6 (WT) mice with 50 μg/mouse (2 mg/kg) of particle or DM, and after 24 hours, mice lungs were lavaged and HMGB1 concentrations were measured in the lavage fluid by ELISA. The MWCNT dose used for the *in vivo* studies was selected based on prior results showing it was the lowest amount required for reproducible measurements of IL-1β dependent inflammation and pathology [78]. The physiochemical characteristics and NLRP3 Inflammasome activating potential of the MWCNT used in these studies has been previously reported [4]. MWCNT exposure increased HMGB1 in the lung lavage fluid (Figure 1A). In order to assess potential sources of HMGB1 following MWCNT exposure in the lung, isolated primary AM and C10 cells were treated with 25 μg/mL MWCNT and extracellular HMGB1 concentrations were assessed after 24 hr. The dosage chosen for *in vitro* studies was selected to eliminate interference of the particle in colorimetric/fluorescent assays that occurs at higher doses, and yet this lower dose retains the ability to induce a significant IL-1β response. MWCNT exposure resulted in increased extracellular HMGB1 in C10 cell supernatant (Figure

1B). Likewise, MWCNT exposure induced a non-significant increase of extracellular HMGB1 in AM supernatants, which was significantly enhanced by stimulation with low levels of LPS (Figure 1C). C10 cells are susceptible to MWCNT cytotoxicity, as measured by the LDH assay [45]. Similarly, MWCNT are cytotoxic to AM [4], suggesting that passive release is a likely source of part of the extracellular HMGB1 pool. Endotoxin stimulated enhancement of HMGB1 secretion in AM also suggests that there is active secretion as well. Together, the data in Figure 1 demonstrate MWCNT induce HMGB1 secretion in the lung, and both epithelial and AM are plausible sources of HMGB1 through passive and active secretion.

*2.5.2. HMGB1 secretion is dependent on caspase-1:* The NLRP3 Inflammasome activates caspase-1, which in turn facilitates pro-IL-1β processing and secretion. Reports suggest that HMGB1 secretion is dependent upon NLRP3 Inflammasome activation of caspase-1 [18, 85]. However, the dependence of HMGB1 secretion on caspase-1 has not been evaluated with nanoparticles such as MWCNT. Therefore, we instilled *caspase-1*$^{-/-}$ mice with MWCNT or DM, and after 24 hours, assessed HMGB1 concentrations in whole lung lavage fluid. *Caspase-1*$^{-/-}$ mice had significantly less HMGB1 than WT (Figure 1A), confirming that HMGB1 secretion is dependent upon caspase-1 in MWCNT exposure models.

*2.5.3. Native HMGB1, but not rHMGB1, contributes to signal 1 of NLRP3 Inflammasome Activation:* The contribution of HMGB1 to particle-induced inflammatory response, specifically the ability of HMGB1 to act as signal 1, has not

been investigated. To elucidate whether HMGB1 can act as the NF-κB activating signal *in vitro*, primary AM were exposed to MWCNT and a dose response of commercially available disulfide form rHMGB1, reported to have NF-κB activating function [26, 22]. rHMGB1 failed to induce IL-1β secretion at any dose in primary AM (high dose shown, Figure 2A), as well as in two other macrophage-like cell models, including: THP-1 and Bone Marrow derived Macrophages (Supplementary Material: S1A, S1B). Likewise, TNF-α was not increased in any of these models (data not shown). Specific HMGB1 isoforms have been identified to contribute more to different disease models, and the rHMGB1 used in this proposal, which has been reported to signal through TLR4 [26], may not be comparable to endogenous HMGB1 in the lung following MWCNT exposure. To elucidate the ability of endogenous, native HMGB1 (nHMGB1) to act as signal 1, primary AM were isolated from C57Bl/6 and exposed to MWCNT *in vitro*, then treated with cell free lung lavage fluid obtained from DM or MWCNT-exposed mice (24 hour exposure period *in vivo* before isolation of cell free lung lavage fluid). In parallel, a second group of MWCNT-exposed C57Bl/6 AM was treated with lung lavage fluid from DM or MWCNT-exposed mice, where HMGB1 had been removed by immunoprecipitation (Figure 2C). Treatment with lung lavage fluid from MWCNT-treated mice enhanced IL-1β secretion in MWCNT-exposed AM, demonstrating that an endogenous signal 1 is present and soluble in the lung lavage fluid of MWCNT- treated mice (Figure 2B). Removal of HMGB1 by immunoprecipiation from the lung lavage fluid prior to treatment resulted in significantly less IL-1β production from MWCNT-exposed AM, indicating that HMGB1 is that endogenous signal 1 following MWCNT exposure. Immuno-blotting and

Coomassie blue staining revealed that the majority of immunoprecipitated protein was HMGB1 (Supplementary Material, S2). Similar experiments were performed in which C57Bl/6 AM were exposed to MWCNT with lavage fluid from *caspase-1*$^{-/-}$ mice. Lavage fluid isolated from *caspase-1*$^{-/-}$ mice exposed to MWCNT failed to induce IL-1β secretion from C57Bl/6 AM exposed to MWCNT *in vitro* (data not shown), supporting the reported role of caspase-1 in HMGB1 secretion and signaling.

*2.5.4. HMGB1 neutralization decreases IL-1β release in vivo:* To translate the contribution of HMGB1 to NLRP3 Inflammasome activity *in vivo*, mice were administered HMGB1 neutralizing antibodies or control IgY antibodies by oropharyngeal aspiration 1 hr following MWCNT instillation. HMGB1 neutralization significantly decreased IL-1β levels in the lung lavage fluid at 1 day (Figure 3A), along with decreased inflammatory markers including neutrophil (trending but non-significant), and eosinophil counts (Figure 3C, 3D). Additionally, there was a non-significant, but trended decrease in total protein and TNF-α, (Supplementary Material: S3A, S3B). However, HMGB1 neutralization did not decrease total cell counts (Figure 3B). Treatment with the isotype control and anti-HMGB1 antibodies induced an increase in neutrophils vs. vehicle only (data not shown), however this had no effect on IL-1β levels, and appeared to be non-inflammatory. Despite the increase in neutrophil numbers with antibody instillation, the anti-inflammatory trends of HMGB1 neutralization remained consistent. Together, this data supports a specific role for extracellular HMGB1 in mediating NLRP3 inflammasome activity, specifically the secretion of IL-1β, *in vivo*. Furthermore, this data suggests an important role for

HMGB1/ IL-1β dependent recruitment of eosinophils in C57Bl/6 mice exposed to MWCNT.

*2.5.5. Caspase-1$^{-/-}$ mice have decreased NLRP3 inflammasome activity:* MWCNT exposure in *caspase-1$^{-/-}$* mice resulted in decreased IL-1β release, along with other standard inflammatory parameters including: total cell count and neutrophil counts (Figure 4A, 4B, 4C). This data supports the critical role of caspase-1 processing of IL-1β and HMGB1 signaling in MWCNT-induced inflammation. However, MWCNT-exposed *caspase-1$^{-/-}$* mice retained similar levels of eosinophil recruitment compared to WT control (Figure 4D). This suggests that despite decreased HMGB1 levels in the lavage fluid, *caspase-1$^{-/-}$* mice have a compensating, HMGB1 independent pathway for recruitment of eosinophils.

**2.6. Discussion**

Due to the diversity of physiochemical properties and potential modifications of MWCNT, *in vitro* screening of inflammatory potential will be critical to identifying their potential to cause lung disease. Past studies by our laboratory have demonstrated that MWCNT physiochemical properties that promote more IL-1β secretion also result in greater pathology [4, 7]. This assessment currently requires stimulation of macrophages with endotoxin, a practice widespread when assessing inflammasome activation by inhaled particles. Pre-sensitization to LPS has been shown to enhance MWCNT-induced inflammation and fibrosis, and LPS has been shown to be a major contributor to environmental particle induced lung disease by integrating with the

hazardous material in the environment [97, 98]. However, it is important to consider the sterile nature of MWCNT-induced inflammation *in vivo*. The MWCNT used in these studies were free from LPS contamination, primarily due to the manufacturing process that requires high temperatures and controlled conditions. The mice used in these studies were kept in SPF conditions, where the contribution of LPS to NLRP3 Inflammasome activity is not evident. The “danger theory” of the inflammatory response indicates that sterile injury is sufficient for NLRP3 inflammasome activation and associated disease through the release of endogenous DAMPs, including HMGB1 [99]. The current two hit hypothesis for MWCNT *in vitro* activation includes MWCNT activation of the NLRP3 Inflammasome through lysosomal membrane permeablization [4], and the activation of NF-kB by an endogenous DAMP (see Figure 5).

Results from this study implicate that HMGB1 plays an integral role in sterile activation of the NLRP3 Inflammasome. The contribution of HMGB1 to sterile inflammation has been of recent interest due to its ability to bind TLR4/RAGE leading to NF-κB activation [86, 87]. While most studies on HMGB1-mediated inflammasome activity have been done following exposure to high levels of endotoxin, bleomycin, or mechanical stress [23, 92, 88], the contribution of HMGB1 to MWCNT-induced inflammation and disease has not hitherto been elucidated. Not only did MWCNT exposure elevate levels of HMGB1, but also we confirmed native HMGB1 participated in NLRP3 inflammasome activation.

HMGB1 secretion has been observed to be through both active (from monocytic cells) and passive mechanisms (secondary to necrosis or apoptosis) [17,

82, 19, 85]. Increased cytotoxicity has been observed with MWCNT exposure in epithelial cells and AM [45, 4], however the pre-dominant form of MWCNT-induced cell death is conflicting, and likely depends upon particle physiochemical and surface properties. However, increased HMGB1 secretion from primary AM exposed to LPS and MWCNT, along with decreased secretion from *Caspase-1*$^{-/-}$ mice, suggests that a portion of the extracellular HMGB1 present following MWCNT exposure is processed through an active caspase-1 mediated secretory mechanism. Higher levels of LPS than those used in this proposal have been shown to induce HMGB1 translocation from the nucleus to the cytosol, where it is then secreted, like IL-1β, through an unconventional pathway [17]. The observation that HMGB1 secretion was dependent on caspase-1 activation suggests that the NLRP3 Inflammasome is integral to the secretory pathway, and is not limited to processing of cytokine precursors.

Others have reported that specific HMGB1 isoforms are required for pro-inflammatory, cytokine-like function or chemokine activity. Specifically, a disulfide bridge between cysteine residues 23 and 45, along with a reduced cysteine residue at 106, constitutes HMGB1 with cytokine-like activity [26, 22, 100]. Fully reduced HMGB1 is considered to be primarily chemotactic. The failure of the disulfide rHMGB1 isoform to act as signal 1 in our model suggests that the endogenous form in the lung, following MWCNT exposure, is distinct from the commercial product. Though most of the HMGB1 immunoprecipitated in these studies was soluble (Figure 2C), it is possible that there was co-immunoprecipiation of immune complexes present at low levels with greater specificity to activate NF-κB, that were not detected due to the insensitive nature of coomassie blue. Others have demonstrated HMGB1

binds to IL-1β, LPS, and extracellular DNA *in situ*, and that these complexes have increased immune-stimulatory activity [101, 102]. Alternatively, since HMGB1 secretion is dependent upon caspase-1, it is possible that HMGB1 is targeted by caspase-1 prior to secretion, and that this cleaved isoform is important in extracellular signaling. However, HMGB1 targeting by caspase-1 has had conflicting reports and was not assessed in these studies [103, 18]. Furthermore, the integration of the NLRP3 Inflammasome into the unconventional secretory pathway may be a pathway around direct caspase-1 cleavage of HMGB1 [104].

IL-1β signaling has been shown to be a significant contributor to neutrophil and eosinophil recruitment after MWCNT exposure [78]. IL-1R null mice have decreased eosinophil and neutrophil recruitment 24 hours after MWCNT exposure. Likewise HMGB1 neutralization in this study, resulting in decreased IL-1β, resulted in decreased eosinophil counts and a decreasing trend in neutrophil recruitment. Similarly, HMGB1 neutralization has been reported to decrease eosinophil recruitment in a murine asthma model using Ova/Albumin sensitization [105]. The mechanism for HMGB1 recruitment of eosinophil and neutrophils remains to be defined, though general cell migration towards HMGB1 has been reported to be dependent on CXCL12 and sustained NF-κB activation [106].

We present a conceptual model for the role of extracellular HMGB1 activity in MWCNT-induced inflammation in Figure 5. This study demonstrates extracellular HMGB1 in MWCNT exposure regulates NLRP3 inflammasome activity by participating in the NF-κB activating step. Though HMGB1 neutralization results in reduced acute NLRP3 Inflammasome activity, the dependence of MWCNT-induced

long-term pathology on HMGB1 remains to be determined. It is plausible that HMGB1 functions as part of the NF-κB activating signal in many other models of particle exposure, which require NLRP3 Inflammasome activity. Therefore, assessment of MWCNT bioactivity (including NLRP3 inflammasome activity) should include measuring the ability of MWCNT and other particles to induce HMGB1 secretion.

## 2.7. Conclusions

These studies establish extracellular HMGB1 as a regulator of NLRP3 inflammasome activity *in vivo* following MWCNT exposure. HMGB1 secretion is dependent upon caspase-1, and this study provides evidence that targeting HMGB1 signaling through extracellular neutralization or secretion pathways (caspase-1 dependent) may have therapeutic implications, however, further studies are needed. Finally, the potency of MWCNT to induce HMGB1 secretion should be considered in future studies delineating inflammatory potential of MWCNT and conceivably other inhaled particulates that act through a similar mechanism.

## 2.8. Other

*2.8.1. Acknowledgments:* The authors thank Center for Environmental Health Sciences core scientists, Mary Buford (Inhalation and Pulmonary Physiology Core), Brittan Postma (Animal Core), Lou Herritt (Molecular Histology and Fluorescence Imaging Core), and Dr. Chris Migliaccio (Inhalation and Pulmonary Physiology Core Director) and Ray Hamilton for contributions of expertise and advice needed to conduct the experiments discussed in this manuscript.

*2.8.2. Authors Contribution:* FJ designed and performed all experiments. AH helped coordinate and supervise these studies. FJ wrote the first draft. AH assisted with draft revisions. FJ and AH approved the final draft.

*2.8.3. Funding Sources:* Research reported in this publication was supported grants from the National Institute Of General Medical Sciences of the National Institutes of Health (NIH) under award number P30GM103338, National Institute of Environmental Health Sciences under award number RC2-ES018742, and a Pre-doctoral fellowship from PhRMA Foundation (Forrest Jessop). The content is solely the responsibility of the authors, and does not necessarily represent the official views of the NIH or PhRMA Foundation.

*2.8.4. Declaration of Interest:* The authors declare no conflicts of interest. The authors alone are responsible for the content and writing of this manuscript.

## 2.9. Figures

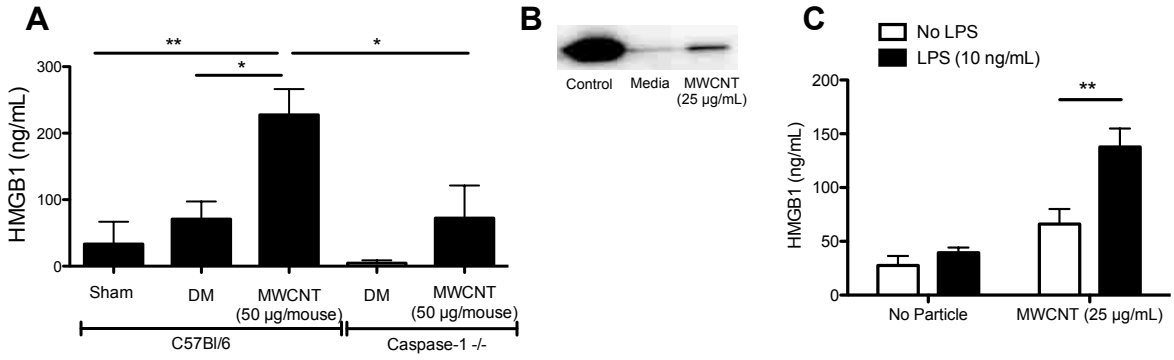


**Figure 2.1.** HMGB1 levels following MWCNT exposure *in vitro* and *in vivo*. **(A)** HMGB1 levels in whole lung lavage fluid 24 hr following MWCNT (50 µg/mouse) or DM instillation in C57Bl/6 or caspase-$1^{-/-}$ null mice. HMGB1 levels were assessed in sham (non-instilled mice) to assess injury caused by instillation of the vehicle. **(B)** Extracellular HMGB1 detected in C10 cell supernatants following 24 hours of exposure to MWCNT (25 µg/mL). **(C)** HMGB1 levels in primary AM cell supernatant 24 hours following MWCNT (25 µg/mL) exposure with (black bar) or without (white bar) LPS (10 ng/mL). *$p<0.05$, **$p<0.01$

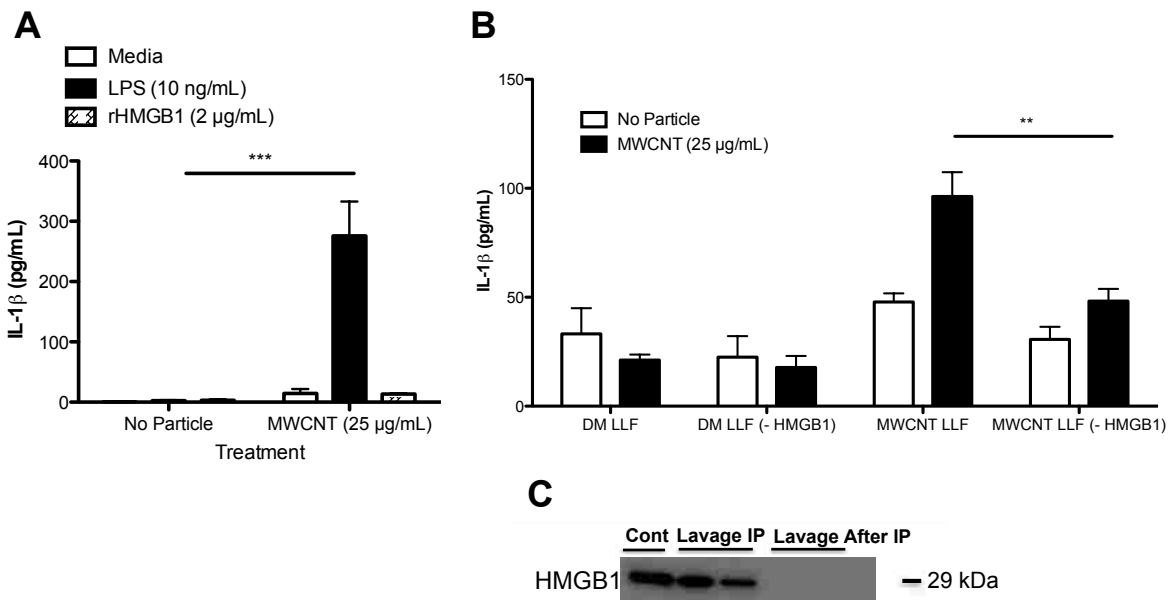


**Figure 2.2.** nHMGB1 not rHMGB1 participates in inflammasome activity *in vitro*. **(A)** IL-1β in primary AM cell supernatants 24 hr following MWCNT exposure and treatment with either LPS (10 ng/mL) or rHMGB1 (2 µg/mL). **(B)** IL-1β in primary AM cell supernatants after 24 hr exposure to MWCNT (black bar, 25 µg/mL) *in vitro*, and exposure to cell free lung lavage fluid from DM-exposed mice (DM LLF) or MWCNT-exposed mice (MWCNT LLF). nHMGB1 was immunoprecipitated out of the lavage fluid to form treatment groups DM LLF (- HMGB1) and MWCNT LLF (-HMGB1). **(C)** Representative Western Blot confirming that nHMGB1 was removed from the lung lavage fluid prior to addition to primary AM *in vitro*. **p<0.01. ***p<0.001.

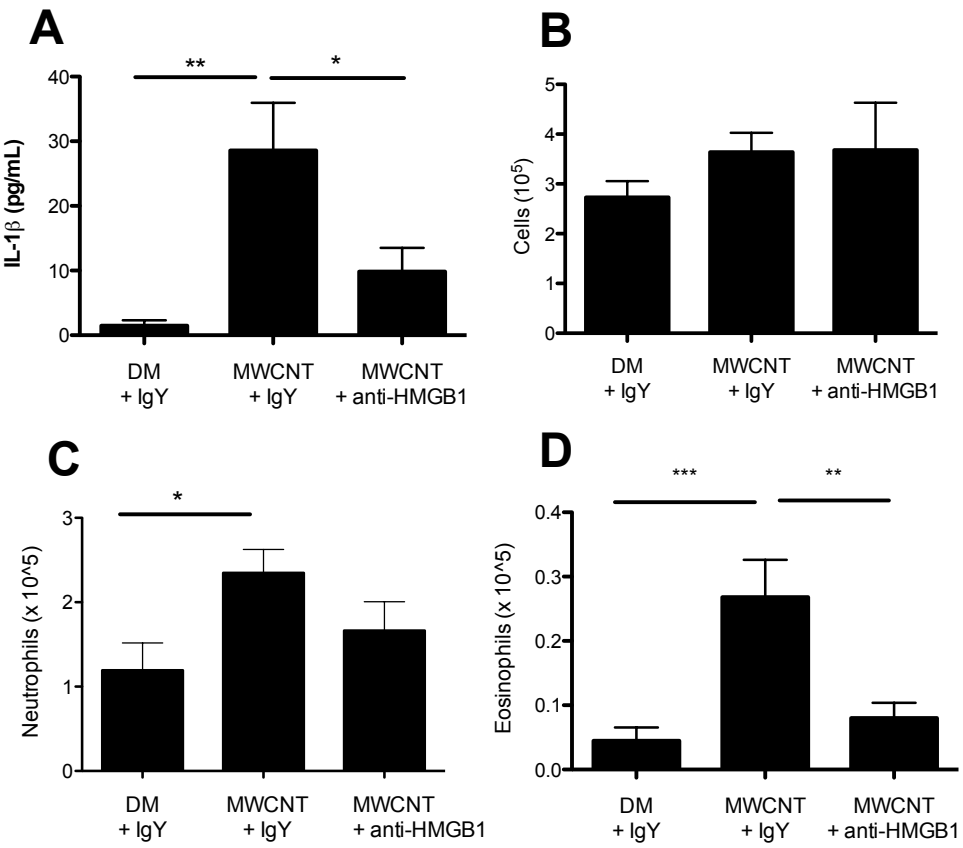


**Figure 2.3.** Neutralization of HMGB1 decreases IL-1β secretion and associated inflammation. **(A)** IL-1β concentration in lung lavage fluid 1 day following MWCNT instillation and treatment with HMGB1 neutralizing antibodies or control antibodies, **(B)** Total cell counts, **(C)** Neutrophil counts, and **(D)** Eosinophil counts in the lung lavage fluid 1 day following treatment MWCNT treatment and administration of antibodies. *p<0.01. **p<0.01. ***p<0.001.

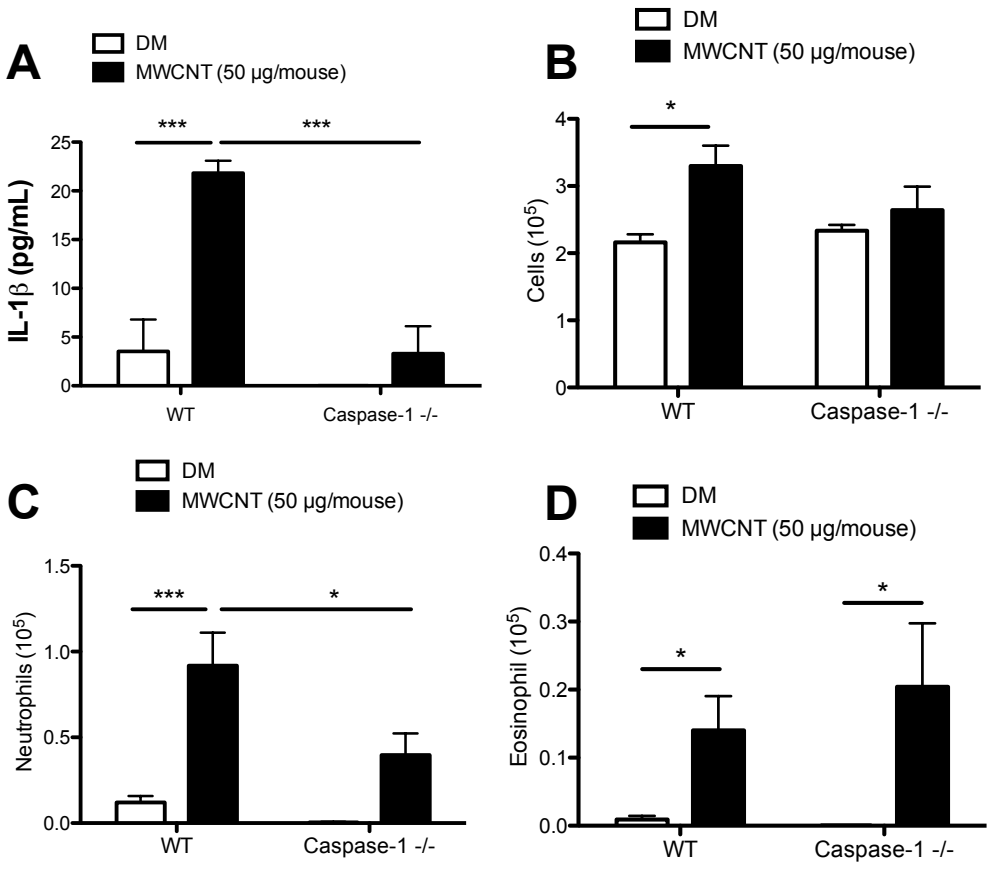


**Figure 2.4.** *Caspase-1*$^{-/-}$ mice have decreased IL-1β and associated inflammation. (A) IL-1β in lung lavage fluid 1 day following MWCNT instillation, (B) total cell counts, (C) neutrophil counts, and (D) eosinophil counts in the lung lavage fluid after 1 day. *p<0.01, ***p<0.001.

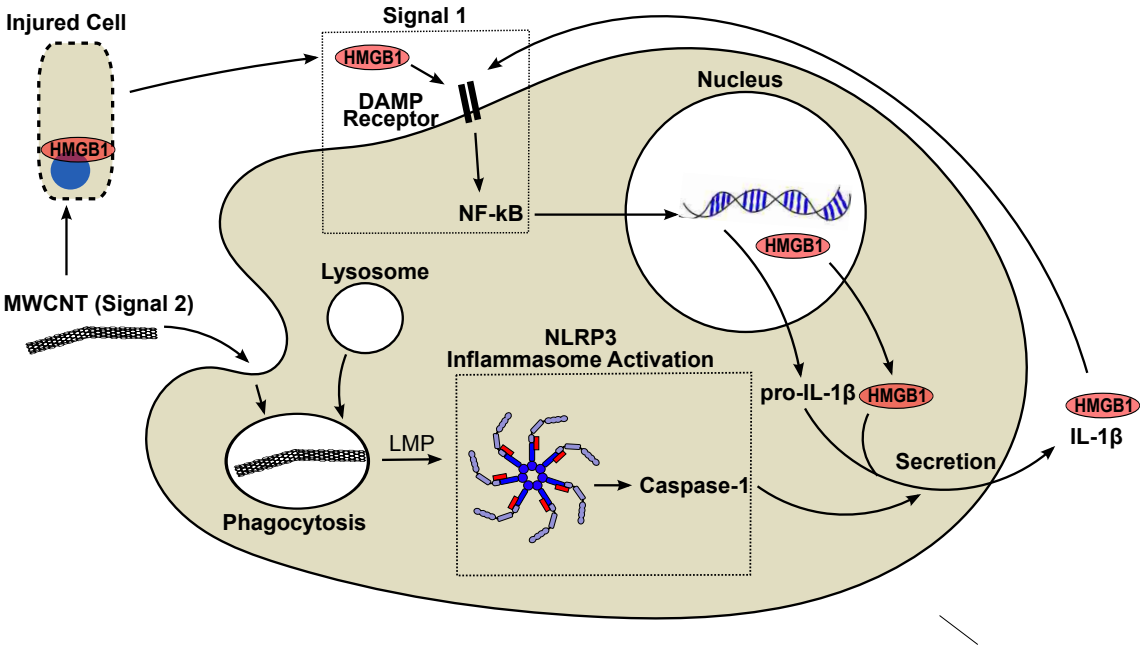


**Figure 2.5.** Model depicts the contribution of HMGB1 to MWCNT-induced inflammation. Macrophages phagocytose MWCNT (signal 2), which induce lysosomal membrane permeablization (LMP), leading to activation of the NLRP3 Inflammasome and caspase-1. Signal 1 is required for activation of NF-κB, which is accomplished by activation of a DAMP recognition receptor such as RAGE or TLR4. HMGB1 is released passively by injured cells or by active secretion from macrophages, and participates in Signal 1.

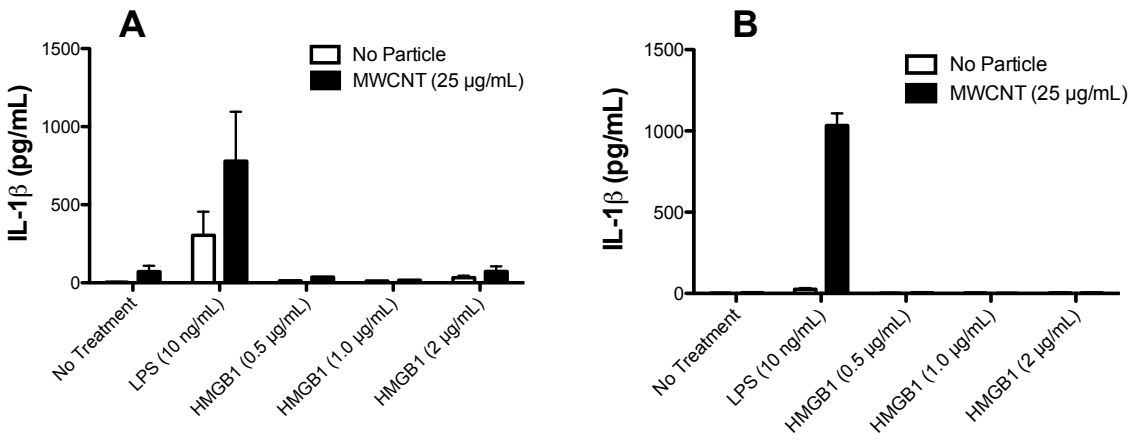


**Supplementary Figure 2.6.** rHMGB1 with MWCNT exposure fails to induce inflammasome activity in THP-1 and Bone Marrow derived Macrophages (BMdM). (A) Differentiated THP-1 were exposed to MWCNT (25 µg/mL) and either LPS (10 ng/mL) or a dose response of rHMGB1 (0.5, 1.0, 2.0 µg/mL). (B) Repeated study in BMdM. IL-1β was assessed by ELISA in the cell supernatants after 24 hr.

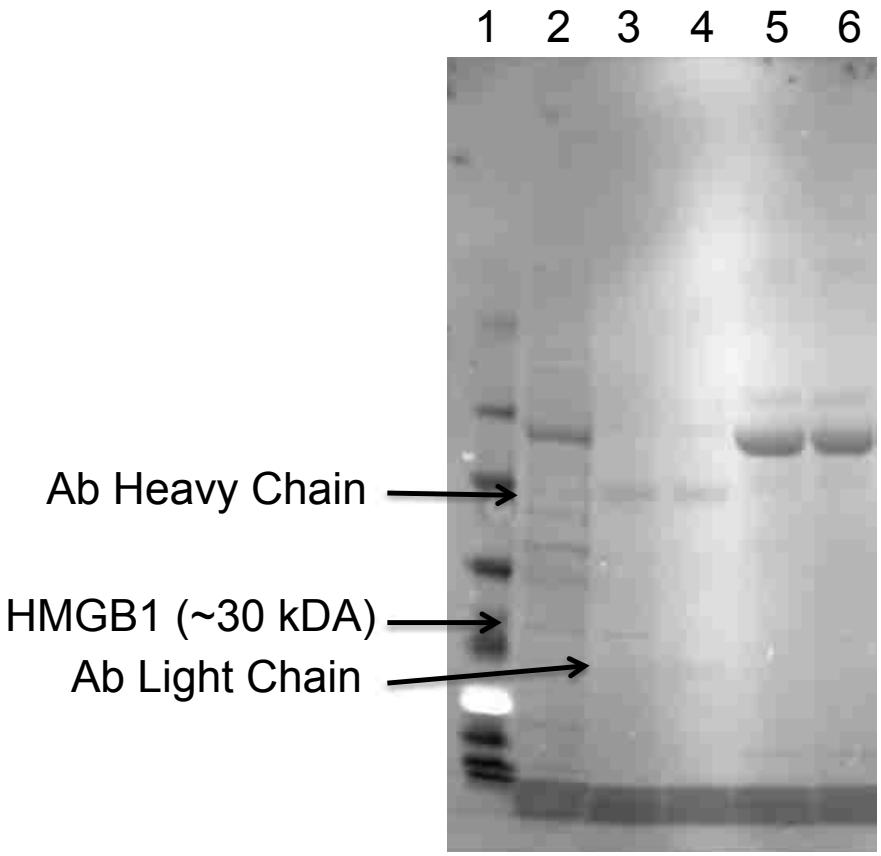


**Supplementary Figure 2.7.** Representative Blot (n=3) of coomassie blue staining of immunoprecipitated HMGB1. Lane 1) molecular mass ruler. 2) Control Cell lysate for identification of HMGB1. 3) Immunoprecipitated HMGB1 from lavage fluid of MWCNT treated mice 24 hr after instillation. 4) Immunoprecipitated HMGB1 from mice treated with DM 24 hr after instillation. 5) Lavage fluid from MWCNT mice after immunoprecipitation of HMGB1. 6) Lavage fluid from DM mice after immunoprecipitation of HMGB1.

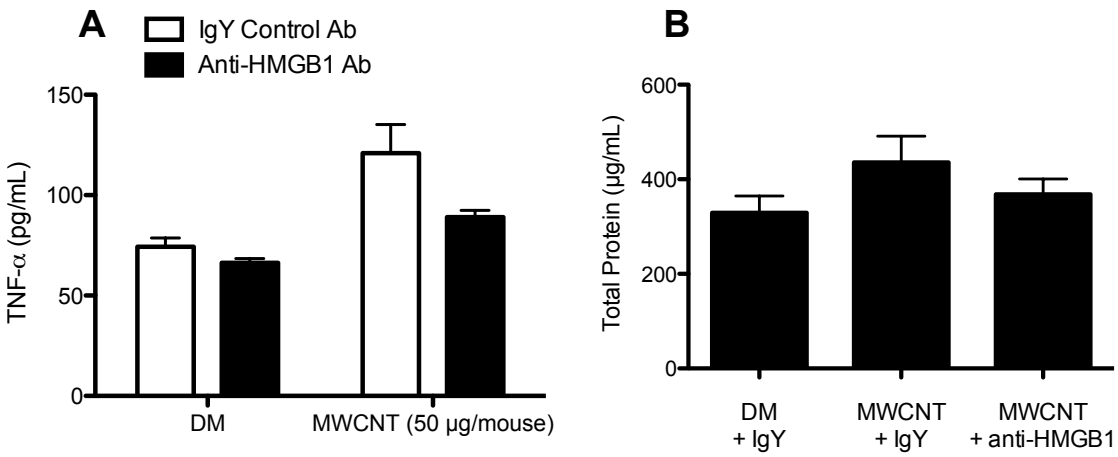


**Supplementary Figure 2.8.** TNF-α (A) and total protein (B) levels in the lavage fluid 24 hr following MWCNT and antibody instillation. TNF-α concentration was measured by ELISA. Total Protein concentration was assessed by the BCA assay.

CHAPTER 3: PHAGOLYSOSOME ACIDIFICATION IS NECESSARY FOR SILICA AND ENGINEERED NANOPARTICLE-INDUCED MEMBRANE PERMEABILIZATION AND RESULTANT NLRP3 INFLAMMASOME ACTIVITY

## 3.0. Manuscript Information Page

**Authors:** Forrest C Jessop[1†], Raymond F. Hamilton[1], Joseph F. Rhoderick [1], Paige Fletcher[1] and Andrij Holian[1]

**Target Journal:** Journal of Biological Chemistry

**Status of Manuscript:**

___ Prepared for submission to a peer-reviewed journal

_X_ Officially submitted to a peer-review journal

___ Accepted by a peer-review journal

___ Published in a peer review journal

Published by American Society for Biochemistry and Molecular Biology

Submitted May, 2016

## 3.1. Phagolysosome acidification is necessary for silica and engineered nanoparticle-induced membrane permeabilization and resultant NLRP3 inflammasome activity

Forrest Jessop*[1], Raymond F. Hamilton Jr*, Joseph F. Rhoderick*, Paige Fletcher* and Andrij Holian*

*Center for Environmental Health Sciences, Department of Biomedical and Pharmaceutical Sciences, University of Montana, Missoula, Montana

Correspondence author[1]

### 3.2. Abstract

NLRP3 inflammasome activation occurs in response to multiple particles including crystalline silica, engineered nanomaterial Multi-Walled Carbon Nanotubes (MWCNT), and Titanium Nanobelts (TNB). NLRP3 inflammasome activity is critical for the development of disease. However, mechanisms that drive persistent NLRP3 inflammasome activity are not fully understood. In this study we investigated the contribution of lysosome membrane permeabilization (LMP) and associated cathepsin B release in the context of silica and nanoparticle-induced NLRP3 inflammasome activity. We demonstrate that silica, MWCNT, and TNB cause significant LMP in Bone Marrow derived Macrophages *in vitro*. Particle-induced LMP was prevented with Bafilomycin A1, an inhibitor of phagolysosome acidification. LMP was also evident in alveolar macrophages *in vivo* 7 d following particle exposure. Cytosolic cathepsin B activity, which occurs following LMP, was responsible for causing NLRP3 inflammasome activity *in vitro* and NLRP3 inflammasome activity persistence *in vivo*. Active cathepsin B regulated both the activation of cathepsin L and the secretion of the alarmin HMGB1 with particle exposure. Together, these data highlight the necessity of phagolysosome acidification in particle-induced LMP. Furthermore they support an NLRP3 inflammasome dependent mechanism that includes active cathepsins in the secretion of HMGB1 with particle exposure.

**Key Words:** NLRP3 inflammasome, MWCNT, TNB, Silica, Lysosome Membrane Permeabilization

### 3.3. Background

Silica was one of the first environmental particles identified to activate the NLRP3 inflammasome [16]. It is now known that many particles, both exogenous and endogenous, environmental and engineered, of many sizes and shapes, are activators of the NLRP3 inflammasome, making inflammasome activity and associated signaling pathways a common target for next generation therapeutics. Gene knockout studies of inflammasome components NLRP3 and caspase-1 in murine models have shown diminished particle-induced acute inflammation and/or fibrosis [107-109]. With the rapid expanding market of engineered nanomaterial (ENM), there is cause for concern as many of these particles, like silica, could potentially cause chronic inflammatory disease. Therefore, there is a serious need to characterize the inflammation-inducing, or bioactive, potential of ENM.

Inhaled particles are phagocytosed by alveolar macrophages, and the phagosome containing particle(s) matures and fuses with lysosomes to attempt to degrade the particle. Most inorganic environmental particles such as silica, and many ENM are resistant to degradation, and consequently, their fate in the phagolysosome is not fully understood. Phagocytized silica particles induce lysosome membrane permeabilization (LMP) resulting in NLRP3 inflammasome assembly [107, 16]. NLRP3 inflammasome assembly results in activation of caspase-1, which cleaves the pro-forms and mediates the secretion of pyrogenic cytokines IL-1$\beta$ and IL-18, which are central to the development of chronic inflammatory lung diseases [110]. Prior studies provide data consistent with ENM-induced LMP and NLRP3 inflammasome activation, however these studies do not specifically quantify LMP or address

mechanisms by which particles cause LMP [111, 5, 112]. Consequently, the mechanisms responsible for LMP and magnitude of LMP caused by bioactive particle exposure require further investigation.

Active lysosomal proteases and low pH are reported to be necessary for removal of protein corona's on nanomaterial [113], which may allow for direct particle-membrane interactions. Critical to phagosome acidification are recruitment and activation of lysosomal vATPases. In addition, optimal activation of lysosomal proteases, such as cathepsin B, requires a low pH environment [114]. Phagolysosome acidification has been reported to play a role in LMP following treatment with Leu-Leu-OMe [16], likely through decreased Dipeptide Peptidase I (cathepsin C) activity, which processes the agent to its active form [115]. Phagolysosome acidification is suspected to play a role in LMP with silica exposure due to its ability to decrease downstream NLRP3 inflammasome activity [16]. Whether Bafilomycin A1 inhibition of NLRP3 inflammasome activity with silica exposure is due to direct inhibition of LMP or inhibition of the activation of cathepsin B is not known. Therefore, the contribution of phagolysosome acidification to silica and nanoparticle-induced LMP remains to be determined. Some reports suggest that active lysosomal protease cathepsin B may directly participate in causing LMP [116, 117, 54, 55]. Once leaked from the lysosome, cathepsin B facilitates NLRP3 inflammasome activation [16]. This is reported to be the case for certain ENM as well [111].

LMP occurs within hours in macrophages following bioactive particle exposure [16]. The persistence of LMP following bioactive particle exposure has not hitherto

been investigated *in vivo*. Evidence of LMP *in vivo* is sparse, let alone in models in which particles are responsible for LMP. The objective of this study was to determine common mechanisms contributing to particle-induced LMP and NLRP3 inflammasome activity with silica and bioactive nanoparticle exposure. We hypothesized that LMP would drive persistent NLRP3 inflammasome activity *in vivo* with particle exposure. Furthermore, we hypothesized that lysosome acidification is necessary for silica and ENM-induced LMP. Multiple particles including silica, Multi-Walled Carbon Nanotubes (MWCNT), Titanium Nanobelts (TNB), and Titanium Nanospheres (TNS) were used in these studies to assess commonality of LMP to persistant NLRP3 inflammasome activity with particle exposure. Further characterizing mechanisms by which LMP occurs and the persistence of LMP following exposure will be necessary to understand dynamics governing chronic NLRP3 inflammasome activity.

## 3.4. Materials and Methods

### *3.4.1. Particle Characteristics and Preparation*

All particles used in these studies have been previously described, in which LPS contamination was determined to be negligible by the Limulus amebocyte lysate assay (Cambrex, Walkersville, MD, USA) [12, 118, 111, 5, 119]. Acid washed crystalline silica (Pennsylvania Glass Sand Corp, Pittsburgh, PA, USA) with average particle size 1.5 – 2 μm was prepared fresh in phosphate-buffered saline (PBS, pH 7.4) and sonicated (550 watts @ 20 kHz) for 1 min in a cup-horn sonicator (Misonix, Inc. Farmingdale, NY, USA) prior to use. MWCNT (Sun Innovations, Inc., Fremont

CA, USA. www.nanomaterialstore.com) was prepared fresh in dispersion medium (DM, 0.6 mg/mL mouse serum albumin (Sigma-Aldrich, Saint Louis, MO, USA) and 0.01 mg/mL 1,2-dipalmitoyl-sn-glycero-3-phosphocholine (Sigma-Aldrich) in PBS) and sonicated (550 watts @ 20 kHz) for 1 min in a cup-horn sonicator [120]. MWCNT were provided by Dr. Nigel Walker and Brad Collins at the National Toxicology Program (NTP) at the National Institute of Environmental Health Sciences (NIEHS). TNB and TNS were prepared and provided by Dr. Nianqiang Wu at West Virginia University (Morgantown, WV, USA) and have been characterized extensively [5, 120]. TNB and TNS were suspended in PBS using a stir bar for 1 hr due to potential fracture by sonication [119].

*3.4.2. Mice*

Both male and female C57Bl/6 and caspase-1 null mice (Jackson Laboratories, Bar Harbor, ME, USA) were used in equal numbers for all studies. Animals were housed in micro-isolators in a specific pathogen-free facility under a 12:12-hr light-dark cycle. Food, bedding, and cages were sterilized by autoclaving. Mice were used between 8-12 wk of age. The University of Montana Institutional Animal Care and Use Committee (Missoula, MT, USA) approved all procedures performed on the animals.

*3.4.3. Bone Marrow derived Macrophages*

BMdM were obtained as described previously [30]. Briefly, wild-type C57Bl/6 were sacrificed and bone marrow was flushed from the isolated femur and tibia with media. Cells were then incubated in T75 culture flasks (20 mL RPMI + 10%FCS) overnight

for stromal cell elimination. Aspirated cells were transferred to new T75 flasks ($15x10^6$ cells/flask in 20 mL media) and 40 µL macrophage colony stimulating factor (M-CSF) added (10 ng/mL stock, R&D Systems). Cultures continued for 7–10 days with re-feeding and M-CSF spiking every 3–4 days.

*3.4.4. In vitro studies*

BMdM were plated in a 96 well plate ($1x10^5$ cells/well) and exposed to particles and LPS (20 ng/mL) for inflammasome priming. Cells were treated with/without the cathepsin B inhibitor CA-074-Me (10 µM, Peptides International, Louisville, KY, USA) or Bafilomycin A1 (100 nM, EnzoLife Sciences, Farmingdale, NY, USA) and cell supernatants collected after 24 hours. Cell supernatants were assessed for IL-1β and IL-18 cytokine levels by ELISA (R&D Systems, Minneapolis, MN, USA). IL-18 was measured by an in-house ELISA previously described [6].

*3.4.5. In vivo and ex vivo studies*

Mice were anaesthetized using isoflurane inhalation and then exposed to silica (40 mg/kg or 1 mg/25 g mouse) or MWCNT, TNB or TNS at 2 mg/kg (50 µg/25 g mouse), by oropharyngeal aspiration [121]. The doses used for these studies were selected based on their inflammatory activity established in prior work [12, 118, 111, 5]. Mice were lavaged after 7 d for analysis of inflammation and LMP. For chronic studies, mice were instilled once a week with silica for 4 consecutive weeks and sacrificed 56 d following the first instillation [12]. Alveolar Macrophages (AM) were isolated from the lavage fluid from both the early (7 d) and chronic time points (56 d) and cultured

*ex vivo* in RPMI + 10% FCS for 24 hr with or without LPS (20 ng/mL) and the cathepsin B inhibitor CA-074-Me (10 μM). Cell supernatants and cell free lavage were assessed for IL-1β and IL-18 by ELISA as previously described. HMGB1 was measured by ELISA using commercially available antibodies (R&D Systems; EMD Millipore, Billerica, MA, USA; Santa-Cruz Biotech, Dallas, TX, USA) as previously described [122]. Whole lung lavage fluid was also assessed for LDH activity (Promega, Madison, WI, USA) and protein content using the BCA assay (Thermo Fisher Scientific, Waltham, MA, USA). Extracellular cathepsin activity was assessed as previously described by our laboratory [123]. Briefly, 2 μg Z-LR-AMC (specific to cathepsin B, cathepsin L and cathepsin V; R&D systems) in PBS was added to 50 μL of whole lung lavage fluid in a total reaction volume of 150 μL. The assays were incubated at 37°C for 1 h then fluorescence was measured using a plate reader at 380 nm excitation and 460 nm emission.

*3.4.6. Lysosome Membrane Permeabilization (LMP) assay*

LMP was assessed using methods modified from Aites et al [60]. Isolated AM were plated in a 96 well plate at 1 x $10^5$ cells per well and allowed to adhere for 2 hours. For BMdM, cells were plated at 2 x $10^5$ cells per well in a 24 well plate. Cells were washed twice with PBS to remove dead cells and debris. AM or BMdM were then incubated with 100 μL (96 well) or 200 μL (24 well) of cytosol extraction buffer (250 mM sucrose, 20 mM Hepes, 10 mM KCl, 1.5 mM $MgCl_2$, 1 mM EDTA, 1 mM EGTA, 0.5 mM pefabloc (Sigma-Aldrich), pH 7.5 + digitonin (Sigma-Aldrich)) for 15 min on ice with rocking. The concentration of digitonin for optimal extraction of the cytosolic

fraction was obtained by titration (BMdM = 12.5 µg/mL; AM = 17.5 µg/mL). 50 µL of extracted cytosol was then added to 50 µL of cathepsin reaction buffer (50 mM sodium acetate, 4 mM EDTA, pH 6.0 + fresh 0.5 mM pefabloc, 8 mM DTT, 50 µM cathepsin L substrate (Z-Phe-Arg-AFC, EnzoLife Sciences)) and read using a plate reader (25 min; 45s intervals; 400 nm excitation; 489 nm emission). β–*N*-acetyl-glucosaminidase (NAG) activity was measured by adding 30 µL cytosolic extract to 100 µL of NAG reaction buffer (0.2 M sodium citrate, pH 4.5 with 300 µg/mL 4-methylumbelliferyl-2-acetamido-2-deoxy-β-D-glucopyranoside (Sigma-Aldrich)) and assessed on a plate reader (20 min; 45s intervals; 356 nm excitation; 444 nm emission). LDH activity was assessed following manufactures instructions (Promega). Extracted cytosolic LDH activity was used as an internal control to which cytosolic cathepsin L or NAG activities were normalized. Cytosolic extract enzyme activities were calculated as a percent of total cell lysate activity in which 200 µg/mL of digitonin was used to completely lyse the cell.

*3.4.7. RNA preparation and RT-PCR*

Isolated AM (4 mice pooled for each N) from mice 7 d following PBS or silica exposure were lysed and total RNA isolated in Trizol (Thermo Fisher Scientific). The RNA Integrity Number (RIN) and total RNA concentration was confirmed using the RNA 6000 Nano Kit (Agilent Technologies, Santa Clara, CA, USA) and Agilent Bioanalyzer 2000. Prior to cDNA synthesis, 100 ng of total RNA was treated with 1-2U of DNAse I (Quanta Biosciences, Gaithersburg, MD, USA). All RNA samples were reverse transcribed using iScript Reverse Transcription Supermix (BioRad, Hercules,

CA, USA) in accordance with the manufacturers protocol. PrimeTime qPCR primers to Caspase-1 (*Casp1*, Prime Time Assay Mm.PT.58.13005595), IL-1β (*Il-1b*, Mm.PT.58.42940223), NLRP3 (*Nlrp3*, Mm.PT.58.42443451), ASC (*Pycard*, Mm.PT.56a.42872867), and reference genes *Adck1* (Mm.PT.56a.41787370) and *Pigo* (Mm.PT.58.6147472) were used for RT-PCR reactions (IDT, Coralville, IA, USA). Efficiency for PrimeTime primers was established via standard curve analysis of at least two biological replicates using cDNA synthesized from AM or genomic DNA isolated from murine lung tissue respectively. Efficiencies for all primer pairs used in PCR analysis >89%. All signals were normalized to *Adck1* and *Pigo* and relative expression levels determined using the REST 2009 v2.0.13 software suite (Qiagen, Valencia, CA, USA).

### *3.4.8. Western Blot*

Isolated cells obtained from lung lavage fluid were lysed directly in RIPA buffer containing HALT™ protease inhibitors (Life Technologies, Carlsbad, CA, USA). Whole lung lavage cells from 4 mice were pooled for each *N*. Lysates were run on 4-12% Bis-Tris SDS-PAGE gels. Anti-NLRP3 antibodies were obtained from R&D Systems. Anti-ASC, Anti-caspase-1, and anti-pro-IL-1β antibodies were obtained from Novus Biologicals (Littleton, CO, USA). The secondary antibodies were donkey anti-rabbit conjugated to horseradish peroxidase (BioLegend, San Diego, CA, USA).

### *3.4.9. Detection of Cathepsin B and Lysotracker™ Red*

Cathepsin B and lysosomes were measured using a CompuCyte iCys Laser Scanning Cytometer (LSC, Westwood, MA, USA). Briefly isolated lung lavage cells were seeded in triplicate wells in a 96-well plate with a glass coverslip bottom (MatTeck Corp. Ashland, MA, USA) at 1 x $10^5$ cells/well. Non-adherent cells were removed by gentle washing once with PBS. Cells were then stained using the Magic Red™ Cathepsin B Detection Kit (ImmunoChemistry Technologies, Bloomington, MN, USA) or LysoTracker Red DND-99 dye (Life Technologies) and counter-stained with Molecular Probes HCS NuclearMask Blue stain (Life Technologies) according to manufacture's instructions. The cathepsin B signal or Lysotracker Red signal was detected using a 561 nm laser as the excitation source and a PMT detector with a 600/50 nm bandpass filter. The nuclear staining was excited with a 405 nm laser and detected with a 440/30 nm bandpass filter/PMT set. Individual passes of the 561 nm and 405 nm lasers were used to avoid any spectral overlap of the "blue" and "red" fluorescent signals. A threshold of "blue" fluorescence was set such that the software draws a contour around the nucleus of the cell. The contour is then expanded by 20 pixels to include the cytoplasm of the cell. Each cell (defined by nuclear staining) is plotted on a histogram showing Red Mean Fluorescent Intensity (MFI). Regions were defined within each well of the 96-well plate to include approximately 1500 cells to achieve sufficient sample representation.

*3.4.10. Statistical analysis*

Statistical analyses involved comparison of means using a one- or two-way ANOVA followed by a Bonferroni's test to compensate for increased type I error. Unpaired *t*

test was utilized for analysis of Western Blots or other data sets that included simple comparisons between two groups. All probabilities were two-tailed. Statistical power was > 0.8 to determine sample size. Statistical significance was defined as a probability of type I error occurring at < 5% ($P$<0.05). The minimum number of experimental replications was 3. Graphics and analyses were performed on PRISM 5.0.

## 3.5. Results

### *3.5.1. Silica and ENM induce LMP in macrophages*

Silica has been shown to cause LMP *in vitro* [16], and LMP has been proposed, but not directly measured with the other ENM used in these studies [111, 5]. While fluorescent probes such as Lysotracker™, acridine orange, and others may provide data suggestive of LMP, they fail to provide quantifiable direct measures of LMP, and can be difficult to interpret. Therefore, we adapted recently reported methods to quantify LMP in macrophages following particle exposure [60]. These assays rely on selective digitonin extraction of the cytosol in order to measure lysosomal cathepsin and hydrolase activity following LMP. Bone Marrow derived Macrophages (BMdM) have successfully been used to model NLRP3 inflammasome activity with particle exposure, and resemble AM responses [124]. Therefore, we utilized BMdM to help determine mechanisms involved in LMP. BMdM were exposed to increasing doses of silica, MWCNT, TNB, and TNS *in vitro* and LMP quantified at 4 hr. We also quantified LMP over an 18 hr time-course. All particles were able to induce LMP with increasing dose (Figure 1A), however, the kinetics of LMP-induction for each particle differed. LMP following silica exposure peaked at 4 hours, while LMP

increased over time with ENM exposures (Figure 1B). These findings reveal important differences between the kinetics of silica and ENM-induced LMP within the first 18 hr of exposure *in vitro*. However, exposure to all particles eventually resulted in significant LMP by 18 hr.

### *3.5.2. Phagolysosome acidification is necessary for particle induced LMP*

Mechanisms by which bioactive particles including silica, MWCNT, and TNB cause LMP have not been determined. Phagolysosome acidification has been reported to play a role in pharmacologically-induced LMP with Leu-Leu-O-Me, and this has been predicted to be the case with silica exposure [16]. The role of phagolysosomal acidification in LMP has not been determined for MWCNT, TNB, or TNS used in these studies. Therefore, we exposed BMdM to silica, MWCNT, TNB, and TNS with or without the vATPase inhibitor Bafilomycin A1. We measured LMP after 4 hr and resultant downstream NLRP3 inflammasome activity (extracellular IL-1$\beta$ and IL-18 levels) after 24 hr. LPS was used to prime the NLRP3 inflammasome, and had no significant effect on LMP (data not shown). Bafilomycin A1 inhibited LMP, as indicated by decreased cytosolic Cathepsin L activity, with all particle exposures (Figure 2A). Leaked NAG can be used as a second indicator of LMP, and has activity independent of cathepsins and a low pH [60]. NAG activity in the cytosolic fraction was significantly decreased with Bafilomycin A1 treatment for all particles, confirming the necessity of phagolysosome acidification in particle-induced LMP. Inhibition of LMP by Bafilomycin A1 was not due to decreased phagocytosis (data not shown).

Finally, inhibition of LMP with Bafilomycin A1 correlated with decreased NLRP3 inflammasome activity, including the release of IL-1β and IL-18 (Figure 2D, 2E).

*3.5.3. Cathepsin B is not necessary for particle-induced LMP*

While most studies agree that cathepsin B is important in activating the NLRP3 inflammasome after LMP, there are reports suggesting a direct role for cathepsin B in facilitating LMP with cholesterol crystals, adjuvants and sphingosine [54, 55, 13, 115]. This relationship has not been determined for silica and ENM exposure. Therefore, to determine if cathepsin B was directly involved in LMP, we exposed BMdM to bioactive particles with or without CA-074-Me treatment and assessed LMP after 4 hr. CA-074-Me has been shown to have increased specificity towards Cathepsin B at the dose used in these studies [16]. CA-074-Me treatment greatly decreased cathepsin L activity in the cytosolic fraction of particle-exposed macrophages (Figure 2A). CA-074-Me did not directly inhibit cathepsin L (Figure 2B). CA-074-Me treatment partially reduced cytosolic NAG activity with silica exposure (Figure 2C), but did not reduce cytosolic NAG activity with ENM exposures (Figure 2D). Together, these findings support the notion that the nanoparticles used in these studies cause LMP independent of cathepsin B, however, cathepsin B may have a marginal or indirect role with silica exposure. Furthermore, these data show that inhibition of active cathepsin B results in inhibition of active cathepsin L, suggesting a protease cascade following particle exposure.

Finally, we measured IL-1β and IL-18 production with particle exposure with or without CA-074-Me treatment at 24 hr to confirm that active cathepsin B plays an

integral role in NLRP3 inflammasome activation. Extracellular IL-1β and IL-18 levels were significantly reduced with CA-074-Me treatment for all particles used (Figure 2E, 2F). These data provide further support to the importance of cathepsin B after LMP in activating the NLRP3 inflammasome *in vitro*.

*3.5.4. Silica exposure results in LMP in vivo*

We have demonstrated that the bioactive particles used in these studies cause LMP, resulting in translocation of cathepsins into the cytosol, and activation of the NLRP3 inflammasome *in vitro*. Direct evidence of LMP *in vivo* is sparse, let alone in models of bioactive particle exposure. Since silica was the most potent inducer of LMP *in vitro*, we utilized silica as a representative particle to determine impacts of particle exposure on cathepsin B expression, lysosomes, and LMP *in vivo*. Using silica for these studies also had the added benefit of not interfering with fluorescent signal in laser scanning cytometry assays, which may occur with MWCNT and TNB. We exposed C57Bl/6 mice to silica and isolated AM after 7 d, then measured intracellular cathepsin B activity using the Magic Red™ assay, which relies on active cathepsin B targeting of a cresyl violet conjugated substrate. This time was chosen based on prior work showing silica, MWCNT, TNB, and TNS exhibited significant cellular inflammation and/or pathology [111, 12, 120, 125], suggesting ongoing NLRP3 inflammasome activity. Silica exposure significantly increased intracellular cathepsin B activity compared to vehicle control (Figure 3A). It is possible that LMP can result in the loss of intact lysosomes [16]. AM isolated 7 d following exposure to silica had a lower mean fluorescence intensity (MFI) of Lysotracker™ Red staining

compared to PBS control when assessed by laser scanning cytometry (Figure 3B). Evaluation of histograms (MFI versus cells counted) revealed that silica exposure caused the formation of two distinct cell populations based on MFI (Figure 3C), suggesting that lysosomal loss could be occurring in a subset of macrophages isolated from the lungs during persistent particle-induced inflammation.

To more directly quantify LMP at 7 d following silica exposure, we extracted the cytosolic fraction from AM and measured leaked lysosomal enzyme activity. Cathepsin L activity was significantly increased in the cytosol of AM from silica-exposed mice compared to PBS-treated mice, confirming LMP *in vivo* (Figure 3D). NAG activity was significantly increased as well (Figure 3E). Together, these data, in conjunction with increased cathepsin B and loss of lysosomal staining, demonstrate LMP *in vivo* following particle exposure.

We previously demonstrated that CA-074-Me did not fully inhibit silica-induced LMP *in vitro*, suggesting LMP can occur independent of cathepsin B activation (Figure 2B, C). To confirm the role of cathepsin B in LMP *in vivo*, we treated AM from silica-exposed mice *ex vivo* with CA-074-Me . CA-074-Me treatment did not significantly reduce LMP, as indicated by no decrease in cytosolic NAG activity (Figure 3E). However, we observed that CA-074-Me treatment did cause a significant decrease in active cathepsin L (Figure 3E), again supporting the notion that cathepsin B regulates the activation of other lysosomal cathepsins.

*3.5.5. NLRP3 Inflammasome activity persists in vivo following particle exposure*

Mechanisms by which NLRP3 inflammasome activity persists following particle exposure are not fully understood. We show with silica exposure that LMP is ongoing at 7 d (Figure 3). We hypothesized LMP would be responsible for persistent NLRP3 inflammasome activity at this time-point. In order to test this, we needed to confirm that NLRP3 inflammasome activity, including the secretion of active IL-1β and IL-18, was persistent *in vivo*. For these reasons, we exposed C57BL/6 and caspase-1 null mice to crystalline silica and assessed pulmonary inflammation at 7 d. C57BL/6 mice had significantly elevated IL-1β and IL-18 levels in the lung lavage fluid (Figure 4A, 4B). Levels of IL-1β and IL-18 were significantly less in caspase-1 null mice compared to wild type C57Bl/6. Total cell counts were similar between silica-exposed mice and ENM-exposed mice at 7 d (Figure 4C), showing consistency with cellular inflammation between various particle exposures. Total protein levels and extracellular LDH activity were increased as well in C57BL/6 mice (Figure 4D, 4E), supporting ongoing inflammation at 7 d.

AM have a critical role in inflammation and the development of disease with particle exposure [12]. We hypothesized that increased NLRP3 inflammasome associated cytokine production *in vivo* was a consequence of persistent NLRP3 inflammasome activity in AM. In order to determine if the NLRP3 inflammasome was persistent in AM *in vivo*, we isolated AM from silica-exposed mice at 7 d and assessed both mRNA and protein levels of NLRP3, ASC, caspase-1, and pro-IL-1β. As predicted, mRNA levels for NLRP3 (Nlrp3), ASC (Pycard), and pro-IL-1β (Il-1β) were significantly increased. Pro-caspase-1 (Casp1) trended upwards but was not significant (Table 1). Protein levels followed a similar pattern, including significantly

increased NLRP3, ASC, and pro-caspase-1 (Figures 4F, 4G). Together, these data support that silica exposure causes NLRP3 inflammasome persistence at 7 d in AM *in vivo*, correlating with ongoing LMP.

### *3.5.6. HMGB1 and cathepsin secretion is dependent upon caspase-1*

The alarmin HMGB1 is an endogenous primer of NLRP3 inflammasome activity through NF-κB, and can be actively secreted from macrophages or passively released from dying cells [122, 11] [85]. Lysosomal cathepsins may also be secreted through similar mechanisms and can participate in extracellular matrix remodeling [63], [126]. An inflammasome dependent and independent secretion pathways for HMGB1 have been reported with infection [85]. We have previously reported that HMGB1 secretion is dependent upon caspase-1 with MWCNT exposure [122]. Whether caspase-1 is necessary for HMGB1 secretion following silica exposure had not been assessed *in vivo*. Therefore, we exposed C57BL/6 and caspase-1 null mice to silica and measured the levels of HMGB1 in the lavage fluid after 7 d. Caspase-1 null mice had significantly less HMGB1 in the lavage fluid compared to C57BL/6 controls (Figure 5A). We also observed significantly less cathepsin activity in silica-exposed caspase-1 null mice lavage fluid compared to silica-exposed C57Bl/6 control (Figure 5B). Together, these data support a novel role for caspase-1 in facilitating both the secretion of HMGB1 and cathepsins with silica exposure.

### *3.5.7. Persistent NLRP3 inflammasome activity is dependent upon Cathepsin B*

Our data support the notion that NLRP3 inflammasome is persistent and active 7 d following silica and ENM exposure *in vivo* (Figure 4), and this correlates with ongoing LMP (Figure 3). We hypothesized that LMP and the release of cathepsin B would be driving forces of persistent NLRP3 inflammasome activity *in vivo* in AM. Consequently, we predicted inhibition of active cathepsin B with CA-074-Me in AM isolated from particle-exposed mice would decrease NLRP3 inflammasome cytokines. Therefore, we isolated AM from C57BL/6 mice 7 d after silica, MWCNT, TNB, and TNS exposure and cultured them *ex vivo* with or without LPS or CA-074-Me to inhibit cathepsin B. Stimulation of cells with low levels of LPS is often used for priming of the NLRP3 inflammasome. After 24 hr we measured IL-1β and IL-18 in cell supernatants (IL-18 data shown only for silica exposure). Isolated AM from silica, MWCNT, and TNB-exposed mice secreted significantly greater amounts of IL-1β than AM from PBS and/or TNS-exposed mice (Figure 6A, 6B). CA-074-Me treatment significantly reduced IL-1β production *ex vivo* with all bioactive particle treatments (Figure 6A, 6B). CA-074-Me also inhibited *ex vivo* production of IL-18 from macrophages from silica-exposed mice (Figure 6C). To confirm this response occurred at a more chronic time point, we utilized a model of chronic lung disease previously established with silica [12]. AM isolated 56 d following silica exposure had significantly more IL-1β and IL-18 secretion that could be mitigated with CA-074-Me treatment (Figure 6D, 6E). Together, these data support persistent NLRP3 inflammasome activity in AM is dependent upon active cathepsin B, which is present in the cytosol after LMP.

HMGB1 has been reported to be dependent upon a cathepsin B associated unconventional secretion pathway with starvation and nigericin co-treatment [11]. However this relationship has not been investigated in a relevant model of particle exposure. Since we observed a dependence of HMGB1 secretion on caspase-1, we predicted that HMGB1 secretion from macrophages could also be mitigated by inhibiting mediators upstream of NLRP3 inflammasome activation (i.e. cathepsin B). We again utilized silica as a representative particle to assess this relationship. Macrophages isolated from silica-exposed mice at 7 d secreted high levels of HMGB1 that could be decreased with CA-074-Me treatment (Figure 6F). These data are the first showing HMGB1 dependence on active cathepsin B in a particle-exposure model, and further support the notion that an active NLRP3 inflammasome regulates the secretion of HMGB1 and cathepsins.

### 3.6. Discussion

Compromised lysosome integrity is an emerging paradigm with ENM exposure, and this includes the potential for ENM to cause LMP [62]. Lysosome dysfunction has been implicated in a number of chronic inflammatory diseases [61]. Evaluation of LMP with particle exposure primarily has been done using acidotropic dyes or immunofluorescent staining to assess colocalization of lysosomal enzymes [62], which can be difficult to interpret. Many nanomaterials, such as MWCNT and TNB, could also interfere with these fluorescent assays, especially at higher doses, further complicating assessment of LMP. Additionally, inhibitors that target lysosome acidification, such as Bafilomycin A1, can also affect fluorescence acidotropic dyes,

preventing mechanistic studies. In this study, we utilized methods adapted from Aits et al., which rely on the saponic qualities of digitionin for selective extraction of the cellular cytosolic fraction [60], allowing for assay of leaked lysosomal enzyme activity. We show that both silica and ENM used in these studies caused a dose-dependent increase in LMP (Figure 1A). We also observed some differences in LMP over time between silica and ENM (Figure 1B), which could be due to multiple factors including mechanisms of uptake. Silica phagocytosis is mediated by MARCO [127], however, many of the uptake mechanisms of the ENM used in these studies have not been determined, but may include caveolin-1 or clatherin-mediated endocytosis [128]. Regardless of uptake mechanism, all particles assessed in these studies caused LMP within 18 hr, consistent with the hypothesis that lysosome dysfunction is the critical pathway following phagocytosis leading to NLRP3 inflammasome activation.

Mechanisms by which silica and nanomaterials cause LMP have not been determined. We demonstrated that phagosome acidification is essential for LMP and downstream NLRP3 inflammasome activity with silica, MWCNT, TNB, and TNS exposure (Figure 2). Phagolysosome acidification has been reported to be necessary for LMP following Leu-Leu-O-Me exposure [16]. However, inhibition of acidification by Bafilomycin A1 may also inhibit activation of cathepsin C, which is important in processing Leu-Leu-O-Me to its active form that induces LMP [116, 16, 115]. Phagolysosome acidification has also been proposed with silica due to its ability to decrease NLRP3 inflammasome associated cytokine production, however direct inhibition of LMP with Bafilomycin A1 was not assessed in these reports [16]. While our results show a role for acidification in particle-induced LMP, they come short of

addressing mechanisms by which particles cause LMP. Lysosome acidification and activation of proteases has been reported to facilitate removal of the protein corona on phagocytosed particles, and thereby may allow for direct particle-membrane interactions [113]. Therefore, after the protein corona is removed, this would support the notion that specific physiochemical characteristics of the particle would define its LMP-inducing potential. Alternatively, some studies have directly implicated cathepsin B in LMP [116, 115, 54, 55]. We show that LMP occurs independent of cathepsin B with ENM exposure, as NAG levels in the cytosolic fraction were not reduced with CA-074-Me treatment (Figure 2, 3). Leaked NAG levels were partially reduced with silica exposure and CA-074-Me treatment in BMdM, suggesting a minor or indirect role for cathepsin B in this model. Particle-induced membrane damage via ROS has also been proposed as a mechanism of LMP [47]. Nonetheless, mechanistic understandings of the contribution of these pathways (ROS and/or direct particle-membrane interactions) to initiating LMP have not been described.

*In vivo* studies supporting LMP are lacking [61]. There are multiple reports of LMP *in vitro* with a broad range of agonists and only one report showing an *in vivo* role for LMP in mammary tissue reduction [129]. Consequently, little is known on the contribution of LMP to NLRP3 associated inflammation beyond what is observed *in vitro*. These studies are the first to show direct evidence of particle-induced LMP in AM 7 d following *in vivo* silica exposure (Figure 3D, 3E). Ongoing LMP, including the leak of active cathepsins into the cytosol, could potentially drive persistent NLRP3 inflammasome activity. Our observation of LMP and increased active cathepsin B in AM (Figure 3A, 3D, 3E) correlated with increased NLRP3 inflammasome activity at 7

d *in vivo* (Figure 4A, 4B). Persistent NLRP3 inflammasome activity in AM was mitigated *ex vivo* with CA-074-Me treatment (Figure 6). Cytosolic cathepsin activity is known to cause NLRP3 inflammasome activation *in vitro*, and therefore the therapeutic effects of CA-074-Me in AM *ex vivo* is likely due to inhibition of cytosolic cathepsin B resulting from ongoing LMP. This would support the hypothesis that cytosolic cathepsin B is responsible for persistence of NLRP3 inflammasome activity.

Further novel findings of this work are that cathepsin B inhibition with CA-074-Me regulates the activity of cathepsin L (Figure 2A, 3D). Others have reported a specific role for cathepsin C in causing LMP and regulating cathepsin B [116]. However, these studies were not done within a relevant particle exposure model, and are not conclusive on the interactions between cathepsin B and cathepsin C. Our findings and these reports may indicate the possibility of a protease cascade within the lysosome following particle exposure. We can conclude that inhibition of cathepsin B suppresses NLRP3 inflammasome activity, and since inhibiting cathepsin B also inhibits other cathepsins, there may also be other intermediate cathepsins regulating NLRP3 inflammasome activity not accounted for. Further studies are required to determine the involvement of other cathepins in NLRP3 inflammasome activation.

It is important to note that we observed significant differences in the magnitude of NLRP3 inflammasome activity in AM at 7 d between silica and MWCNT exposures (Figure 5A, 5B). This is likely due to a number of factors involved in IL-1$\beta$ production including differences in particle dose, surface area, physiochemical properties, and clearance. Because of these differences, it is difficult to directly compare bioactivity of

ENM to silica without further dosimetry evaluation, although the critical pathway (lysosome membrane permeabilization) is the same.

HMGB1 is a Danger associated Molecular Pattern/alarmin that is released by dead or dying cells, and can be actively secreted by macrophages [85, 17]. Once outside of the cell, HMGB1 has both pro-inflammatory and chemotactic activity [130, 22]. Both HMGB1 and IL-18 have been implicated in autoimmune diseases such as SLE, which has increased prevalence in individuals with silicosis [24, 3, 25]. We have previously reported that HMGB1 participates in sterile priming of the NLRP3 inflammasome *in vitro* and *in vivo* with MWCNT exposure [122]. While we did not investigate the contribution of HMGB1 in silica or TNB-associated NLRP3 inflammasome activity, we suspect a commonality with MWCNT exposure. HMGB1 release has been reported to be dependent upon NLRP3 inflammasome activation with endotoxemia, ATP, and nigericin exposure [18]. In these studies, we further show that HMGB1 secretion *in vivo* is dependent upon caspase-1 and cathepsin B with silica exposure (Figure 5A, 6F). Extracellular cathepsin activity was also dependent upon Caspase-1, suggesting the NLRP3 inflammasome is regulating unconventional secretion of both HMGB1 and proteases. An autophagy-based unconventional secretion pathway has been reported for the secretion of HMGB1 and NLRP3 inflammasome associated cytokines with nigericin and starvation [11]. Autophagic activity has been reported to be altered with silica exposure [131], however, further studies are needed to determine if autophagy contributes to an NLRP3 inflammasome dependent secretion pathway following silica and ENM exposure.

In summary, this study demonstrates several novel findings that further our understanding of mechanisms driving persistent NLRP3 inflammasome activity and particle-induced LMP. First, we highlight the necessity of phagolysosome acidification as a common prerequisite to particle-induced LMP, and show cathepsin B does not play a direct role in causing LMP. Secondly, we provide evidence of LMP in AM *in vivo*, and resultant cytosolic cathepsin B activity drives persistent NLRP3 inflammasome activity in AM *ex vivo*. Finally, we provide evidence supporting a cathepsin B and NLRP3 inflammasome associated mechanism for the secretion of HMGB1. These findings are highlighted in Figure 7. These studies support that targeting cathepsin B and/or LMP through lysosomal stabilization may be a therapeutic strategy for reducing particle-induced chronic inflammatory disease.

### 3.7. Other

*3.7.1. Acknowledgements:* The authors are grateful for the technical support obtained through the CEHS Molecular Histology and Fluorescence Imaging, Inhalation and Pulmonary Physiology Cores, and Fluorescence Cytometry Core facilities. We extend a special thanks to the technical staff of these cores including Pam Shaw, Britt Postma, Mary Buford, and Lou Herritt. The authors thank Dr. Christopher T. Migliaccio and Kevin Trout for scientific advice, as well as Dr. Elizabeth Putnam, Dr. Kevan Roberts, and Dr. John Hoidal for independent review of the manuscript.

*3.7.2. Author Contributions:* FJ designed and carried out both the in vitro, and 7 d in vivo and ex vivo studies in the manuscript, and performed statistical analysis. FJ

wrote the first draft of the manuscript. RFH performed the *ex vivo* studies and cytokine analysis on AM isolated 56 d after silica exposure. RFH helped with the statistical analysis. JFR performed mRNA quantification by RT-PCR for the 7 d studies and assisted with BMdM *in vitro* studies. PF assisted with the caspase-1 null mouse studies. AH assisted FJ in overall study design and coordination. All authors helped further draft the manuscript and approved the final manuscript

*3.7.3. Funding Sources:* This work was support by a research grant from NIEHS (R01ES023209), Institutional Idea Awards from NCRR (P20 RR017670) and NIGMS (P30 GM103338), and a S10 Shared instrument grant (S10RR026325-01). Additionally, Forrest Jessop was supported in part by a PhRMA Foundation Individual Pre-doctoral Fellowship. The content of this manuscript is solely the responsibility of the authors and does not necessarily represent the views of the National Institute of Health or the PhRMA Foundation.

*3.7.8. Conflicts of Interest:* The authors declare that they have no competing interests.

Table 3: NLRP3 Inflammasome components are increased with silica exposure

| Gene | Fold Change | Std. Error | P Value |
|---|---|---|---|
| *Casp1* | 1.774 | 0.719 – 4.804 | 0.356 |
| *Il-1β* | 6.509 | 1.227 – 24.183 | 0.033* |
| *Nlrp3* | 2.773 | 1.770 – 4.774 | 0.000*** |
| *Pycard* | 2.390 | 1.159 – 3.752 | 0.004*** |

Lung lavage cells were collected at 7 d after silica exposure for analysis of mRNA expression levels. Expression is presented as fold change caused by particle treatment over PBS control after normalization to reference genes. Values are shown as mean ± *SD* (*N*=4). * $P < 0.05$, *** $P < 0.001$ indicates significant increase in transcription compared to PBS control.

### 3.8. Figures

FIGURE 1

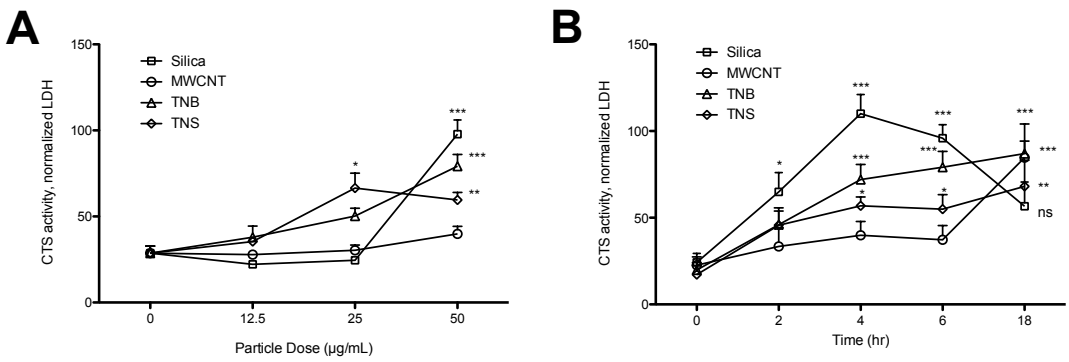


**Figure 3.1.** *Silica and ENM exposure cause LMP in macrophages*. (A) BMdM were exposed to increasing doses of silica, MWCNT, TNB, and TNS and LMP (leaked cathepsin L) measured in the cytosolic fraction at 4 hr. (B) LMP over time with particle dose of 50 µg/mL. Data are presented as mean ± *SEM* (*N*=3). *P < 0.05, **P < 0.01, ***P < 0.001 when compared to baseline.

FIGURE 2

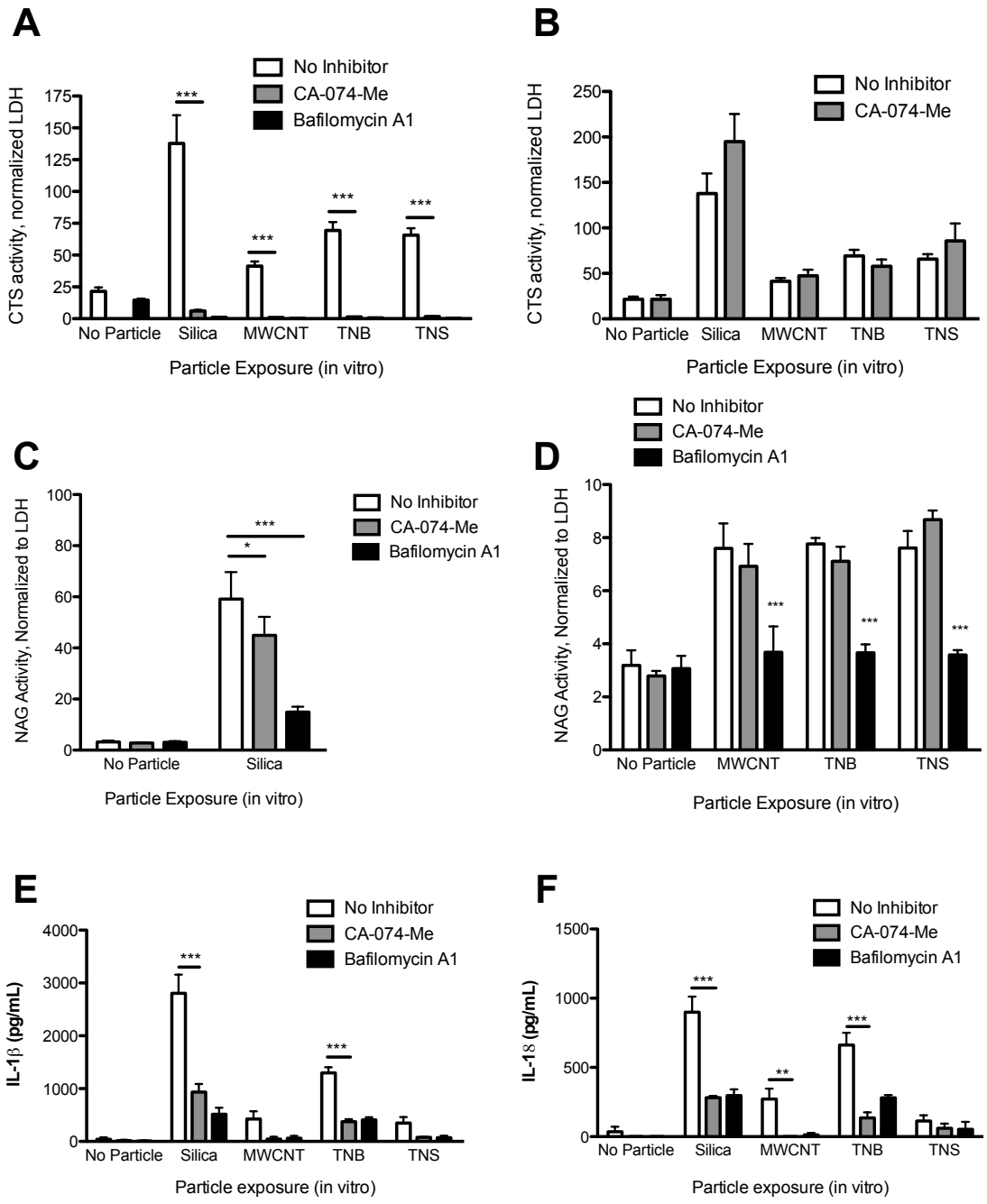


**Figure 3.2.** *Particle-induced LMP in macrophages is dependent on phagolysosome acidification in vitro*. BMdM were exposed to silica, MWCNT, TNB, or TNS (all 50 μg/mL) with or without Bafilomycin A1 (100 nM) or CA-074-Me (10 μM) and LMP

assessed after 4 hr. (A) Cathepsin L activity in the cytosolic fraction. (B) CA-074-Me does not inhibit Cathepsin L activity when CA-074-Me (10 μM) was added *in situ* to cellular extracts and incubated for 30 minutes. (C) NAG activity in the cytosolic fraction following exposure (crystalline silica only). (D) NAG activity in the cytosolic fraction following MWCNT, TNB, and TNS exposure. (D) IL-1β levels in BMdM cell supernatants 24 hr after particle exposure, LPS stimulation (20 ng/mL), and treatment with Bafilomycin A1 (100 nM) or CA-074-Me (10 μM). (E) IL-18 levels in the cell supernatants after 24 hr. Data show mean ± *SEM* (*N*=3). **P* < 0.05, ***P* < 0.01, ****P* < 0.001 indicate significance compared to particle exposures without CA-074-Me or Bafilomycin A1 treatment.

FIGURE 3

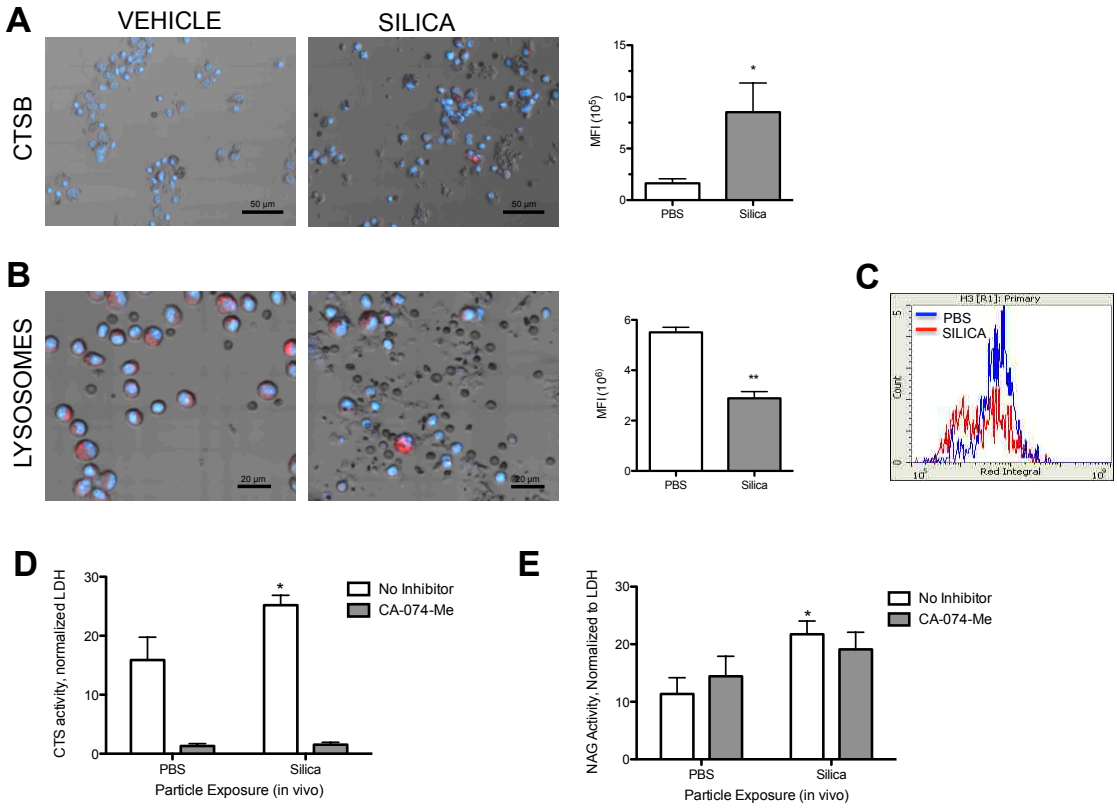


**Figure 3.3.** *LMP is increased in AM 7 d following silica exposure in vivo*. AM were isolated 7 d following silica (40 mg/kg) or PBS exposure and assessed for active cathepsin B, lysosomal loss with Lysotracker Red™, and leaked lysosomal enzymes cathepsin L and NAG using digitonin extraction. (A) Representative LSC images (40X scan) and figure showing Mean Fluorescent Intensity (MFI per total cells counted) of cathepsin B for combined experiments (N=4, 2 mice pooled for each N). (*B*) Representative LSC images (60X scan) of Lysotracker Red™ staining with figure showing MFI of Lysotracker Red™ for combined experiments. (*C*) Histogram overlays of Lysotracker Red™ MFI integrals from combined experiments (N=4, 2 mice pooled for each N). (D) Cathepsin L activity in cytosolic fraction. (E) NAG activity in cytosolic

fraction. CA-074-Me (10 μM) was added to AM cultures for 2 hours *ex vivo*. Data are shown as mean ± *SEM* (*N*=4). **P* < 0.05, ***P* < 0.01, ****P* < 0.001 indicate significance when compared to control.

FIGURE 4

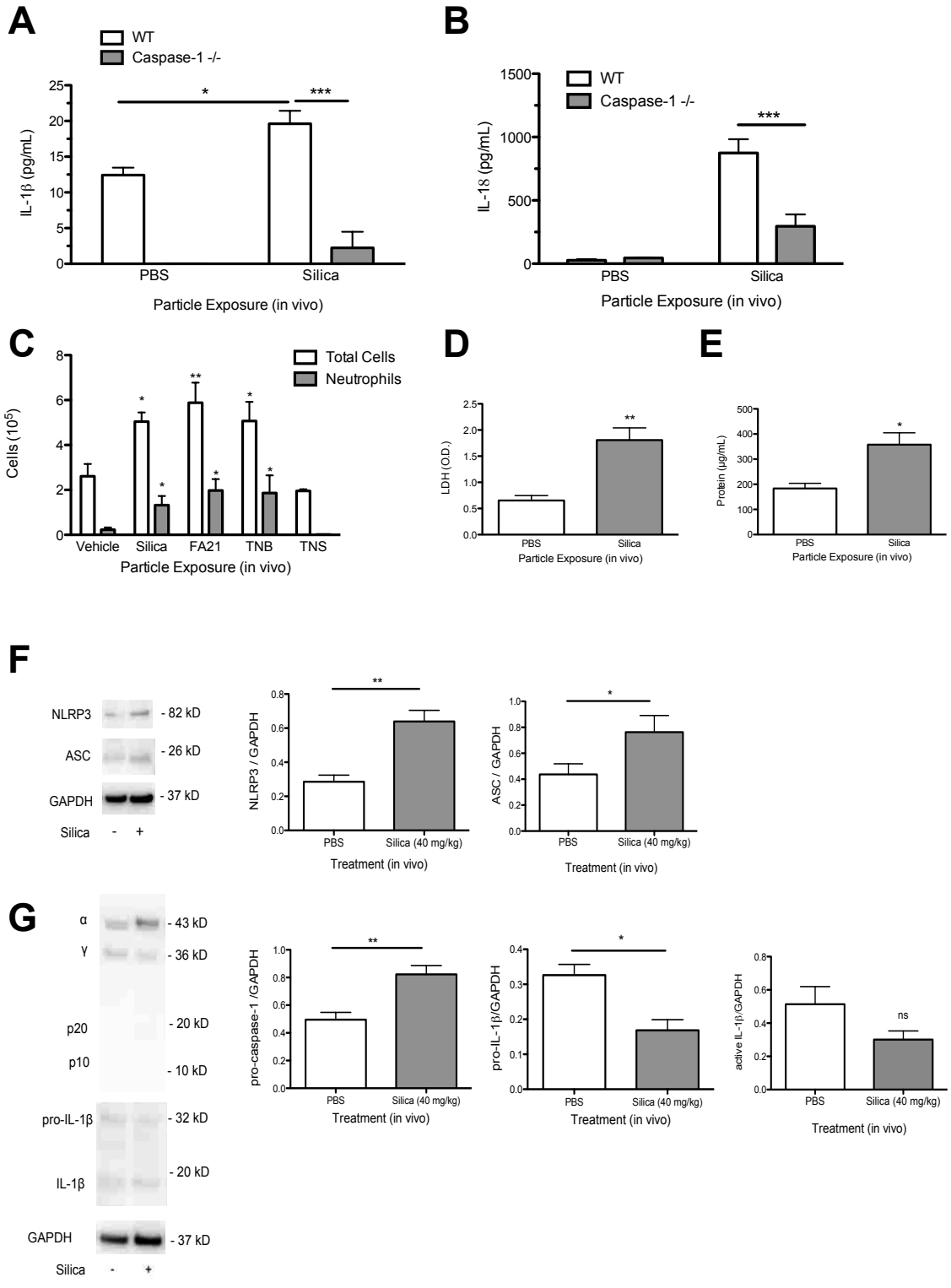
A
WT
Caspase-1 -/-
IL-1β (pg/mL)
PBS
Silica
Particle Exposure (in vivo)
B
IL-18 (pg/mL)
C
Total Cells
Neutrophils
Cells (10^5)
Vehicle
Silica
FA21
TNB
TNS
D
LDH (O.D.)
E
Protein (μg/mL)
F
NLRP3
ASC
GAPDH
- 82 kD
- 26 kD
- 37 kD
NLRP3 / GAPDH
ASC / GAPDH
Silica (40 mg/kg)
Treatment (in vivo)
G
α
γ
p20
p10
pro-IL-1β
IL-1β
- 43 kD
- 36 kD
- 20 kD
- 10 kD
- 32 kD
- 20 kD
- 37 kD
pro-caspase-1 /GAPDH
pro-IL-1β/GAPDH
active IL-1β/GAPDH
ns

**Figure 4.4.** *Bioactive particle exposure causes persistent NLRP3 inflammasome activity in vivo*. (A) IL-1β levels in the whole lavage fluid of C57Bl/6 and caspase-1 null mice 7 d following instillation of PBS or silica (40 mg/kg). (B) IL-18 levels in lung lavage fluid at 7 d. (C) Cell counts 7 d after silica and ENM (2 mg/kg) instillation. (D) LDH and (E) total protein levels in the lavage fluid of silica or PBS exposed C57Bl/6 mice at 7 d. (F) Intracellular NLRP3 and ASC protein levels in isolated AM from C57Bl/6 mice 7 d following silica exposure. (*G*) Intracellular caspase-1, pro-IL-1β, and cleaved IL-1β protein levels. Western Blots shown are representative of 3 separate experiments with lung lavage cells from 3 mice pooled for each lysate. All samples were derived at the same time and processed in parallel for western blot analysis. Data are presented as mean ± *SEM* (*N*= 3 to 4). **P* < 0.05, ***P* < 0.01, ****P* < 0.001.

FIGURE 5

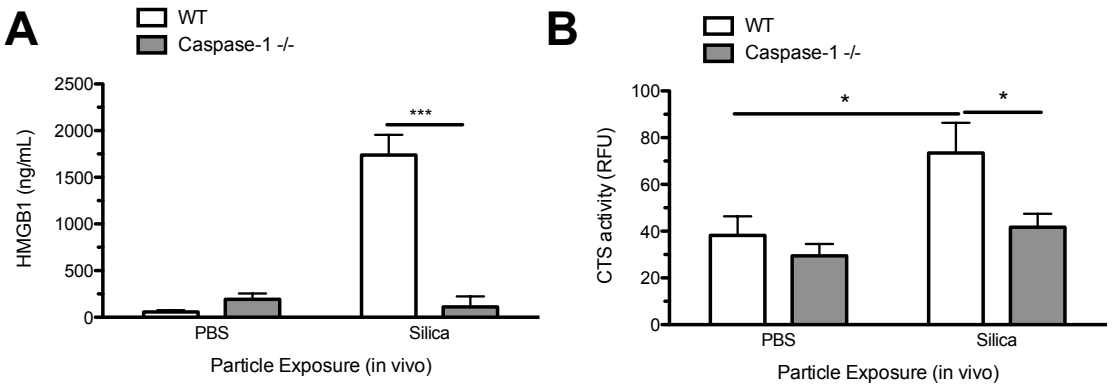


**Figure 3.5.** *Secretion of HMGB1 and cathepsins is dependent upon caspase-1 in vivo.* (A) HMGB1 levels in the lavage fluid of C57Bl/6 and caspase-1 null mice 7 d following exposure to silica (40 mg/kg). (B) Cathepsin (CTS) activity in the lavage fluid at 7 d. Data are presented as mean ± *SEM* (*N*=4). **P* < 0.05, ****P* < 0.001.

FIGURE 6

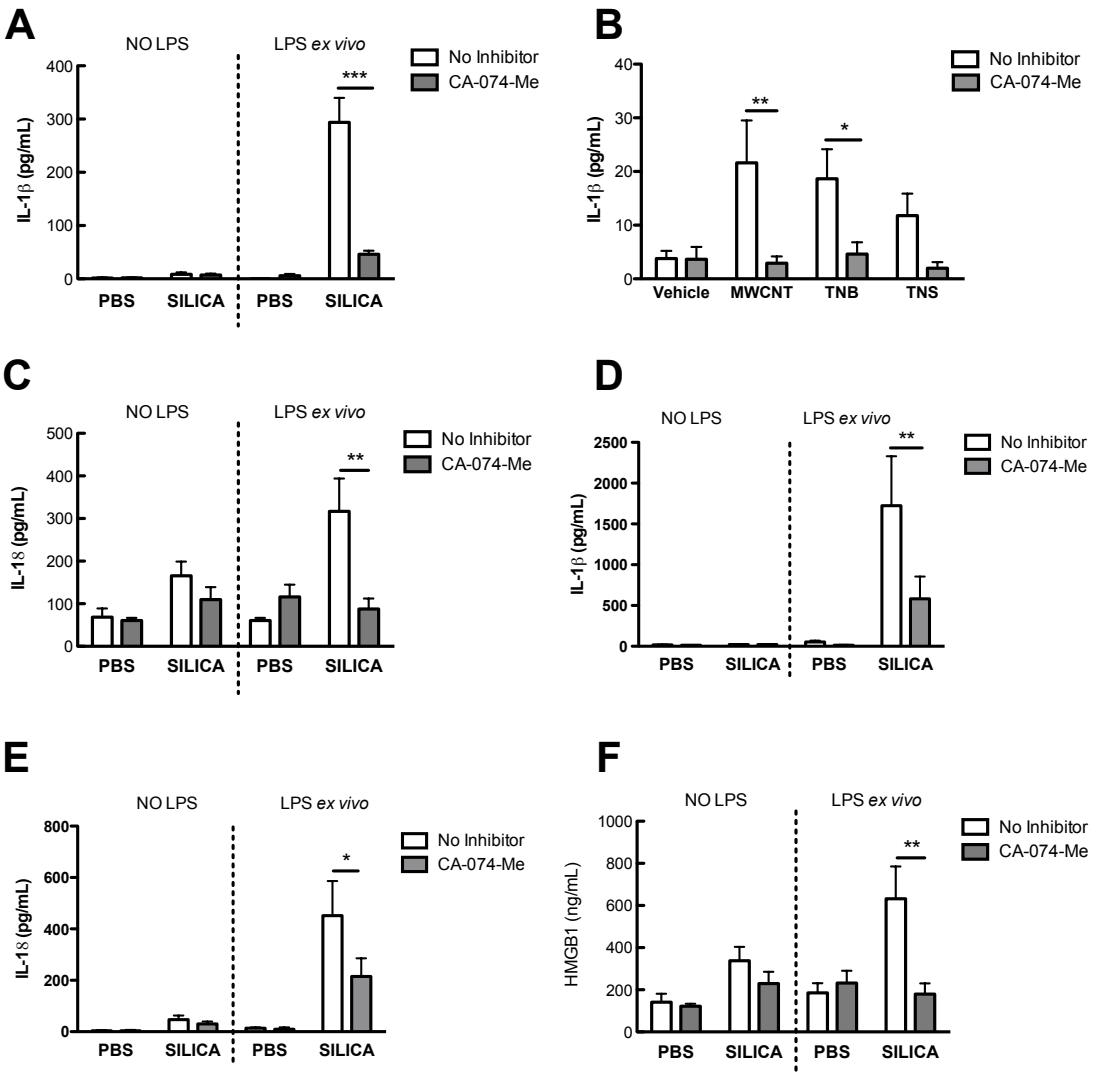


**Figure 3.6.** *Cathepsin B activity drives persistent NLRP3 inflammasome activity and HMGB1 release from AM ex vivo.* AM were isolated from C57BL/6 mice 7 d following silica (40 mg/kg), MWCNT, TNB, and/or TNS (2 mg/kg) exposure and cultured *ex vivo* with/without LPS (20 ng/mL) stimulation and CA-074-Me (10 μM). Cytokine levels were measured in cell supernatants after 24 hr of *ex vivo* culture. (A) IL-1β levels in supernatants of AM from silica or PBS exposed mice (7 d). (B) IL-1β levels in supernatants of AM from MWCNT, TNB, and TNS or vehicle exposed mice (7 d).

(C) IL-18 levels in supernatants of AM from silica or PBS exposed mice (7 d). (D) IL-1β levels in supernatants of AM from silica or PBS exposed mice (56 d). (E) IL-18 levels in supernatants of AM from silica or PBS exposed mice (56 d) (F) HMGB1 levels in supernatants of AM from silica or PBS exposed mice (7 d). Data are shown as mean ± SEM (N=4). *$P < 0.05$. **$P < 0.01$. ***$P < 0.001$.

FIGURE 7

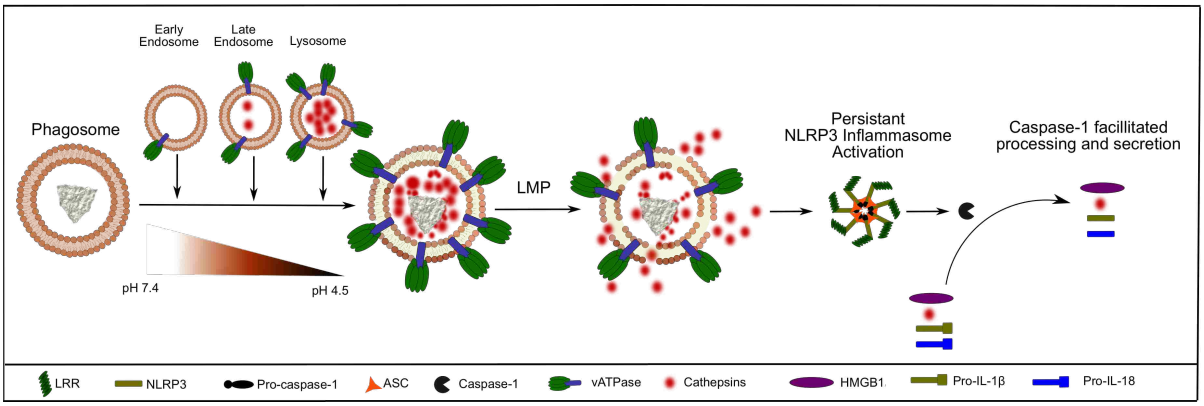


**Figure 3.7.** *Model of particle-induced LMP and resultant NLRP3 inflammasome activity.* Phagosomes containing the particle become more acidic as they move down the endocytic pathway and fuse with lysosomes. Phagolysosome acidification is necessary for particle-induced LMP. LMP results in the release of cathepsins into the cytosol, which in turn activate the NLRP3 inflammasome. NLRP3 inflammasome activity regulates the secretion of pyrogenic cytokines IL-1β and IL-18, as well as the alarmin HMGB1.

# CHAPTER 4: AUTOPHAGY DEFICIENCY IN MACROPHAGES ENHANCES NLRP3 INFLAMMASOME ACTIVITY AND CHRONIC LUNG DISEASE FOLLOWING SILICA EXPOSURE

## 4.0. Manuscript Information Page

**Authors:** Forrest C Jessop, Raymond F. Hamilton, Joseph F. Rhoderick, Pamela K Shaw and Andrij Holian

**Target Journal:** Journal of Immunology

Status of Manuscript:

___ Prepared for submission to a peer-reviewed journal

_X_ Officially submitted to a peer-review journal

___ Accepted by a peer-review journal

___ Published in a peer review journal

Published by American Association of Immunologists, Inc.

Submitted April, 2016

## 4.1. Autophagy deficiency in macrophages enhances NLRP3 inflammasome activity and chronic lung disease following silica exposure

Forrest C Jessop[1], Raymond F. Hamilton[1], Joseph F. Rhoderick [1], Pamela K Shaw[1] and Andrij Holian[1†]

[1]Center for Environmental Health Sciences, University of Montana, Missoula, Montana

[†]Corresponding author

Email Addresses:

FJ: forrest.jessop@umontana.edu

RFH: Raymond.Hamilton@umontana.edu

JFR: fred.rhoderick@umontana.edu

PKS: pamela.shaw@umontana.edu

AH: andrij.holian@umontana.edu

## 4.2. Abstract

Autophagy is an important metabolic mechanism that can promote cellular survival following injury. The specific contribution of autophagy to silica-induced inflammation and disease is not known. The objective of these studies was to determine the effects of silica exposure on the autophagic pathway in macrophages, as well as the general contribution of autophagy in macrophages to inflammation and disease. Silica exposure enhanced autophagic activity in vitro in Bone Marrow derived Macrophages and in vivo in Alveolar Macrophages isolated from silica-exposed mice. Impairment of autophagy in myeloid cells in vivo using $Atg5^{fl/fl}$LysM-$Cre^{+}$ mice resulted in enhanced cytotoxicity and inflammation after silica exposure compared to littermate controls, including elevated IL-18 and the alarmin HMGB1 in the whole lavage fluid. Autophagy deficiency caused some spontaneous inflammation and disease. Greater silica-induced acute inflammation in $Atg5^{fl/fl}$LysM-$Cre^{+}$ mice correlated with increased fibrosis and chronic lung disease. These studies demonstrate a critical role for autophagy in suppressing silica-induced cytotoxicity and inflammation in disease development. Furthermore, these data highlights the importance of basal autophagy in macrophages and other myeloid cells in maintaining lung homeostasis.

**Keywords:** Autophagy, NLRP3 Inflammasome, HMGB1, IL-1β, IL-18, Silica

### 4.3. Background

Autophagy is critical in maintaining cell homeostasis and is generally considered a pro-survival mechanism. While there are multiple types of autophagy, these studies focus primarily on macroautophagy, which has a fundamental responsibility of sequestering and degrading large macromolecular protein structures and damaged organelles [67]. In the autophagic process, cytosolic microtubule-associated protein 1A/1B-light chain 3 (LC3-I) is cleaved to the LC3-II isoform and incorporated into the forming autophagosome membrane. Atg5 is a critical protein required for autophagosome elongation and LC3 lipidation [132]. Macromolecular structures are targeted towards the autophagic pathway through hyper-ubiquitination and the autophagy specific chaperone SQSTM1 (p62) [69]. Targeted material and p62 is sequestered within autophagosomes, which fuse with lysosomes in order to degrade and recycle the target and carrier proteins. Autophagy is reported to be a primary mechanism for degradation of the AIM2 and NLRP3 inflammasomes [72]. Therefore, regulating autophagy could possibly have profound implications in macrophage responses to pro-inflammatory and cytotoxic environmental particles.

Recent reports highlight that silica exposure and the development of pneumoconiosis continues to be a significant health concern [133]. There are few studies investigating the contribution of autophagy to lung disease, let alone those caused by exposure to hazardous particulates such as silica. Failure of autophagy to degrade inflammasomes and clear bulk damaged organelles and protein aggregates are thought to contribute to the development of chronic lung disease. However, the state of autophagy appears to vary with different types of chronic lung diseases [134].

Autophagy is reported to be greatly enhanced in Chronic Obstructive Pulmonary Disease in epithelial cells, while autophagic flux is impaired in isolated alveolar macrophages following cigarette smoke exposure [135, 136]. On the other hand, autophagy is reportedly decreased in bleomycin-induced fibrosis *in vivo*, and in human Idiopathic Pulmonary Fibrosis and Cystic Fibrosis [137, 138]. The role and state of autophagy in silicosis has not been determined, but may differ from these other lung diseases due to alternative mechanisms of action.

Chronic NLRP3 inflammasome activity and cell death is reported to drive the development of pathology following silica exposure [107]. Previous studies have shown that innate immune function is sufficient for the development of fibrosis in a mouse model of silicosis, suggesting a critical role for macrophages in the chronic inflammatory response [12]. A primary mechanism by which silica induces NLRP3 inflammasome activation and cell death in macrophages is through permeablization of phagolysosomes [16]. The autophagic pathway also shares lysosomes as a common endpoint for degradation of sequestered material. However, the consequences of silica exposure on autophagic flux through the lysosome are not known.

In the current study, we investigated the contribution of autophagy in lung macrophages, in response to silica-induced inflammation and disease. For this study we used $Atg5^{fl/fl}$LysM-$Cre^{+}$ mice, which lack essential machinery necessary for the formation of autophagosomes in cells that express high levels of lysozyme, which include macrophages and other myeloid cell populations [139]. Therefore, we

expected that there would be greater inflammation and disease following silica exposure in mice in which autophagic activity has been impaired.

## 4.4. Material and Methods

### *4.4.1. Particle preparation*

Acid washed crystalline silica (Min-U-Sil-5; mean particle diameter 1.5-2 μm) was obtained from Pennsylvania Glass Sand Corp (Pittsburgh, PA, USA). Silica was determined to have insignificant levels of endotoxin (LPS) by the Limulus amoebocyte lysate assay (Cambrex, Walkersvill, MD, USA) as previously described [12, 140]. Prior to instillation into mice or addition to cell cultures, silica particles were suspended in PBS and sonicated for >1 min (550 watts @ 20 kHz) by a cup-horn sonicator in a circulating water bath (Misonix, Inc. Farmingdale, NY, USA).

### *4.4.2. Mice*

Transgenic GFP-LC3 mice, which express green fluorescent protein (GFP) fused to microtubule-associated protein 1A/1B-light chain 3 (LC3), were generously donated by Dr. Aruni Bhatnagar (University of Louisville, KY, USA) and have been previously described [141]. Homozygous $Atg5^{fl/fl}$ mice were obtained from the RIKEN BRC through the National Bio-Resource Project of the MEXT, Japan, courtesy of Dr. Noboru Mizushima [142]. LysM-$Cre^{+}$ mice were obtained from Jackson Laboratories. Crossing of homozygous $Atg5^{fl/fl}$ mice with LysM-$Cre^{+}$ to generate the $Atg5^{fl/fl}$LysM-$Cre^{+}$ mice was tracked and confirmed by PCR as previously described [142, 143]. Autophagy knockout in was confirmed by Western Blot in Bone Marrow derived

Macrophages (BMdM) from Atg5$^{fl/fl}$LysM-Cre$^{+}$ mice. Western Blot analysis included confirming deficiency in Atg5 (data not shown) and blocked lipidation of LC3-I to LC3-II. Both male and female C57Bl/6 (Jackson Laboratories, Bar Harbor, ME, USA), GFP-LC3 and Atg5$^{fl/fl}$LysM-Cre$^{+}$ mice were used in equal numbers for all studies. Mice were housed in micro-isolators in a specific pathogen-free facility under a 12:12-hr light-dark cycle. Food, bedding, and cages were sterilized by autoclaving. Mice were used between 8-16 wk of age. The University of Montana Institutional Animal Care and Use Committee (Missoula, MT, USA) approved all procedures performed on the animals.

*4.4.3. Bone Marrow derived Macrophages*

Bone Marrow derived Macrophages (BMdM) were generated as described previously [140]. Briefly, BMdM were obtained by flushing the femur and tibia following sacrifice of C57Bl/6, GFP-LC3, and Atg5$^{fl/fl}$LysM-Cre$^{+}$ and/or Littermate control mice. Bone marrow isolate was then cultured in T75 culture flasks with 20 mL of RPMI (10 % FCS) overnight for stromal cell elimination. Non-adherent cells were aspirated and seeded in a new T75 flask (15 x $10^6$ cells/flask) in 20 mL and 40 µL Macrophage Colony Stimulating Factor (M-CSF, 10 ng/mL stock, R&D Systems, Minneapolis, MN, USA) added to each flask. Cultures were maintained for 7-10 days with re-feeding every 3-4 days.

*4.4.4. In vitro studies*

BMdM from Atg5$^{fl/fl}$LysM-Cre$^{+}$ mice and littermate controls were plated at 1x10$^{5}$ cells/well in a 96 well plate and exposed to silica (100 µg/mL) and LPS (20 ng/mL) to prime the NLRP3 inflammasome. After 24 hr, cell supernatants were collected and assessed for markers of inflammation and cell death. For analysis of GFP-LC3 in BMdM, cells were plated in a 96 well culture dish with a glass bottom coverslip (MatTeck Corp. Ashland, MA, USA) at 1x10$^{5}$ cells/well. Macrophages were then exposed to silica (100 µg/mL) with or without Bafilomycin A1 (100 nM, EnzoLife Sciences, Farmingdale, NY, USA) to inhibit autophagic flux. BMdM were also treated with 3-methyladenine (3-MA, 5 µM, Sigma-Aldrich, Saint Louis, MO, USA) to inhibit autophagosome formation. After 24 hr, GFP-LC3 was assessed by laser scanning cytometry.

*4.4.5. In vivo studies*

Atg5$^{fl/fl}$LysM-Cre$^{+}$ mice and littermate control mice were instilled with silica at 40 mg/kg (~1 mg/mouse), which has previously been shown to induce sufficient acute inflammation *in vivo* [12, 140]. Mice were sacrificed 24 hr after silica exposure for analysis of the whole lung lavage fluid and cell differentials. Mice were lavaged by instilling, aspirating, and re-instilling 1 mL of cold PBS (3X) to concentrate lavage cytokines. An additional two more rounds of 1 mL PBS instillation/aspiration were performed to maximize cell retrieval. Isolated whole lung lavage cells were counted using a Coulter Z2 particle counter (Beckman Coulter, Brea, CA, USA). Cells were then stained for differential analysis using Wright's Geimsa and a Hematek 2000

autostainer (Miles-Bayer-Siemens Diagnostics, Deerfield, IL, USA). Macrophage area on differential slides was assessed via ImageJ Analysis Software. Using similar methods, whole lung lavage cells were isolated from C57Bl/6 or GFP-LC3 mice 7 d following silica exposure for analysis of autophagy by confocal microscopy or Western Blot. For chronic studies, $Atg5^{fl/fl}$LysM-$Cre^{+}$ mice and littermate control mice were instilled with silica (40 mg/kg) once a week for 4 consecutive weeks as described previously [12, 140]. Twenty eight days after the final instillation (day 56), the mice were sacrificed and their lungs inflated with 4% paraformaldehyde for histology. Fixed lungs were embedded in paraffin and sectioned (7 μm), and mounted on Superfrost+ VWR slides (VWR, Radnor, PA, USA). Sections were stained with Gomori's Trichrome (EMD Chemicals, Gibbstown, NJ, USA) or hematoxylin-eosin (RAS Harris Hematoxylin and Shandon Alcohol Eosin) using a Leica ST5010 Autostainer (Buffalo Grove, IL, USA).

*4.4.6. Laser Scanning Cytometry*

GFP-LC3 was assessed using a CompuCyte iCys Laser Scanning Cytometer (LSC; Westwood, MA, USA). Non-adherent BMdM were removed prior to analysis by gentle washing of each well once with PBS. GFP-LC3 positive cells were counter-stained with Molecular Probes HCS NuclearMask Blue (Life Technologies, Carlsbad, CA, USA) according to manufacture's instructions. GFP-LC3 was detected using a 488 nm laser as the excitation source and a PMT detector with a 530/30 nm bandpass filter. The nuclear staining was excited with a 405 nm laser and detected with a 440/30 nm bandpass filter/PMT set. The iCys was programmed to make 0.15

μm x-steps (setting pixel size/resolution) on an automated stage using a 60x inverted objective to interrogate a field size of 150 μm x 125.6 μm each step. Individual passes of the 488 nm and 405 nm lasers were used to avoid any spectral overlap of the "blue" and "green" fluorescent signals. A threshold of "blue" fluorescence was set such that the software draws a contour around the nucleus of the cell. The contour is then expanded by 25 pixels to include the cytoplasm of the cell. Each cell (as defined by nuclear staining) is plotted on a histogram showing green Median Fluorescent Intensity (MFI). Additionally, GFP puncta were counted per each cell using standard integrated filters and threshold within the CompuCyte software. Regions were defined within each well of the 96-well plate to include approximately 1500 cells to achieve sufficient sample representation. Isolated lung lavage cells from GFP-LC3 mice were seeded at 1 x $10^5$ cells/well in RPMI in an 4-well glass bottom dish (Greiner Bio-One, Monroe, NC, USA), counterstained with Molecular Probes HCS NuclearMask Blue (Life Technologies), and examined immediately using an Olympus FV 1000 IX inverted laser scanning confocal microscope.

*4.4.7. Cytokine and Cytotoxicity Assays*

BMdM cell supernatants and whole lung lavage fluid were assayed for LDH activity (Promega, Madison, WI, USA). Cytokines IL-1$\beta$, CXCL1, and IL-1$\alpha$ were measured by ELISA (R&D systems, Minneapolis, MN, USA). HMGB1 was assessed by an in-house ELISA as previously described [122]. IL-18 was also assessed by an in-house ELISA [6]. Extracellular cathepsin activity was assessed as previously described by our laboratory [123]. Briefly, 2 μg Z-LR-AMC (specific to cathepsin B, cathepsin L and

cathepsin V; R&D systems) in PBS was added to 50 µL of whole lung lavage fluid in a total reaction volume of 150 µL. The assays were incubated at 37°C for 1 h then fluorescence was measured using a plate reader at 380 nm excitation and 460 nm emission.

*4.4.8. Western Blot*

BMdM or cells isolated from lung lavage fluid were lysed directly in RIPA buffer containing HALT$^{TM}$ protease inhibitors (Life Technologies). For *in vivo* assessment of autophagic markers, whole lung lavage cells from 4 mice were pooled for each *N*. Lysates were run on 12-4% Bis-Tris SDS-PAGE gels. Anti-LC3, p62, ubiquitin, and GAPDH antibodies were obtained from Cell Signaling (Danvers, MA, USA). GAPDH was used as the loading control. Protein bands were quantified with Image J software (NIH, Bethesda, MD, USA).

*4.4.9. Microscopy and pathology scoring*

Gomori's Trichrome and H&E stained mouse lung tissue sections were imaged using a Zeiss Axioskop attached to a Zeiss digital camera. Two expert observers scored the lung disease using a 5-point scale (0, 1, 2, 3, and 4) with 0 being no effect and 4 being maximum lung pathology evident. The scorers were blinded to mouse treatments. Cronbach's-$\alpha$ was used to assess the reliability between the scorers. Inter-scorer reliability was significant at 0.86.

*4.4.10. Statistical analysis*

Statistical analyses involved comparison of means using a one- or two-way ANOVA followed by a Bonferroni's test or Holm- Šídák test to compensate for increased type I error. Unpaired *t* test was utilized for analysis of Western Blots or other data sets that included simple comparisons between two groups. Statistical power was > 0.8 to determine sample size. Statistical significance was defined as a probability of type I error occurring at < 5% ($P<0.05$). The minimum number of experimental replications was 3. Graphics and analyses were performed on PRISM 5.0.

## 4.5. Results

*4.5.1. Silica particle increases autophagy in macrophages*

Crystalline silica is reported to cause lysosome membrane permeabilization, which consequently leads to NLRP3 inflammasome activity and the activation of cell death pathways [16]. Silica's ability to compromise lysosomal integrity and cause intracellular damage likely has broad impacts on other cell pathways, including autophagy, however this relationship has not been investigated sufficiently. Therefore, to assess the effects of silica exposure on autophagy, we exposed BMdM from GFP-LC3 mice to silica and measured changes in GFP-LC3 expression and compartmentalization after 24 hr. BMdM were used for these studies due to their consistency in response with Alveolar Macrophages (AM) in prior studies by our laboratory [124]. In order to test silica's ability to increase autophagosome formation and/or block autophagic flux, Bafilomycin A1, an inhibitor of lysosomal vATPases, was added along with the particle [144]. 3-MA is an inhibitor of class III PI3-kinases

and prevents autophagosome formation [71], and was added to the BMdM cultures to further test silica's ability to induce autophagy. A dose of 100 μg/mL of silica was used for these studies based on prior reports by our laboratory in which this dose was shown to maximize inflammasome activity while minimizing cell death [127]. Silica exposure caused a marginal increase in median fluorescent intensity (MFI) of GFP-LC3 per cell and a significantly increased number of GFP-LC3 puncta/cell (Figure 1A, 1B, and 1C). 3-MA effectively blocked autophagy in silica-exposed BMdM, indicating silica exposure results in autophagic induction. As expected, Bafilomycin A1 treatment of control cells resulted in an accumulation of GFP-LC3. When Bafilomycin A1 was added to silica-exposed cells, there was an increase in GFP-LC3 when compared to Bafilomycin A1 only treated cells, which further supports the notion that silica exposure is increasing autophagosome formation but not necessarily blocking autophagic flux through the lysosome.

To further confirm that silica exposure was increasing autophagy rather than blocking autophagic flux, we assessed LC3-I and LC3-II, the autophagy associated ubiquitin-specific chaperone p62, and total ubiquitinated protein levels by Western Blot [144, 145]. Both intracellular p62 and total ubiquitinated protein levels were elevated in BMdM 24 hr following silica exposure (Figure 1D). Silica exposure increased LC3-II, consistent with increased autophagosome formation and with the observed increase in number of GFP-Puncta/Cell shown in Figure 1B. When silica-exposed cells were treated with Bafilomycin A1, we saw further increases in LC3-II, p62, and total ubiquitinated protein when compared to Bafilomycin A1-treated control. Together, these data further support the notion that silica exposure increases

induction of autophagy in macrophages, but does not necessarily result in impaired autophagic flux through the lysosome.

*4.5.2. Silica exposure enhances autophagy in AM in vivo*

To determine if silica exposure increases autophagy in AM *in vivo*, we instilled C57Bl/6 mice with crystalline silica and assessed autophagy markers in isolated lung lavage cells lysates after 7 d. Lung lavage cells at this time are primarily composed of AM with some neutrophil influx (Figure 2A). Isolated AM from silica-exposed mice exhibited increased LC3-I and LC3-II levels, indicating increased autophagy (Figure 2B). P62 levels were also significantly elevated (Figure 2B), as well as was total ubiquitinated protein (Data not shown). Isolated lung lavage cells from GFP-LC3 mice at 7 d had increased GFP-LC3 fluorescence and puncta (Figure 2C), further supporting our findings by Western Blot. Together, these data provide consistency in in the autophagic response to silica exposure between BMdM *in vitro* and AM *in vivo*.

*4.5.3. Autophagy deficiency in macrophages enhances cell death and HMGB1 release*

Autophagy has been reported to be a primary mechanism for the degradation of assembled inflammasomes, specifically AIM2 and NLRP3 [72]. Consequently, autophagy can potentially regulate the secretion of inflammasome-associated cytokines. The role of autophagy in regulating NRLP3 inflammasome activity following exposure to silica has not been previously described. Additionally, autophagy is generally regarded as a cell survival mechanism, and may act to

prevent silica-induced cytotoxicity. In order to test the role of autophagy in silica-induced NLRP3 inflammasome activity and cell death, we generated BMdM from $Atg5^{fl/fl}$LysM-$Cre^{+}$ mice, which are deficient in autophagosome formation. Though $Atg5^{fl/fl}$LysM-$Cre^{+}$ mice have been utilized by multiple other groups [146, 139, 11, 143], we confirmed BMdM generated from these mice exhibited impaired autophagy to establish reproducibility of the model. This included specifically determining Atg5 depletion (data not shown) and defective lipidation of LC3-I to LC3-II (Figure 3A). We then exposed BMdM generated from littermate control and $Atg5^{fl/fl}$LysM-$Cre^{+}$ mice to silica and LPS, which was added simultaneously with the particle in order to prime the NLRP3 inflammasome and cause cytokine production over 24 hr. Silica exposure did not significantly increase extracellular IL-1$\beta$ levels in BMdM cultures from $Atg5^{fl/fl}$LysM-$Cre^{+}$ mice when compared to littermate controls (Figure 3B). However, there was spontaneous (background) release of IL-1$\beta$ at low levels from non silica-exposed autophagy deficient BMdM. This suggested some basal level of NLRP3 inflammasome activity in macrophages in which autophagy is impaired. $Atg5^{fl/fl}$LysM-$Cre^{+}$ macrophages were more susceptible to cell death than littermate controls, as indicated by increased LDH in cell supernatants following silica exposure (Figure 3C). HMGB1 release has been associated with NLRP3 inflammasome activation and cell death with bacterial infection, and exposure to carbon nanotubes [122, 20]. We observed increased HMGB1 release from silica exposed $Atg5^{fl/fl}$LysM-$Cre^{+}$ BMdM compared to silica-exposed littermate controls (Figure 3D). We suspect HMGB1 release was due in part to more cell death. These data are consistent with the notion that autophagy functions to prevent silica-induced cytotoxicity, and supports the

proposal that autophagy deficiency results in some spontaneous NLRP3 inflammasome activity.

*4.5.4. Autophagy deficiency enhances silica-induced acute inflammation in vivo*

In order to determine if autophagy impairment in macrophages results in increased acute inflammation and cytotoxicity *in vivo*, we exposed $Atg5^{fl/fl}$LysM-$Cre^{+}$ mice to silica and assessed parameters of inflammation in the whole lung lavage fluid after 24 hr. Silica exposure resulted in significant increases in total protein, HMGB1, and IL-18 in the lavage fluid of $Atg5^{fl/fl}$LysM-$Cre^{+}$ mice compared to silica-exposed littermate controls (Figure 4A, 4B, 4C). IL-1β was not significantly increased in $Atg5^{fl/fl}$LysM-$Cre^{+}$ mouse lavage fluid compared to silica-exposed littermate controls, but was significantly increased over PBS-exposed animals (Figure 4D). We observed some spontaneous (background) IL-18 production in $Atg5^{fl/fl}$LysM-$Cre^{+}$ mice (Figure 4C). Consistent with our findings in BMdM exposed to silica *in vitro*, LDH levels were greater in the lavage fluid of $Atg5^{fl/fl}$LysM-$Cre^{+}$ mice compared to littermate controls (Figure 4E). Extracellular Cathepsin activity was also increased in autophagy deficient mice compared to littermate controls, though not significantly (Figure 4F). These data support the notion that depletion of autophagy in macrophages causes some basal NRLP3 inflammasome activity. Furthermore, the observation that inflammation and cytotoxicity (LDH) were exacerbated in $Atg5^{fl/fl}$LysM-$Cre^{+}$ mice demonstrates a fundamental role for autophagic suppression of silica-induced lung injury.

*4.5.5. Autophagy deficiency in macrophages causes a basal pro-inflammatory phenotype in vivo*

In our assessment of the acute inflammatory response following silica exposure, some findings suggested a basal phenotype when autophagy was impaired, including spontaneous IL-18 production (Figure 4C). We also observed increased cell numbers, mainly due to increased neutrophils in the $Atg5^{fl/fl}$LysM-$Cre^{+}$ mice (Figure 5A) suggesting background inflammation. Neutrophil influx in PBS-exposed $Atg^{fl/fl}$LysM-$Cre^{+}$ mice correlated with elevated CXCL1 in the lavage fluid (Figure 5B). Other investigators have reported similar observations, as well as elevated levels of IL-1$\alpha$ [139, 146]. However, we did not observe increased IL-1$\alpha$ in the whole lung lavage fluid of $Atg^{fl/fl}$LysM-$Cre^{+}$ mice, and there was no significant difference in IL-1$\alpha$ after silica exposure between autophagy deficient and littermate control mice (Figure 5C). This discrepancy could be due to differences in lung lavage fluid levels or more likely the interstitial/intracellular levels assayed with whole lung homogenization used in the other studies [139]. During differential analysis, we noticed that AM from $Atg5^{fl/fl}$LysM-$Cre^{+}$ mice were much larger than those observed in littermate controls (Figure 5D), which may indicate further differences in macrophage activity and phenotype. These data highlight the importance of macrophage-associated autophagy in maintaining homeostasis, and that knocking out autophagy in macrophages results in an unusual basal phenotype that may contribute to greater inflammation following particle exposure.

*4.5.6. Autophagy deficiency in macrophages increases silica-induced lung pathology*

Next, we examined whether autophagy deficiency in macrophages and other cells of myeloid origin results in greater chronic disease *in vivo* following silica exposure. $Atg5^{fl/fl}$LysM-$Cre^{+}$ mice and littermate controls were exposed to silica (40 mg/kg) once a week for 4 consecutive weeks, then we evaluated the mice at 56 d following the first instillation for pathology and fibrosis [12]. We observed no differences in weight between littermate controls and $Atg5^{fl/fl}$LysM-$Cre^{+}$ over the course of this study (data not shown). Autophagy deficient mice exposed to silica exhibited more significant pathology than littermate controls exposed to silica (Figure 6A). In parallel, we observed more pathology and fibrosis in the silica exposed $Atg5^{fl/fl}$LysM-$Cre^{+}$ mice as determined by Trichrome staining (Figure 6B). PBS exposed $Atg5^{fl/fl}$ LysM-$Cre^{+}$ mice had slightly elevated pathology score compared to littermate controls, consistent with the altered phenotype and elevated IL-18 levels at baseline as previously discussed. These studies demonstrate that autophagy in macrophages is important in mitigating silica-induced chronic disease.

### 4.6. Discussion

NLRP3 inflammasome activity in macrophages is a central driver of silica-induced chronic inflammation and lung disease [107], [12]. An inherent role for autophagy is to sequester and degrade inflammasomes and inflammasome cytokines such as pro-IL-1β [72, 147, 71]. Therefore, autophagic stimulation is being investigated as a potential therapeutic target for chronic inflammatory conditions. Ineffective autophagic suppression of NLRP3 inflammasome activity may, in part, be a mechanism contributing to chronic NLRP3 inflammasome activity with silica

exposure. We initially hypothesized that silica-induced NLRP3 inflammasome activity would be due, in part, to impaired autophagic flux through the lysosome. This has been reported to be the case for rare-earth nanomaterials [73]. There is some evidence of altered autophagic activity with silica exposure *in vivo*, including an accumulation of p62 within granulomas [148], though a very high dose of silica was used in those studies. Others reported that autophagy is impaired in isolated human lung AM from individuals with silicosis, including increased levels of LC3, p62, and Beclin-1 [131]. In the same study, autophagy alteration by silica was suggested to contribute to AM sensitization to LPS stimulation, though exactly how this occurs was not clear. Our data showing increased LC3-II, p62, and total ubiquitination *in vitro* and *vivo* are consistent with reports in human AM (Figure 1 and 2). We were also able to show that 3-MA effectively inhibited silica-induced autophagy (Figure 1), indicating that silica-exposure is causing autophagic induction. Secondly, through inhibiting lysosomal activity with Bafilomycin A1, we demonstrated further accumulation of autophagic carrier proteins (Figure 1), which supports the hypothesis that the primary outcome of silica exposure on the autophagic pathway is induction and not necessarily impaired autophagic flux. Silica exposure is known to induce lysosome membrane permeabilization (LMP), which can result NLRP3 inflammasome activation and cytotoxicity [16]. Increased autophagy following silica exposure may be a mechanism to mitigate the cytotoxic and pro-inflammatory outcomes of LMP.

Our studies are the first to utilize $Atg5^{fl/fl}$LysM-$Cre^{+}$ mice to test the contribution of autophagy in macrophages to silica-induced NLRP3 inflammasome activity and chronic disease. Others have utilized this mouse model to test the role of myeloid

cell-mediated autophagy in inflammation and disease burden with *Mycobacterium tuberculosis* [139]. In that report, inflammation and disease were significantly enhanced in Atg5$^{fl/fl}$LysM-Cre$^{+}$ mice compared to littermate controls. A second study by different investigators reported enhanced inflammation and disease with LPS and/or Bleomycin induced lung injury in Atg7$^{fl/fl}$LysM-Cre$^{+}$ mice, which are also defective in autophagosome formation [146]. Likewise, we observed significantly greater levels of pro-inflammatory mediators IL-18 and HMGB1 (Figure 5), increased extracellular LDH, and chronic disease (Figure 6) in Atg5$^{fl/fl}$LysM-Cre$^{+}$ mice with silica exposure. The studies strongly support an integral role for autophagy as an important mechanism in suppressing cell death with silica exposure as well as mitigating NLRP3 inflammasome activity.

Two additional important findings in this study include the observation that silica exposure increases IL-18 and HMGB1 (Figure 4), and release of these pro-inflammatory mediators is enhanced in autophagy deficient mice. HMGB1 is a nuclear architectural protein that is actively secreted from macrophages with active NLRP3 inflammasomes, and is passively released from dead or dying cells [19, 18, 11]. Extracellular HMGB1 acts as a Danger Associated Molecular Pattern, and can contribute to sterile priming of the NLRP3 inflammasome [100]. Exacerbated HMGB1 levels in the lavage fluid of silica-exposed Atg5$^{fl/fl}$LysM-Cre$^{+}$ mice are consistent with increased cell death (Figure 4). The observation that Atg5$^{fl/fl}$LysM-Cre$^{+}$ have increased neutrophil numbers at baseline (Figure 5), and high levels of HMGB1 after silica exposure could be due, in part, to more neutrophil cell death, though this was not investigated in these studies. The presence of high levels of both IL-18 and

HMGB1 in autophagy deficient mice, and greater chronic disease, indicate that these two inflammatory mediators could contribute more to particle-induced chronic lung disease than appreciated. IL-1R null mice exposed to Multi-walled Carbon Nanotubes (another particle that activates the NLRP3 inflammasome), while protected from excessive acute inflammation, develop more severe chronic disease [78]. These studies indicate that IL-1R signaling may not be as important in chronic disease, but rather other signals including IL-18 and/or HMGB1 could be more important contributors to chronic pathology. This notion is further supported by the fact that we observed spontaneous IL-18 release and some lung pathology in PBS-exposed autophagy deficient mice (Figure 4C, Figure 6B). Others have also reported increased neutrophils, IL-18, and spontaneous disease at baseline in $Atg7^{fl/fl}$LysM-$Cre^{+}$ mice [146]. IL-18 neutralizing antibodies but not Anakinra, the IL-1R antagonist, were effective at reducing spontaneous disease in $Atg7^{fl/fl}$LysM-$Cre^{+}$ mice [146]. This may likely be true for $Atg5^{fl/fl}$LysM-$Cre^{+}$ mice, though this was not determined. Finally, IL-18 and HMGB1 have been implicated in autoimmune disorders such as SLE, which has greater prevalence among individuals with silicosis [25, 24]. Further studies will be needed to elucidate the role of HMGB1 and IL-18 in silica-induced lung inflammation and its subsequent contribution to systemic disease.

An additional novel finding of this work is that the macrophages in $Atg5^{fl/fl}$LysM-$Cre^{+}$ mice were significantly larger than littermate controls. Defective autophagy has been reported to negatively impact lipid metabolism and cholesterol trafficking [149], and contribute to foam cell formation in atherosclerosis [150]. Foam cells have been observed in silicosis, and may contribute to the fibrotic response [151]. While the

mechanism responsible for larger AM was not investigated, future studies should include further characterization of AM populations from autophagy-deficient mice, including assessing the impacts of Atg5 depletion in macrophages on foam cell formation.

In conclusion, silica exposure increases autophagic activity in macrophages *in vitro* and *vivo*. Knocking out Atg5, which is required for autophagosome formation, causes enhanced acute inflammation (predominantly HMGB1 and IL-18 release), increased cell death, and exacerbated chronic disease (see Figure 7). Furthermore, Atg5 depletion causes spontaneous NLRP3 inflammasome activity and disease, with IL-18 being the predominant NLRP3 inflammasome cytokine being released. These studies show the importance of autophagy in macrophages to suppressing silica-induced inflammation and cytotoxicity that drive chronic disease, and maintaining lung homeostasis. The mechanisms described in these studies may also be critical for suppression of inflammation and disease following exposure to other NLRP3 inflammasome activating particles including asbestos, uric acid crystals, cholesterol crystals, and engineered nanoparticles, and supports future studies of the role of autophagy with exposure to these agents.

### 4.7. Other

4.*7.1. Acknowledgements:* The authors appreciate the technical support obtained through the CEHS Molecular Histology and Fluorescence Imaging, Inhalation and Pulmonary Physiology, and Fluorescence Cytometry Core facilities. We extend a special thanks to the technical staff of these cores including Britt Postma, Mary

Buford, and Lou Herritt. We also acknowledge Dr. Noboru Mizushima for developing and providing the $Atg5^{fl/fl}$ mice. Finally, we thank Dr. John Hoidal at University of Utah School of Medicine, for independently reviewing data presented in this study.

*4.7.2. Authors' Contributions:* FJ designed and carried out all of the studies in the manuscript. RFH assisted in statistical analysis and scoring lung pathology for the *in vivo* studies. JFR assisted in mouse genotyping to confirm $Atg5^{fl/fl}$ LysM-$Cre^{+}$ and littermate controls, as well as assisted in the BMdM studies. PKS assisted with GFP-LC3 imaging and quantification. AH assisted FJ in overall study design and coordination. FJ wrote the first draft of the manuscript. AH, RFH, PKS and JFR helped further draft the manuscript. All authors read/approved the final manuscript.

*4.7.3. Funding Sources:* This work was support by research grants from NIEHS (R01ES023209), Shared Instrument grant (S10RR026325-01), and Institutional Develoment (IDeA) Awards from NCRR (P20 RR017670), and NIGMS (P30 GM103338). Additionally, Forrest Jessop was supported in part by a PhRMA Foundation Individual Pre-doctoral Fellowship. The content of this manuscript is solely the responsibility of the authors and does not necessarily represent the views of the National Institute of Health or the PhRMA Foundation.

*4.7.4. Competing Interests:* The authors declare no competing interest.

## 4.8. Figures

FIGURE 1

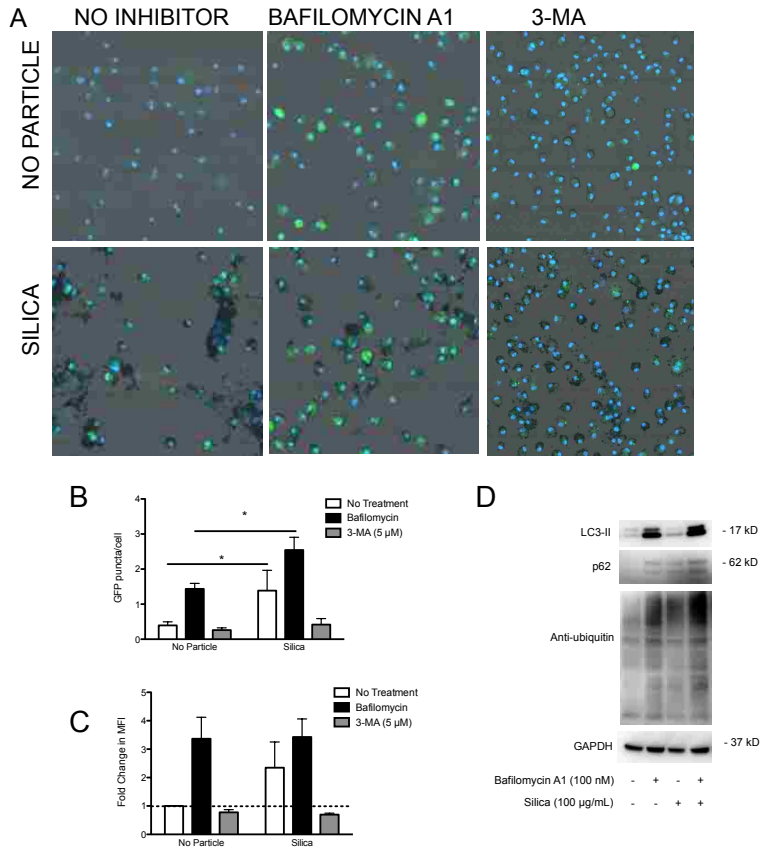


**Figure 4.1.** *Autophagy is increased in vitro in BMdM 24 hr following silica exposure.* (A) Representative images of GFP-LC3 expression in BMdM following exposure to silica (100 μg/mL) with or without Bafilomycin A1 treatment (100 μM) and 3-MA treatment (5 μM). Images were captured using a 60X scan (B) Average GFP-LC3 puncta per cell for combined experiments (*N*=3). (C) Median Fluorescent Intensity (MFI) of combined experiments (*N*= 3). (D) Representative western blot of three separate experiments showing LC3, p62, and total ubiquitination levels in BMdM exposed to silica with or without Bafilomycin A1 treatment (100 μM). Graphs show median ± SEM. **P* < 0.05 indicates significance with two-way ANOVA and a one-tailed post test.

FIGURE 2

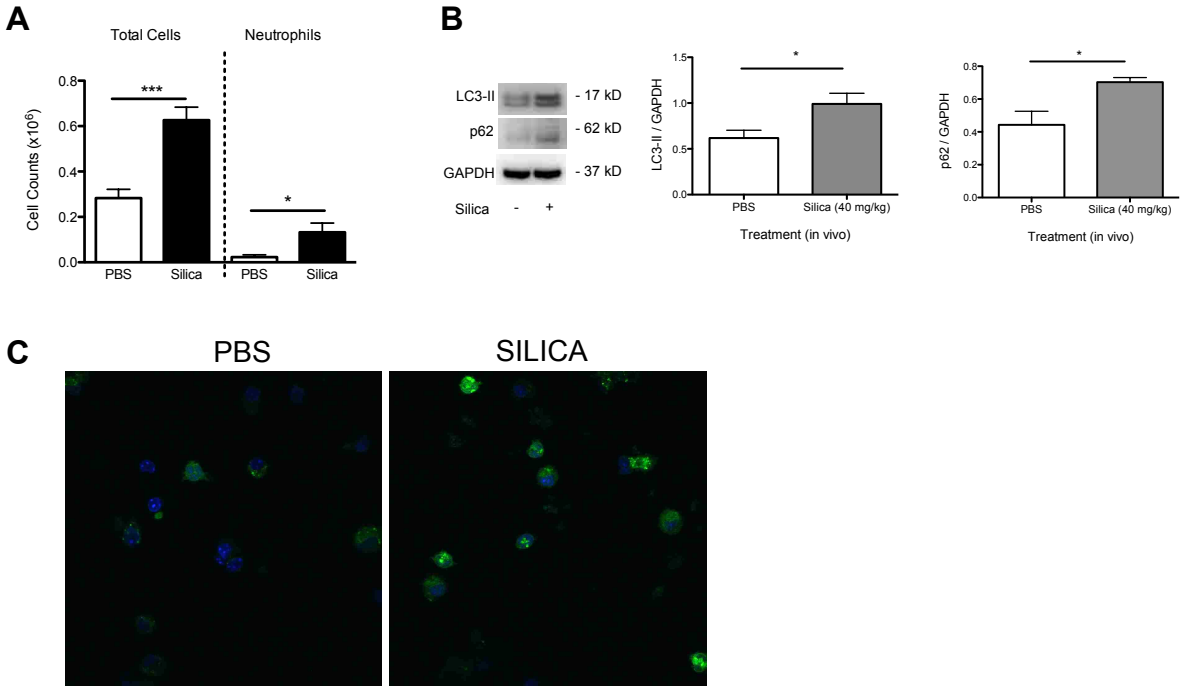


**Figure 4.2.** *Silica exposure increases autophagy in AM in vivo.* (A) Cell counts in the lung lavage fluid 7 d after silica exposure (40 mg/kg). (B) Representative Western Blot and densitometry graph of combined experiments showing LC3 and p62 levels in isolated AM 7 d following instillation of silica (40 mg/kg). (C) Representative images of AM isolated 7 d post silica exposure in GFP-LC3 mice (60X). *N*=4 for each treatment group. 2 mice were pooled for each *N* for sufficient protein for Western Blot analysis. Graphs show mean ± SEM. **P* < 0.05, ****P* < 0.001 indicates significance over PBS-exposed mice using a two-tailed t-test.

FIGURE 3

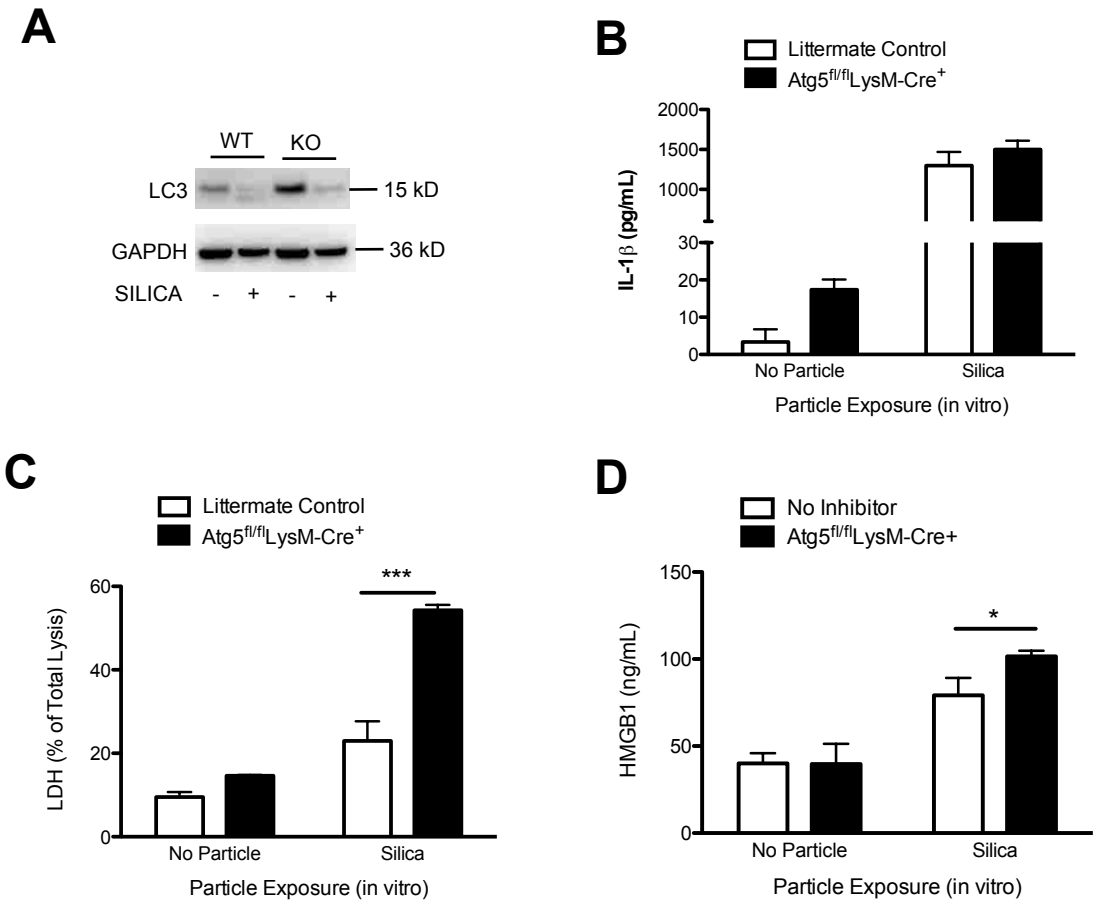


**Figure 4.3.** *Autophagy deficient BMdM are more susceptible to cell death and have enhanced HMGB1 release.* BMdM were exposed to silica (100 µg/mL) and LPS (20 ng/mL) and cell supernatants or lysates assessed after 24 hr. (A) Representative Western Blot showing defective autophagy in Atg5$^{fl/fl}$LysM-Cre$^{+}$ mouse BMdM, indicated by impaired LC3-I lipidation to LC3-II. (B) IL-1β levels in cell supernatants 24 hr after particle exposure. (C) Percent extracellular LDH activity in cell supernatants (compared to activity from total cell lysates). (D) Extracellular HMGB1 24 hr after particle exposure. Graphs show mean ± SEM (*N*=6 for each group). *$P$ < 0.05, ***$P$ < 0.001 indicate significance with 2-way ANOVA.

FIGURE 4

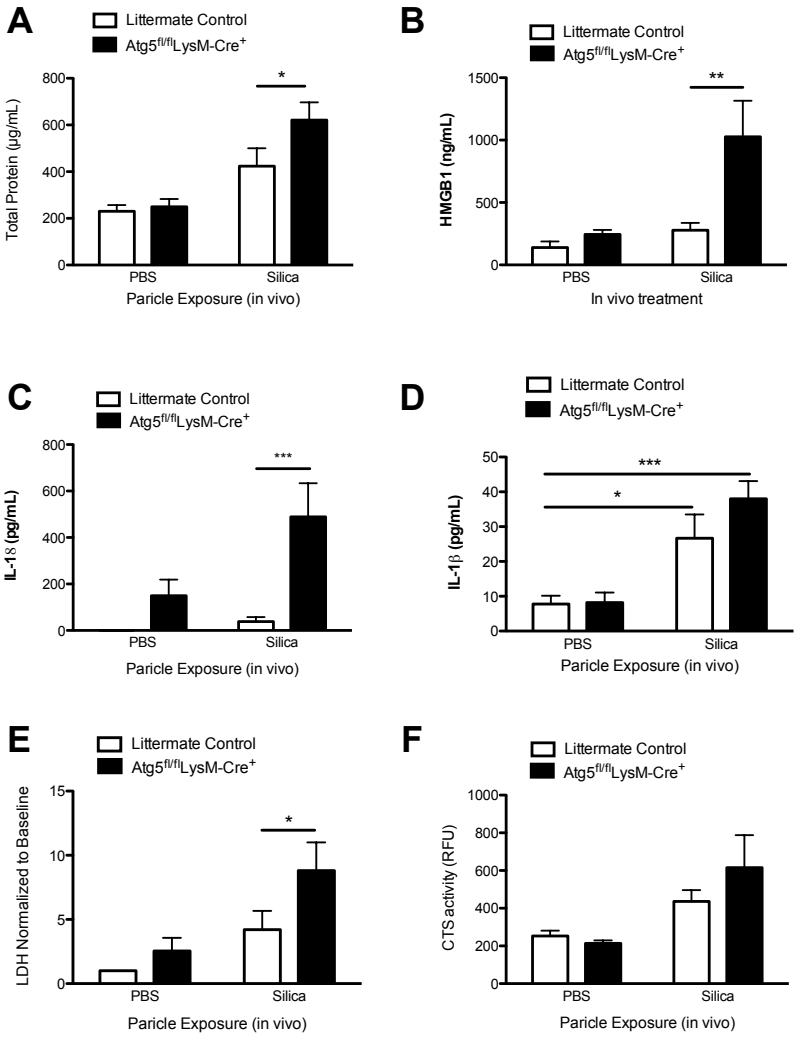


**Figure 4.4.** *Atg5 depletion in macrophages in vivo enhances acute inflammation.* Autophagy deficient and littermate control mice were instilled with 40 mg/kg silica or PBS and assessed for indicators of inflammation in the lavage fluid after 24 hr including: (A) Total protein, (B) HMGB1, (C) IL-18, (D) IL-1β, (E) LDH, and (F) cathepsin activity. Graphs show mean ± SEM (*N*=8 for all treatment groups). **P* < 0.05, ***P* < 0.01, ****P* < 0.001 compared to silica-exposed littermate control using a 2-way ANOVA.

FIGURE 5

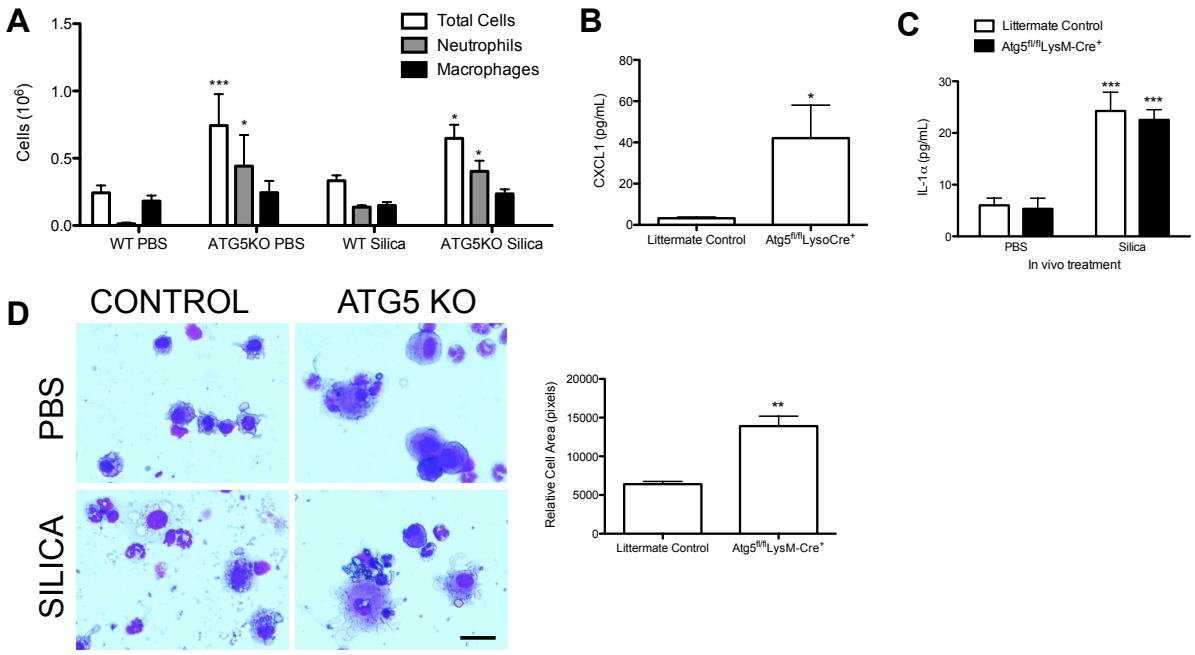


**Figure 4.5.** *Basal phenotype observed in Atg5$^{fl/fl}$LysM-Cre$^{+}$ mice.* Autophagy deficient and littermate control mice were instilled with 40 mg/kg silica or PBS and assessed sacrificed after 24 hr. (A) Total combined cell counts, and macrophage and neutrophil counts in the lavage fluid. (B) CXCL1 levels in the lavage fluid. (C) IL-1$\alpha$ levels in the lavage fluid. (D) Cytospins showing increased macrophage area on slide. Black Bar indicates 20 μm. Graphs show mean ± SEM (*N*=8 mice per treatment group). **P* < 0.05, ***P* < 0.01, ***P* < 0.001 when comparing to PBS-exposed littermate control.

FIGURE 6

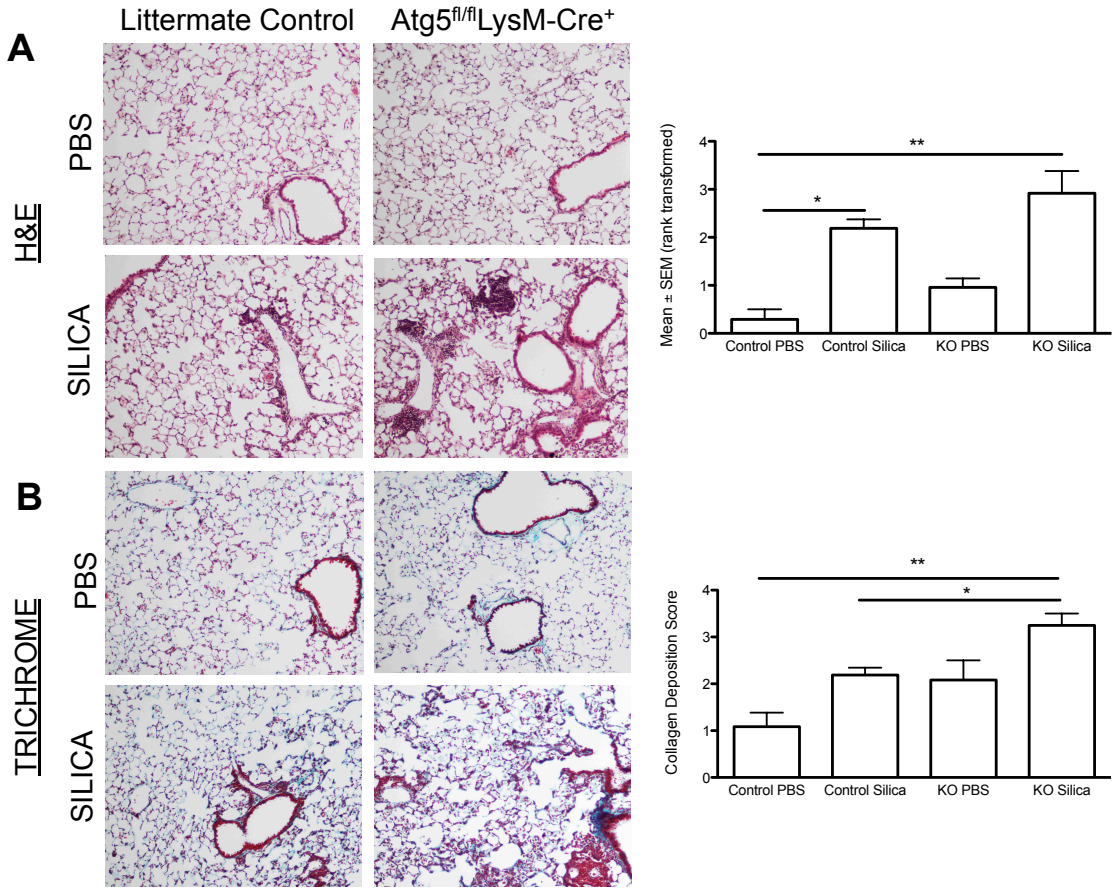


**Figure 4.6.** *Atg5 depletion in macrophages in vivo results in enhanced pathology and collagen deposition with silica exposure.* Mice were exposed to silica (40 mg/kg) once a week for 4 consecutive weeks, and then sacrificed 28 days following the final instillation (day 56). (A) H&E stained lung sections showing increased pathology. (B) Trichrome stained sections showing increased collagen and pathology. Images were captured at 20X magnification. Graphs show mean rank score ± SEM (*N*=3 for each treatment group) **P* < 0.05, ***P* < 0.01 indicates significance following rank transformation and post-hoc analysis using the Kruskal-Wallis test with Dunn's multiple-comparison post test.

FIGURE 7

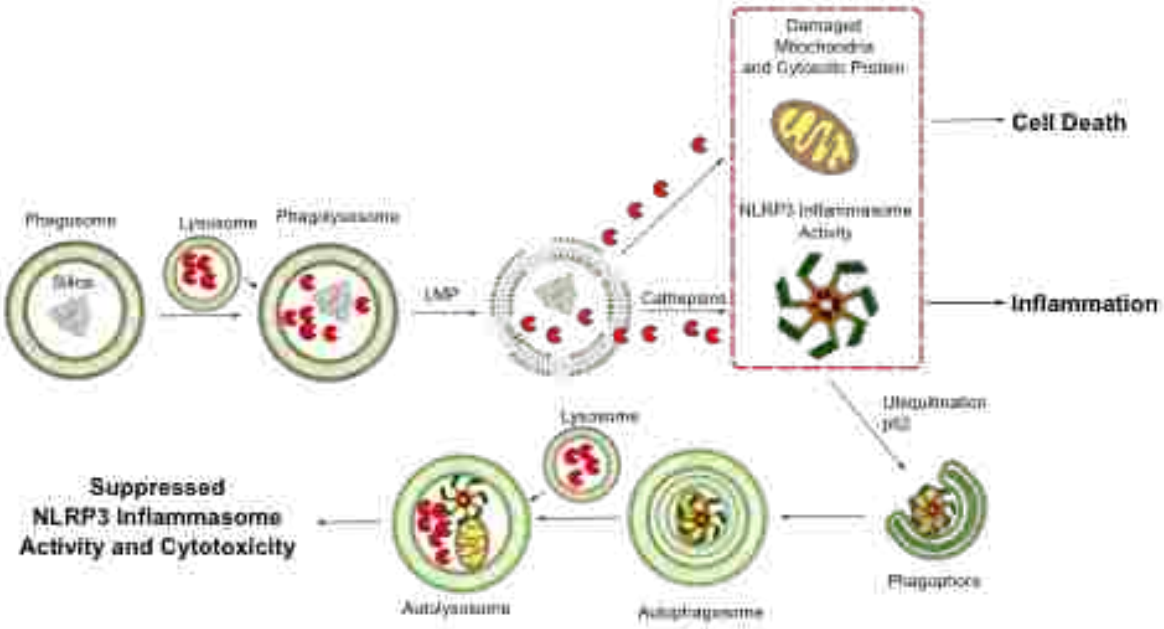


**Figure 4.7.** *Model of autophagy suppression of NLRP3-inflammasome associated inflammation and cytotoxicity*. Silica exposure causes phagolysosome membrane permeabilization resulting in the release of lysosomal contents into the cytosol including cathepsins. This results in both activation of the NLRP3 inflammasome and damage of cellular proteins and organelles, and leads to cytotoxicity. Mitochondrial damage, which results in ROS, is used as a representative example of downstream consequences of LMP. Autophagy is increased following silica exposure in order to suppress NLRP3-inflammasome activity and rescue cells from cytotoxicity, and thereby mitigate chronic inflammation and disease.

# 5.0. CHAPTER 5: UNIFYING THEORY

## 5.1. Overview

Chronic NLRP3 inflammasome activity is critical to the development of multiple ILD. The studies in this dissertation address specific gaps of knowledge related to NLRP3 inflammasome activation and persistence in macrophages in the lungs following bioactive particle exposure. Summaries of critical findings for each manuscript, limitations, and proposed future studies are discussed below. A unifying theory of the the mechanisms and consequences of lysosome membrane permeabilization based on the findings in these studies are summarized in the unifying model (Figure 5.1)

## 5.2. HMGB1 participates in NLRP3 inflammasome priming

The current two hit hypotheses for particle-induced NLRP3 inflammasome activity includes priming by an endogenous alarmin (signal 1), and NLRP3 inflammasome assembly (Signal 2) which results from LMP. Signal 1 had not hitherto been determined with particle exposures. We identify HMGB1 as participating in priming of the NLRP3 inflammasome with MWCNT exposure in Chapter 2. Central findings of Chapter 2 are summarized below:

- *HMGB1 is released from macrophages and epithelial cells following MWCNT exposure (Figure 1.1)*
- *HMGB1 secretion from macrophages is dependent on caspase-1 (Figure 1.1, Figure 3.5)*
- *Extracellular HMGB1 participates in priming of the NLRP3 inflammasome with MWCNT exposure (Figure 2.2, 2.3).*

*While this relationship was not assessed for other particle exposures, we predict a similar activity in other models of sterile injury.*

A Specific redox form of HMGB1 has been proposed to promote NF-κB activity [100, 22]. In these studies, a disulfide bride between cysteine residues C23 and C45 and a cysteine residue C106 are reported to be important for binding to TLR4. Our data suggest that the specific NF-κB activating redox HMGB1 isoform did not prime the NLRP3 inflammasome (Figure 2.2), suggesting other potential isoforms or HMGB1 complexes were responsible. Future studies should include identifying the HMGB1 isoform *in vivo* responsible for NLRP3 inflammasome priming. Necrosis and lysosome mediated cell death was observed following bioactive particle exposure, so it is very possible that HMGB1 is associated in immune complexes that may include nucleic acid. HMGB1/DNA immune complexes have been implicated in SLE, which has increased prevalence in individuals with chronic lung disease associated with particle exposure [25, 29, 3]. Therefore, future studies should include measuring HMGB1/DNA immune complexes in serum following particle exposure and in individuals with chronic lung diseases. The studies were performed at an acute time point (24 hr), which does not necessarily mean HMGB1 contributes to continuous priming of the NLRP3 inflammasome, driving chronic disease. However, HMGB1 was present in high levels in the lavage fluid 7 d after silica exposure, and was being secreted from macrophages at this time point (Figure 3.5, 3.6). Increased HMGB1 levels have also been observed 4 d following MWCNT exposure (data not shown). These data are consistent with HMGB1 driving persistent NLRP3 inflammasome

activity. Future studies should include administration of HMGB1 neutralizing antibodies or A-box (the truncated form that acts as a competitive receptor antagonist [152]) in order to test the role of HMGB1 in driving persistent NLRP3 inflammasome activity and the development of ILD.

### 5.3. LMP and Cathepsin B drive persistent NLRP3 inflammasome activity

Studies on the role of HMGB1 in priming the NLRP3 inflammasome revealed that secretion was dependent upon active caspase-1. The next logical step was to investigate whether HMGB1 secretion was dependent upon upstream activators of the NLRP3 inflammasome, including cathepsin B. We identified cathepsin B activity as the critical pathway driving persistent NLRP3 inflammasome activity and HMGB1 release with particle exposure. LMP results in cathepsin release into the cytosol, which can, in turn, drive persistent NLRP3 inflammasome activity. These studies suggest targeting cathepsin B and/or LMP may block both signal 1 and signal 2, and effectively reduce persistent NLRP3 inflammasome activity following particle exposure. Important findings from Chapter 3 are summarized below:

- *Particle-induced LMP is dependent upon Phagolysosome acidification (Figure 3.2, Figure 3.3)*
- *Silica exposure causes LMP in vivo (Figure 3.3.)*
- *Active Cathepsin B regulates active Cathepsin L (Figure 3.2, Figure 3.3)*

- *Cytosolic cathepsin B (following LMP) drives persistent NLRP3 inflammasome activity and HMGB1 secretion (Figure 3.6)*

The dependence of HMGB1 and cathepsin secretion on active caspase-1 supports the notion that the NRLP3 inflammasome regulates unconventional secretion. Others have reported this as well, and suggest autophagy is a platform by which NLRP3 inflammasome associated cytokines and HMGB1 are packaged [66, 11]. The Golgi Reassembly and Stacking Protein (GRASP) is reported to be associated with the unconventional secretosome [66]. Despite these reports, unconventional secretion mechanisms remain largely undetermined.

A second important finding presented in Chapter 3 includes the dependence of cathepsin L activation on active cathepsin B. These data have significant implications challenging the current hypothesis that cathepsin B or associated substrates could be directly responsible for binding NLRP3. Others have reported that NLRP3 inflammasome activation is not defective in cathepsin-B deficient macrophages, raising doubts on the specificity of cathepsin B following LMP. Multiple cathepsins may facilitate NLRP3 inflammasome activation with particle exposure [13, 153]. Our findings support this notion. Future studies should include determining the relative contribution of other lysosomal cathepsins to NLRP3 inflammasome activation following particle-induced LMP.

Finally, we hypothesize that targeting LMP and cathepsin B may be a viable approach to reducing both signal 1 and signal 2 following particle exposures. It is important to consider that while LMP is a common event driving particle-induced

LMP, other downstream factors likely contribute to the divergence of ILD. In order to target LMP more effectively, it will be necessary to understand how particles induce LMP. We show that phagolysosome acidification is necessary for particle-induced LMP. The protein corona has been implicating in decreasing particle bioactivity, possibly through buffering membrane interactions [113]. While these studies do not directly address how particles cause LMP, they provide significant support that the protein corona may be important in buffering particle-induced LMP. Further, our findings support that specific physiochemical characteristics of the particles define both their LMP and downstream NLRP3 inflammasome activating potential. With the adaptation of the LMP assay developed by Aits et al [60], these associations between particle physiochemical characteristics and LMP-inducing potential can now be more readily quantified. Future studies should include altering particle physiochemical characteristics (size, shape, charge, solubility, protein corona etc.) and measuring LMP using this assay.

### 5.4. Autophagy suppresses silica-induced inflammation and lung disease

Autophagy is reported to be a primary degradation pathway for NLRP3 and AIM inflammasomes [71, 147, 72]. Furthermore, autophagy may be protective during cellular injury. The contribution of autophagy in macrophages to particle-induced inflammation and disease had not hitherto been determined. We hypothesized that autophagy would be an important mechanism for suppressing silica-induced cytotoxicity and inflammation. Important findings of Chapter 4 are summarized below.

- *Silica exposure increases autophagy (Figure 4.1.,4.2.)*

- *Autophagy deficiency enhances cytotoxicity in macrophages in vitro (Figure 4.3.)*
- *Autophagy deficiency in macrophages enhances NLRP3 inflammasome activity (primarily IL-18), HMGB1 secretion, and cytotoxicity in vivo (Figure 4.4.)*
- *Knocking out autophagy in macrophages causes basal inflammation and altered macrophage phenotype (Figure 4.5.)*
- *Autophagy deficiency in macrophages results in chronic lung disease, which is further exacerbated with silica exposure (Figure 4.6)*

Findings from chapter 4 support our hypothesis that autophagy is a mechanism to suppress cellular injury and inflammation with silica exposure. An important observation was that in autophagy deficient mice, IL-18 was significantly increased as well as chronic pathology. Furthermore, HMGB1 release was greatly enhanced. This would suggest greater roles for IL-18 and HMGB1 in driving chronic lung disease than previously appreciated. Future studies should include assessing the dependence of chronic disease on IL-18 and HMGB1.

Enhanced autophagy via overexpression of Atg5 has been reported to provide an overall protective advantage in mice challenged with oxidative stress, and can increase their lifespan [154]. In addition to sequestering damaged cellular components the NLRP3 inflammasome, autophagy has been reported to facilitate recapture of permeabilized lysosomes following acute kidney injury [155]. Whether

this is true for macrophages in the lungs following silica and other ENM exposures has not been determined, but may be an additional mechanism of cellular survival. Enhancing autophagy as a possible therapeutic approach was not investigated in these studies, but should be included in future research.

### 5.5. Unifying Theory

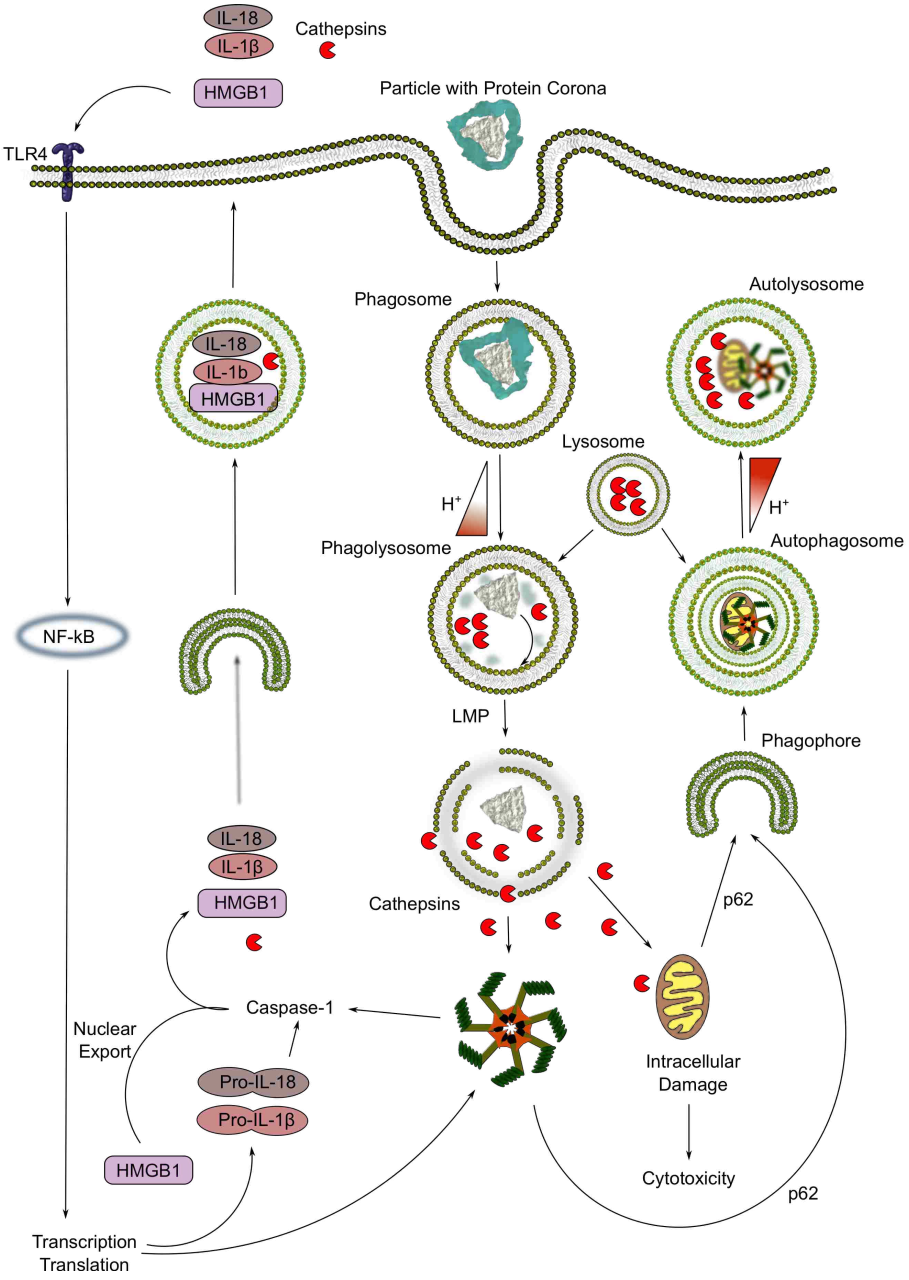

**Figure 5.1.** *Mechanisms and consequences of LMP following exposure to bioactive particles*. The model depicted illustrates common mechanisms contributing to persistent NLRP3 inflammasome activity following bioactive particle exposure in macrophages. Following inhalation, bioactive particles are phagocytosed by lung macrophages. The phagosome containing the particle matures in the endocytic pathway and fuses with lysosomes in order to degrade the particle. The low pH of the phagolysosome allows for removal of the protein/lipid corona surrounding the particle, which could lead to particle-membrane interactions. Inhibition of lysosomal vATPases with Bafilomycin A1 prevents LMP, highlighting the importance of acidification in licensing particles or other endogenous mechanisms to cause LMP. Following LMP, cathepsins translocate into the cytosol facilitating NLRP3 inflammasome activation and causing intracellular damage. NLRP3 inflammasome assembly and activation of caspase-1 mediates the unconventional secretion pathway for cytokines, HMGB1, and cathepsins. Once actively secreted or released from dying cells, extracellular HMGB1 can participate in priming of the NLRP3 inflammasome. Additionally, particle exposure causes cellular injury resulting in increased autophagic induction. Autophagy acts to suppress NLRP3 inflammasome activity and cytotoxicity, however in the face of LMP, autophagy may not function normally. Future research should include assessing the therapeutic merit of inhibiting LMP and/or HMGB1 release, or enhancing autophagy in the context of murine models of particle-induced ILD and models of ILD not associated with particle exposure.

## Acknowledgments

First and foremost, I would like to express my utmost gratitude and appreciation for my mentor, Dr. Andrij Holian, who has made all of this work possible. He has been the best mentor an undergraduate and graduate student could ask for. I would like to thank my dissertation committee members, Dr. Liz Putnam, Dr. Kevan Roberts, Dr. Christopher Migliaccio, and Dr. John Hoidal. I want to extend a special thanks to Dr. Christopher Migliaccio, who has been a friend and mentor from the very beginning. I also want to extend my utmost appreciation to Dr. John Hoidal, who took me in at the University of Utah and has supported me ever since in my research endeavors.

I want to thank the technical staff and admin of CEHS who are the bread and butter behind the research. I want to extend a special thanks to Britt Postma and Mary Buford for all the hours they helped me with mice over the years. Fred Rhoderick and Ray Hamilton have been an enormous support and resource as well. I want to thank Pam Shaw and Lou Herritt for helping with all things microscopic or flow-cytometry based. I offer my appreciation to Paulette Jones and Patrick Dye who have helped keep me in line, and been so supportive.

I want to thank my fellow graduate students, especially Kevan Trout, who I have often consulted. I offer a special thanks to Paige Fletcher who helped with some of this work.

Finally, I want to thank my wonderful wife who is my better half and could practically be getting a research doctorate herself at this point, and my wonderful children.

# REFERENCES

1. G. John Gibson RL, Yves Sibille, Bo Lundback. The European Lung White Book: Respiratory Health and Disease in Europe. United Kingdom: European Resipratory Society; 2013.

2. Gasse P, Riteau N, Charron S, Girre S, Fick L, Petrilli V et al. Uric acid is a danger signal activating NALP3 inflammasome in lung injury inflammation and fibrosis. Am J Respir Crit Care Med. 2009;179(10):903-13. doi:10.1164/rccm.200808-1274OC.

3. Leung CC, Yu IT, Chen W. Silicosis. Lancet. 2012;379(9830):2008-18. doi:10.1016/S0140-6736(12)60235-9.

4. Hamilton RF, Jr., Buford M, Xiang C, Wu N, Holian A. NLRP3 inflammasome activation in murine alveolar macrophages and related lung pathology is associated with MWCNT nickel contamination. Inhalation toxicology. 2012;24(14):995-1008. doi:10.3109/08958378.2012.745633.

5. Hamilton RF, Wu N, Porter D, Buford M, Wolfarth M, Holian A. Particle length-dependent titanium dioxide nanomaterials toxicity and bioactivity. Part Fibre Toxicol. 2009;6:35. doi:10.1186/1743-8977-6-35.

6. Hamilton RF, Wu N, Xiang C, Li M, Yang F, Wolfarth M et al. Synthesis, characterization, and bioactivity of carboxylic acid-functionalized titanium dioxide nanobelts. Part Fibre Toxicol. 2014;11:43. doi:10.1186/s12989-014-0043-7.

7. Hamilton RFJ, Wu Z, Mitra S, Shaw PK, Holian A. Effect of MWCNT size, carboxylation, and purification on in vitro and in vivo toxicity, inflammation and lung pathology. Part Fibre Toxicol. 2013;10(1743-8977 (Electronic)).

8. Hosseinian N, Cho Y, Lockey RF, Kolliputi N. The role of the NLRP3 inflammasome in pulmonary diseases. Ther Adv Respir Dis. 2015;9(4):188-97. doi:10.1177/1753465815586335.

9. Guo H, Callaway JB, Ting JP. Inflammasomes: mechanism of action, role in disease, and therapeutics. Nat Med. 2015;21(7):677-87. doi:10.1038/nm.3893.

10. Dinarello CA. A clinical perspective of IL-1beta as the gatekeeper of inflammation. Eur J Immunol. 2011;41(5):1203-17. doi:10.1002/eji.201141550.

11. Dupont N, Jiang S, Pilli M, Ornatowski W, Bhattacharya D, Deretic V. Autophagy-based unconventional secretory pathway for extracellular delivery of IL-1beta. The EMBO journal. 2011;30(23):4701-11. doi:10.1038/emboj.2011.398.

12. Beamer CA, Migliaccio CT, Jessop F, Trapkus M, Yuan D, Holian A. Innate immune processes are sufficient for driving silicosis in mice. Journal of leukocyte biology. 2010;88(3):547-57. doi:10.1189/jlb.0210108.

13. Duewell P, Kono H, Rayner KJ, Sirois CM, Vladimer G, Bauernfeind FG et al. NLRP3 inflammasomes are required for atherogenesis and activated by cholesterol crystals. Nature. 2010;464(7293):1357-61. doi:10.1038/nature08938.

14. Juliana C, Fernandes-Alnemri T, Kang S, Farias A, Qin F, Alnemri ES. Non-transcriptional priming and deubiquitination regulate NLRP3 inflammasome activation. J Biol Chem. 2012;287(43):36617-22. doi:10.1074/jbc.M112.407130.

15. Py BF, Kim MS, Vakifahmetoglu-Norberg H, Yuan J. Deubiquitination of NLRP3 by BRCC3 critically regulates inflammasome activity. Mol Cell. 2013;49(2):331-8. doi:10.1016/j.molcel.2012.11.009.

16. Hornung V, Bauernfeind F, Halle A, Samstad EO, Kono H, Rock KL et al. Silica crystals and aluminum salts activate the NALP3 inflammasome through phagosomal destabilization. Nature immunology. 2008;9(8):847-56. doi:10.1038/ni.1631.

17. Gardella S, Andrei C, Ferrera D, Lotti LV, Torrisi MR, Bianchi ME et al. The nuclear protein HMGB1 is secreted by monocytes via a non-classical, vesicle-mediated secretory pathway. EMBO Rep. 2002;3(10):995-1001. doi:10.1093/embo-reports/kvf198.

18. Lamkanfi M, Sarkar A, Vande Walle L, Vitari AC, Amer AO, Wewers MD et al. Inflammasome-dependent release of the alarmin HMGB1 in endotoxemia. J Immunol. 2010;185(7):4385-92. doi:10.4049/jimmunol.1000803.

19. Scaffidi P, Misteli T, Bianchi ME. Release of chromatin protein HMGB1 by necrotic cells triggers inflammation. Nature. 2002;418(6894):191-5. doi:10.1038/nature00858.

20. Willingham SB, Allen IC, Bergstralh DT, Brickey WJ, Huang MT, Taxman DJ et al. NLRP3 (NALP3, Cryopyrin) facilitates in vivo caspase-1 activation, necrosis, and HMGB1 release via inflammasome-dependent and -independent pathways. J Immunol. 2009;183(3):2008-15. doi:10.4049/jimmunol.0900138.

21. Tang D, Kang R, Livesey KM, Cheh CW, Farkas A, Loughran P et al. Endogenous HMGB1 regulates autophagy. J Cell Biol. 2010;190(5):881-92. doi:10.1083/jcb.200911078.

22. Yang H, Lundback P, Ottosson L, Erlandsson-Harris H, Venereau E, Bianchi ME et al. Redox modification of cysteine residues regulates the cytokine activity of high

mobility group box-1 (HMGB1). Mol Med. 2012;18(1):250-9. doi:10.2119/molmed.2011.00389.

23. Hamada N, Maeyama T, Kawaguchi T, Yoshimi M, Fukumoto J, Yamada M et al. The role of high mobility group box1 in pulmonary fibrosis. American journal of respiratory cell and molecular biology. 2008;39(4):440-7. doi:10.1165/rcmb.2007-0330OC.

24. Dinarello CA. Interleukin-18 and the pathogenesis of inflammatory diseases. Semin Nephrol. 2007;27(1):98-114. doi:10.1016/j.semnephrol.2006.09.013.

25. Lu M, Yu S, Xu W, Gao B, Xiong S. HMGB1 Promotes Systemic Lupus Erythematosus by Enhancing Macrophage Inflammatory Response. J Immunol Res. 2015;2015:946748. doi:10.1155/2015/946748.

26. Yang H, Hreggvidsdottir HS, Palmblad K, Wang H, Ochani M, Li J et al. A critical cysteine is required for HMGB1 binding to Toll-like receptor 4 and activation of macrophage cytokine release. Proceedings of the National Academy of Sciences of the United States of America. 2010;107(26):11942-7. doi:10.1073/pnas.1003893107.

27. Schmidt AM, Hori O, Chen JX, Li JF, Crandall J, Zhang J et al. Advanced glycation endproducts interacting with their endothelial receptor induce expression of vascular cell adhesion molecule-1 (VCAM-1) in cultured human endothelial cells and in mice. A potential mechanism for the accelerated vasculopathy of diabetes. J Clin Invest. 1995;96(3):1395-403. doi:10.1172/JCI118175.

28. Yang D, Chen Q, Yang H, Tracey KJ, Bustin M, Oppenheim JJ. High mobility group box-1 protein induces the migration and activation of human dendritic cells and

acts as an alarmin. Journal of leukocyte biology. 2007;81(1):59-66. doi:10.1189/jlb.0306180.

29. Tian J, Avalos AM, Mao SY, Chen B, Senthil K, Wu H et al. Toll-like receptor 9-dependent activation by DNA-containing immune complexes is mediated by HMGB1 and RAGE. Nature immunology. 2007;8(5):487-96. doi:10.1038/ni1457.

30. Yu M, Wang H, Ding A, Golenbock DT, Latz E, Czura CJ et al. HMGB1 signals through toll-like receptor (TLR) 4 and TLR2. Shock. 2006;26(2):174-9. doi:10.1097/01.shk.0000225404.51320.82.

31. Huang H, Evankovich J, Yan W, Nace G, Zhang L, Ross M et al. Endogenous histones function as alarmins in sterile inflammatory liver injury through Toll-like receptor 9 in mice. Hepatology. 2011;54(3):999-1008. doi:10.1002/hep.24501.

32. Rabolli V, Badissi AA, Devosse R, Uwambayinema F, Yakoub Y, Palmai-Pallag M et al. The alarmin IL-1alpha is a master cytokine in acute lung inflammation induced by silica micro- and nanoparticles. Part Fibre Toxicol. 2014;11(1):69. doi:10.1186/s12989-014-0069-x.

33. Jiang D, Liang J, Fan J, Yu S, Chen S, Luo Y et al. Regulation of lung injury and repair by Toll-like receptors and hyaluronan. Nat Med. 2005;11(11):1173-9. doi:10.1038/nm1315.

34. Scheibner KA, Lutz MA, Boodoo S, Fenton MJ, Powell JD, Horton MR. Hyaluronan fragments act as an endogenous danger signal by engaging TLR2. J Immunol. 2006;177(2):1272-81.

35. Lee GS, Subramanian N, Kim AI, Aksentijevich I, Goldbach-Mansky R, Sacks DB et al. The calcium-sensing receptor regulates the NLRP3 inflammasome through Ca2+ and cAMP. Nature. 2012;492(7427):123-7. doi:10.1038/nature11588.

36. Chen K, Zhang J, Zhang W, Zhang J, Yang J, Li K et al. ATP-P2X4 signaling mediates NLRP3 inflammasome activation: a novel pathway of diabetic nephropathy. Int J Biochem Cell Biol. 2013;45(5):932-43. doi:10.1016/j.biocel.2013.02.009.

37. Hofmann MA, Drury S, Fu C, Qu W, Taguchi A, Lu Y et al. RAGE mediates a novel proinflammatory axis: a central cell surface receptor for S100/calgranulin polypeptides. Cell. 1999;97(7):889-901.

38. Wittkowski H, Sturrock A, van Zoelen MA, Viemann D, van der Poll T, Hoidal JR et al. Neutrophil-derived S100A12 in acute lung injury and respiratory distress syndrome. Crit Care Med. 2007;35(5):1369-75. doi:10.1097/01.CCM.0000262386.32287.29.

39. Oka T, Hikoso S, Yamaguchi O, Taneike M, Takeda T, Tamai T et al. Mitochondrial DNA that escapes from autophagy causes inflammation and heart failure. Nature. 2012;485(7397):251-5. doi:10.1038/nature10992.

40. Suliman HB, Welty-Wolf KE, Carraway MS, Schwartz DA, Hollingsworth JW, Piantadosi CA. Toll-like receptor 4 mediates mitochondrial DNA damage and biogenic responses after heat-inactivated E. coli. FASEB journal : official publication of the Federation of American Societies for Experimental Biology. 2005;19(11):1531-3. doi:10.1096/fj.04-3500fje.

41. Deane R, Du Yan S, Submamaryan RK, LaRue B, Jovanovic S, Hogg E et al. RAGE mediates amyloid-beta peptide transport across the blood-brain barrier and accumulation in brain. Nat Med. 2003;9(7):907-13. doi:10.1038/nm890.

42. Halle A, Hornung V, Petzold GC, Stewart CR, Monks BG, Reinheckel T et al. The NALP3 inflammasome is involved in the innate immune response to amyloid-beta. Nature immunology. 2008;9(8):857-65. doi:10.1038/ni.1636.

43. Kumagai Y, Takeuchi O, Akira S. TLR9 as a key receptor for the recognition of DNA. Adv Drug Deliv Rev. 2008;60(7):795-804. doi:10.1016/j.addr.2007.12.004.

44. Alexopoulou L, Holt AC, Medzhitov R, Flavell RA. Recognition of double-stranded RNA and activation of NF-kappaB by Toll-like receptor 3. Nature. 2001;413(6857):732-8. doi:10.1038/35099560.

45. Beamer CA, Girtsman TA, Seaver BP, Finsaas KJ, Migliaccio CT, Perry VK et al. IL-33 mediates multi-walled carbon nanotube (MWCNT)-induced airway hyper-reactivity via the mobilization of innate helper cells in the lung. Nanotoxicology. 2013;7(6):1070-81. doi:10.3109/17435390.2012.702230.

46. Brennan TV, Lin L, Huang X, Cardona DM, Li Z, Dredge K et al. Heparan sulfate, an endogenous TLR4 agonist, promotes acute GVHD after allogeneic stem cell transplantation. Blood. 2012;120(14):2899-908. doi:10.1182/blood-2011-07-368720.

47. Boya P, Kroemer G. Lysosomal membrane permeabilization in cell death. Oncogene. 2008;27(50):6434-51. doi:10.1038/onc.2008.310.

48. Kurz T, Terman A, Gustafsson B, Brunk UT. Lysosomes in iron metabolism, ageing and apoptosis. Histochem Cell Biol. 2008;129(4):389-406. doi:10.1007/s00418-008-0394-y.

49. Kurz T, Terman A, Gustafsson B, Brunk UT. Lysosomes and oxidative stress in aging and apoptosis. Biochim Biophys Acta. 2008;1780(11):1291-303. doi:10.1016/j.bbagen.2008.01.009.

50. Persson HL, Kurz T, Eaton JW, Brunk UT. Radiation-induced cell death: importance of lysosomal destabilization. Biochem J. 2005;389(Pt 3):877-84. doi:10.1042/BJ20050271.

51. Wei X, Jiang W, Yu J, Ding L, Hu J, Jiang G. Effects of SiO2 nanoparticles on phospholipid membrane integrity and fluidity. J Hazard Mater. 2015;287:217-24. doi:10.1016/j.jhazmat.2015.01.063.

52. Pavan C, Rabolli V, Tomatis M, Fubini B, Lison D. Why does the hemolytic activity of silica predict its pro-inflammatory activity? Part Fibre Toxicol. 2014;11:76. doi:10.1186/s12989-014-0076-y.

53. Hamilton RF, Jr., Xiang C, Li M, Ka I, Yang F, Ma D et al. Purification and sidewall functionalization of multiwalled carbon nanotubes and resulting bioactivity in two macrophage models. Inhalation toxicology. 2013;25(4):199-210. doi:10.3109/08958378.2013.775197.

54. Taha TA, Kitatani K, Bielawski J, Cho W, Hannun YA, Obeid LM. Tumor necrosis factor induces the loss of sphingosine kinase-1 by a cathepsin B-dependent mechanism. J Biol Chem. 2005;280(17):17196-202. doi:10.1074/jbc.M413744200.

55. Werneburg NW, Guicciardi ME, Bronk SF, Gores GJ. Tumor necrosis factor-alpha-associated lysosomal permeabilization is cathepsin B dependent. Am J Physiol Gastrointest Liver Physiol. 2002;283(4):G947-56. doi:10.1152/ajpgi.00151.2002.

56. Fehrenbacher N, Bastholm L, Kirkegaard-Sorensen T, Rafn B, Bottzauw T, Nielsen C et al. Sensitization to the lysosomal cell death pathway by oncogene-induced down-regulation of lysosome-associated membrane proteins 1 and 2. Cancer Res. 2008;68(16):6623-33. doi:10.1158/0008-5472.CAN-08-0463.

57. Mora R, Dokic I, Kees T, Huber CM, Keitel D, Geibig R et al. Sphingolipid rheostat alterations related to transformation can be exploited for specific induction of lysosomal cell death in murine and human glioma. Glia. 2010;58(11):1364-83. doi:10.1002/glia.21013.

58. Yamashima T. Hsp70.1 and related lysosomal factors for necrotic neuronal death. J Neurochem. 2012;120(4):477-94. doi:10.1111/j.1471-4159.2011.07596.x.

59. Johansson AC, Appelqvist H, Nilsson C, Kagedal K, Roberg K, Ollinger K. Regulation of apoptosis-associated lysosomal membrane permeabilization. Apoptosis. 2010;15(5):527-40. doi:10.1007/s10495-009-0452-5.

60. Aits S, Jaattela M, Nylandsted J. Methods for the quantification of lysosomal membrane permeabilization: a hallmark of lysosomal cell death. Methods Cell Biol. 2015;126:261-85. doi:10.1016/bs.mcb.2014.10.032.

61. Appelqvist H, Waster P, Kagedal K, Ollinger K. The lysosome: from waste bag to potential therapeutic target. Journal of molecular cell biology. 2013;5(4):214-26. doi:10.1093/jmcb/mjt022.

62. Stern ST, Adiseshaiah PP, Crist RM. Autophagy and lysosomal dysfunction as emerging mechanisms of nanomaterial toxicity. Part Fibre Toxicol. 2012;9:20. doi:10.1186/1743-8977-9-20.

63. Wolters PJ, Chapman HA. Importance of lysosomal cysteine proteases in lung disease. Respir Res. 2000;1(3):170-7. doi:10.1186/rr29.

64. Ryter SW, Nakahira K, Haspel JA, Choi AM. Autophagy in pulmonary diseases. Annual review of physiology. 2012;74:377-401. doi:10.1146/annurev-physiol-020911-153348.

65. Boyle KB, Randow F. The role of 'eat-me' signals and autophagy cargo receptors in innate immunity. Current opinion in microbiology. 2013;16(3):339-48. doi:10.1016/j.mib.2013.03.010.

66. Deretic V, Jiang S, Dupont N. Autophagy intersections with conventional and unconventional secretion in tissue development, remodeling and inflammation. Trends Cell Biol. 2012;22(8):397-406. doi:10.1016/j.tcb.2012.04.008.

67. Wirawan E, Vanden Berghe T, Lippens S, Agostinis P, Vandenabeele P. Autophagy: for better or for worse. Cell research. 2012;22(1):43-61. doi:10.1038/cr.2011.152.

68. Alers S, Loffler AS, Wesselborg S, Stork B. Role of AMPK-mTOR-Ulk1/2 in the regulation of autophagy: cross talk, shortcuts, and feedbacks. Mol Cell Biol. 2012;32(1):2-11. doi:10.1128/MCB.06159-11.

69. Pankiv S, Clausen TH, Lamark T, Brech A, Bruun JA, Outzen H et al. p62/SQSTM1 binds directly to Atg8/LC3 to facilitate degradation of ubiquitinated protein aggregates by autophagy. J Biol Chem. 2007;282(33):24131-45. doi:10.1074/jbc.M702824200.

70. Eskelinen EL, Reggiori F, Baba M, Kovacs AL, Seglen PO. Seeing is believing: the impact of electron microscopy on autophagy research. Autophagy. 2011;7(9):935-56.

71. Harris J, Hartman M, Roche C, Zeng SG, O'Shea A, Sharp FA et al. Autophagy controls IL-1beta secretion by targeting pro-IL-1beta for degradation. J Biol Chem. 2011;286(11):9587-97. doi:10.1074/jbc.M110.202911.

72. Shi CS, Shenderov K, Huang NN, Kabat J, Abu-Asab M, Fitzgerald KA et al. Activation of autophagy by inflammatory signals limits IL-1beta production by targeting ubiquitinated inflammasomes for destruction. Nature immunology. 2012;13(3):255-63. doi:10.1038/ni.2215.

73. Li R, Ji Z, Qin H, Kang X, Sun B, Wang M et al. Interference in autophagosome fusion by rare earth nanoparticles disrupts autophagic flux and regulation of an interleukin-1beta producing inflammasome. ACS nano. 2014;8(10):10280-92. doi:10.1021/nn505002w.

74. Hamilton RF, Buford MC, Wood MB, Arnone B, Morandi M, Holian A. Engineered carbon nanoparticles alter macrophage immune function and initiate airway hyper-responsiveness in the BALB/c mouse model. Nanotoxicology. 2007;1(2):104-17. doi:Doi 10.1080/17435390600926939.

75. Mercer RR, Hubbs AF, Scabilloni JF, Wang L, Battelli LA, Friend S et al. Pulmonary fibrotic response to aspiration of multi-walled carbon nanotubes. Particle and fibre toxicology. 2011;8:21. doi:10.1186/1743-8977-8-21.

76. Mercer RR, Scabilloni JF, Hubbs AF, Battelli LA, McKinney W, Friend S et al. Distribution and fibrotic response following inhalation exposure to multi-walled carbon

nanotubes. Particle and fibre toxicology. 2013;10(1):33. doi:10.1186/1743-8977-10-33.

77. Glista-Baker EE, Taylor AJ, Sayers BC, Thompson EA, Bonner JC. Nickel Nanoparticles cause exaggerated lung and airway remodeling in mice lacking the T-box transcription factor, TBX21 (T-bet). Particle and fibre toxicology. 2014;11(1):7. doi:10.1186/1743-8977-11-7.

78. Girtsman TA, Beamer CA, Wu N, Buford M, Holian A. IL-1R signalling is critical for regulation of multi-walled carbon nanotubes-induced acute lung inflammation in C57Bl/6 mice. Nanotoxicology. 2012. doi:10.3109/17435390.2012.744110.

79. Palomaki J, Valimaki E, Sund J, Vippola M, Clausen PA, Jensen KA et al. Long, needle-like carbon nanotubes and asbestos activate the NLRP3 inflammasome through a similar mechanism. ACS nano. 2011;5(9):6861-70. doi:10.1021/nn200595c.

80. Martinon F, Burns K, Tschopp J. The inflammasome: a molecular platform triggering activation of inflammatory caspases and processing of proIL-beta. Molecular cell. 2002;10(2):417-26.

81. Ghonime MG, Shamaa OR, Das S, Eldomany RA, Fernandes-Alnemri T, Alnemri ES et al. Inflammasome Priming by Lipopolysaccharide Is Dependent upon ERK Signaling and Proteasome Function. J Immunol. 2014. doi:10.4049/jimmunol.1301974.

82. Pisetsky DS. The Expression of HMGB1 on Microparticles Released During Cell Activation and Cell Death in vitro and in vivo. Mol Med. 2014. doi:10.2119/molmed.2014.00014.

83. Stros M. HMGB proteins: interactions with DNA and chromatin. Biochim Biophys Acta. 2010;1799(1-2):101-13. doi:10.1016/j.bbagrm.2009.09.008.

84. Yang H, Rivera Z, Jube S, Nasu M, Bertino P, Goparaju C et al. Programmed necrosis induced by asbestos in human mesothelial cells causes high-mobility group box 1 protein release and resultant inflammation. Proceedings of the National Academy of Sciences of the United States of America. 2010;107(28):12611-6. doi:10.1073/pnas.1006542107.

85. Willingham SB, Allen IC, Bergstralh DT, Brickey WJ, Huang MT, Taxman DJ et al. NLRP3 (NALP3, Cryopyrin) facilitates in vivo caspase-1 activation, necrosis, and HMGB1 release via inflammasome-dependent and -independent pathways. J Immunol. 2009;183(3):2008-15. doi:10.4049/jimmunol.0900138.

86. Park JS, Gamboni-Robertson F, He Q, Svetkauskaite D, Kim JY, Strassheim D et al. High mobility group box 1 protein interacts with multiple Toll-like receptors. Am J Physiol Cell Physiol. 2006;290(3):C917-24. doi:10.1152/ajpcell.00401.2005.

87. Ullah MA, Loh Z, Gan WJ, Zhang V, Yang H, Li JH et al. Receptor for advanced glycation end products and its ligand high-mobility group box-1 mediate allergic airway sensitization and airway inflammation. J Allergy Clin Immunol. 2014. doi:10.1016/j.jaci.2013.12.1035.

88. Wang H, Bloom O, Zhang M, Vishnubhakat JM, Ombrellino M, Che J et al. HMG-1 as a late mediator of endotoxin lethality in mice. Science. 1999;285(5425):248-51.

89. Wang H, Yang H, Tracey KJ. Extracellular role of HMGB1 in inflammation and sepsis. Journal of internal medicine. 2004;255(3):320-31.

90. Ueno H, Matsuda T, Hashimoto S, Amaya F, Kitamura Y, Tanaka M et al. Contributions of high mobility group box protein in experimental and clinical acute lung injury. American journal of respiratory and critical care medicine. 2004;170(12):1310-6. doi:10.1164/rccm.200402-188OC.

91. Kim JY, Park JS, Strassheim D, Douglas I, Diaz del Valle F, Asehnoune K et al. HMGB1 contributes to the development of acute lung injury after hemorrhage. American journal of physiology Lung cellular and molecular physiology. 2005;288(5):L958-65. doi:10.1152/ajplung.00359.2004.

92. van Zoelen MA, Ishizaka A, Wolthuls EK, Choi G, van der Poll T, Schultz MJ. Pulmonary levels of high-mobility group box 1 during mechanical ventilation and ventilator-associated pneumonia. Shock. 2008;29(4):441-5. doi:10.1097/SHK.0b013e318157eddd.

93. Porter D, Sriram K, Wolfarth M, Jefferson A, Schwegler-Berry D, Andrew M et al. A biocompatible medium for nanoparticle dispersion. Nanotoxicology. 2008;2(3):144-54. doi:Doi 10.1080/17435390802318349.

94. Lacher SE, Johnson C, Jessop F, Holian A, Migliaccio CT. Murine pulmonary inflammation model: a comparative study of anesthesia and instillation methods. Inhalation toxicology. 2010;22(1):77-83. doi:10.3109/08958370902929969.

95. Dave SH, Tilstra JS, Matsuoka K, Li F, DeMarco RA, Beer-Stolz D et al. Ethyl pyruvate decreases HMGB1 release and ameliorates murine colitis. J Leukoc Biol. 2009;86(3):633-43. doi:10.1189/jlb.1008662.

96. Liou TG, Adler FR, Keogh RH, Li Y, Jensen JL, Walsh W et al. Sputum biomarkers and the prediction of clinical outcomes in patients with cystic fibrosis. PloS one. 2012;7(8):e42748. doi:10.1371/journal.pone.0042748.

97. Cesta MF, Ryman-Rasmussen JP, Wallace DG, Masinde T, Hurlburt G, Taylor AJ et al. Bacterial lipopolysaccharide enhances PDGF signaling and pulmonary fibrosis in rats exposed to carbon nanotubes. Am J Respir Cell Mol Biol. 2010;43(2):142-51. doi:10.1165/rcmb.2009-0113OC.

98. Schwartz DA. Inhaled endotoxin, a risk for airway disease in some people. Respir Physiol. 2001;128(1):47-55.

99. Chen GY, Nunez G. Sterile inflammation: sensing and reacting to damage. Nat Rev Immunol. 2010;10(12):826-37. doi:10.1038/nri2873.

100. Venereau E, Casalgrandi M, Schiraldi M, Antoine DJ, Cattaneo A, De Marchis F et al. Mutually exclusive redox forms of HMGB1 promote cell recruitment or proinflammatory cytokine release. J Exp Med. 2012;209(9):1519-28. doi:10.1084/jem.20120189.

101. Hreggvidsdottir HS, Ostberg T, Wahamaa H, Schierbeck H, Aveberger AC, Klevenvall L et al. The alarmin HMGB1 acts in synergy with endogenous and exogenous danger signals to promote inflammation. J Leukoc Biol. 2009;86(3):655-62. doi:10.1189/jlb.0908548.

102. Sha Y, Zmijewski J, Xu Z, Abraham E. HMGB1 develops enhanced proinflammatory activity by binding to cytokines. J Immunol. 2008;180(4):2531-7.

103. Leblanc PM, Doggett TA, Choi J, Hancock MA, Durocher Y, Frank F et al. An Immunogenic Peptide in the A-box of HMGB1 Protein Reverses Apoptosis-induced

Tolerance through RAGE Receptor. J Biol Chem. 2014;289(11):7777-86. doi:10.1074/jbc.M113.541474.

104. Dupont N, Jiang S, Pilli M, Ornatowski W, Bhattacharya D, Deretic V. Autophagy-based unconventional secretory pathway for extracellular delivery of IL-1beta. Embo J. 2011;30(23):4701-11. doi:10.1038/emboj.2011.398.

105. Shim EJ, Chun E, Lee HS, Bang BR, Kim TW, Cho SH et al. The role of high-mobility group box-1 (HMGB1) in the pathogenesis of asthma. Clin Exp Allergy. 2012;42(6):958-65. doi:10.1111/j.1365-2222.2012.03998.x.

106. Kew RR, Penzo M, Habiel DM, Marcu KB. The IKKalpha-dependent NF-kappaB p52/RelB noncanonical pathway is essential to sustain a CXCL12 autocrine loop in cells migrating in response to HMGB1. J Immunol. 2012;188(5):2380-6. doi:10.4049/jimmunol.1102454.

107. Cassel SL, Eisenbarth SC, Iyer SS, Sadler JJ, Colegio OR, Tephly LA et al. The Nalp3 inflammasome is essential for the development of silicosis. Proceedings of the National Academy of Sciences of the United States of America. 2008;105(26):9035-40. doi:10.1073/pnas.0803933105.

108. Dostert C, Petrilli V, Van Bruggen R, Steele C, Mossman BT, Tschopp J. Innate immune activation through Nalp3 inflammasome sensing of asbestos and silica. Science. 2008;320(5876):674-7. doi:10.1126/science.1156995.

109. Munoz-Planillo R, Kuffa P, Martinez-Colon G, Smith BL, Rajendiran TM, Nunez G. K(+) efflux is the common trigger of NLRP3 inflammasome activation by bacterial toxins and particulate matter. Immunity. 2013;38(6):1142-53. doi:10.1016/j.immuni.2013.05.016.

110. Netea MG, van de Veerdonk FL, van der Meer JW, Dinarello CA, Joosten LA. Inflammasome-independent regulation of IL-1-family cytokines. Annu Rev Immunol. 2015;33:49-77. doi:10.1146/annurev-immunol-032414-112306.

111. Hamilton RF, Jr., Buford M, Xiang C, Wu N, Holian A. NLRP3 inflammasome activation in murine alveolar macrophages and related lung pathology is associated with MWCNT nickel contamination. Inhalation toxicology. 2012;24(14):995-1008. doi:10.3109/08958378.2012.745633.

112. Meunier E, Coste A, Olagnier D, Authier H, Lefevre L, Dardenne C et al. Double-walled carbon nanotubes trigger IL-1beta release in human monocytes through Nlrp3 inflammasome activation. Nanomedicine. 2012;8(6):987-95. doi:10.1016/j.nano.2011.11.004.

113. Wang F, Yu L, Monopoli MP, Sandin P, Mahon E, Salvati A et al. The biomolecular corona is retained during nanoparticle uptake and protects the cells from the damage induced by cationic nanoparticles until degraded in the lysosomes. Nanomedicine. 2013;9(8):1159-68. doi:10.1016/j.nano.2013.04.010.

114. Lennon-Dumenil AM, Bakker AH, Maehr R, Fiebiger E, Overkleeft HS, Rosemblatt M et al. Analysis of protease activity in live antigen-presenting cells shows regulation of the phagosomal proteolytic contents during dendritic cell activation. J Exp Med. 2002;196(4):529-40.

115. Jacobson LS, Lima H, Jr., Goldberg MF, Gocheva V, Tsiperson V, Sutterwala FS et al. Cathepsin-mediated necrosis controls the adaptive immune response by Th2 (T helper type 2)-associated adjuvants. J Biol Chem. 2013;288(11):7481-91. doi:10.1074/jbc.M112.400655.

116. Brojatsch J, Lima H, Kar AK, Jacobson LS, Muehlbauer SM, Chandran K et al. A proteolytic cascade controls lysosome rupture and necrotic cell death mediated by lysosome-destabilizing adjuvants. PLoS One. 2014;9(6):e95032. doi:10.1371/journal.pone.0095032.

117. Moles A, Tarrats N, Fernandez-Checa JC, Mari M. Cathepsin B overexpression due to acid sphingomyelinase ablation promotes liver fibrosis in Niemann-Pick disease. J Biol Chem. 2012;287(2):1178-88. doi:10.1074/jbc.M111.272393.

118. Girtsman TA, Beamer CA, Wu N, Buford M, Holian A. IL-1R signalling is critical for regulation of multi-walled carbon nanotubes-induced acute lung inflammation in C57Bl/6 mice. Nanotoxicology. 2014;8(1):17-27. doi:10.3109/17435390.2012.744110.

119. Xia T, Hamilton RF, Bonner JC, Crandall ED, Elder A, Fazlollahi F et al. Interlaboratory evaluation of in vitro cytotoxicity and inflammatory responses to engineered nanomaterials: the NIEHS Nano GO Consortium. Environmental health perspectives. 2013;121(6):683-90. doi:10.1289/ehp.1306561.

120. Porter DW, Wu N, Hubbs AF, Mercer RR, Funk K, Meng F et al. Differential mouse pulmonary dose and time course responses to titanium dioxide nanospheres and nanobelts. Toxicol Sci. 2013;131(1):179-93. doi:10.1093/toxsci/kfs261.

121. Lacher SE, Johnson C, Jessop F, Holian A, Migliaccio CT. Murine pulmonary inflammation model: a comparative study of anesthesia and instillation methods. Inhalation toxicology. 2010;22(1):77-83. doi:10.3109/08958370902929969.

122. Jessop F, Holian A. Extracellular HMGB1 regulates multi-walled carbon nanotube-induced inflammation in vivo. Nanotoxicology. 2015;9:365-72. doi:10.3109/17435390.2014.933904.

123. Sager TM, Wolfarth MW, Andrew M, Hubbs A, Friend S, Chen TH et al. Effect of multi-walled carbon nanotube surface modification on bioactivity in the C57BL/6 mouse model. Nanotoxicology. 2014;8(3):317-27. doi:10.3109/17435390.2013.779757.

124. Migliaccio CT, Hamilton RF, Jr., Holian A. Increase in a distinct pulmonary macrophage subset possessing an antigen-presenting cell phenotype and in vitro APC activity following silica exposure. Toxicol Appl Pharmacol. 2005;205(2):168-76. doi:10.1016/j.taap.2004.11.005.

125. Solano-Lopez C, Zeidler-Erdely PC, Hubbs AF, Reynolds SH, Roberts JR, Taylor MD et al. Welding fume exposure and associated inflammatory and hyperplastic changes in the lungs of tumor susceptible a/j mice. Toxicol Pathol. 2006;34(4):364-72. doi:10.1080/01926230600815122.

126. Valimaki E, Miettinen JJ, Lietzen N, Matikainen S, Nyman TA. Monosodium urate activates Src/Pyk2/PI3 kinase and cathepsin dependent unconventional protein secretion from human primary macrophages. Mol Cell Proteomics. 2013;12(3):749-63. doi:10.1074/mcp.M112.024661.

127. Biswas R, Hamilton RF, Jr., Holian A. Role of lysosomes in silica-induced inflammasome activation and inflammation in absence of MARCO. J Immunol Res. 2014;2014:304180. doi:10.1155/2014/304180.

128. Kuhn DA, Vanhecke D, Michen B, Blank F, Gehr P, Petri-Fink A et al. Different endocytotic uptake mechanisms for nanoparticles in epithelial cells and macrophages. Beilstein J Nanotechnol. 2014;5:1625-36. doi:10.3762/bjnano.5.174.

129. Kreuzaler PA, Staniszewska AD, Li W, Omidvar N, Kedjouar B, Turkson J et al. Stat3 controls lysosomal-mediated cell death in vivo. Nat Cell Biol. 2011;13(3):303-9. doi:10.1038/ncb2171.

130. Tsung A, Tohme S, Billiar TR. High-mobility group box-1 in sterile inflammation. Journal of internal medicine. 2014;276(5):425-43. doi:10.1111/joim.12276.

131. Chen S, Yuan J, Yao S, Jin Y, Chen G, Tian W et al. Lipopolysaccharides may aggravate apoptosis through accumulation of autophagosomes in alveolar macrophages of human silicosis. Autophagy. 2015;11(12):2346-57. doi:10.1080/15548627.2015.1109765.

132. Mizushima N, Ohsumi Y, Yoshimori T. Autophagosome formation in mammalian cells. Cell Struct Funct. 2002;27(6):421-9.

133. Cohen RA, Petsonk EL, Rose C, Young B, Regier M, Najmuddin A et al. Lung Pathology in U.S. Coal Workers with Rapidly Progressive Pneumoconiosis Implicates Silica and Silicates. Am J Respir Crit Care Med. 2016;193(6):673-80. doi:10.1164/rccm.201505-1014OC.

134. Nakahira K, Choi AM. Autophagy: a potential therapeutic target in lung diseases. Am J Physiol Lung Cell Mol Physiol. 2013;305(2):L93-107. doi:10.1152/ajplung.00072.2013.

135. Chen ZH, Kim HP, Sciurba FC, Lee SJ, Feghali-Bostwick C, Stolz DB et al. Egr-1 regulates autophagy in cigarette smoke-induced chronic obstructive pulmonary disease. PLoS One. 2008;3(10):e3316. doi:10.1371/journal.pone.0003316.

136. Monick MM, Powers LS, Walters K, Lovan N, Zhang M, Gerke A et al. Identification of an autophagy defect in smokers' alveolar macrophages. J Immunol. 2010;185(9):5425-35. doi:10.4049/jimmunol.1001603.

137. Patel AS, Lin L, Geyer A, Haspel JA, An CH, Cao J et al. Autophagy in idiopathic pulmonary fibrosis. PLoS One. 2012;7(7):e41394. doi:10.1371/journal.pone.0041394.

138. Luciani A, Villella VR, Esposito S, Brunetti-Pierri N, Medina D, Settembre C et al. Defective CFTR induces aggresome formation and lung inflammation in cystic fibrosis through ROS-mediated autophagy inhibition. Nat Cell Biol. 2010;12(9):863-75. doi:10.1038/ncb2090.

139. Castillo EF, Dekonenko A, Arko-Mensah J, Mandell MA, Dupont N, Jiang S et al. Autophagy protects against active tuberculosis by suppressing bacterial burden and inflammation. Proceedings of the National Academy of Sciences of the United States of America. 2012;109(46):E3168-76. doi:10.1073/pnas.1210500109.

140. Migliaccio CT, Buford MC, Jessop F, Holian A. The IL-4Ralpha pathway in macrophages and its potential role in silica-induced pulmonary fibrosis. Journal of leukocyte biology. 2008;83(3):630-9. doi:10.1189/jlb.0807533.

141. Mizushima N, Yamamoto A, Matsui M, Yoshimori T, Ohsumi Y. In vivo analysis of autophagy in response to nutrient starvation using transgenic mice expressing a

fluorescent autophagosome marker. Mol Biol Cell. 2004;15(3):1101-11. doi:10.1091/mbc.E03-09-0704.

142. Hara T, Nakamura K, Matsui M, Yamamoto A, Nakahara Y, Suzuki-Migishima R et al. Suppression of basal autophagy in neural cells causes neurodegenerative disease in mice. Nature. 2006;441(7095):885-9. doi:10.1038/nature04724.

143. Zhao Z, Thackray LB, Miller BC, Lynn TM, Becker MM, Ward E et al. Coronavirus replication does not require the autophagy gene ATG5. Autophagy. 2007;3(6):581-5.

144. Klionsky DJ, Elazar Z, Seglen PO, Rubinsztein DC. Does bafilomycin A1 block the fusion of autophagosomes with lysosomes? Autophagy. 2008;4(7):849-50.

145. Matsumoto G, Wada K, Okuno M, Kurosawa M, Nukina N. Serine 403 phosphorylation of p62/SQSTM1 regulates selective autophagic clearance of ubiquitinated proteins. Mol Cell. 2011;44(2):279-89. doi:10.1016/j.molcel.2011.07.039.

146. Abdel Fattah E, Bhattacharya A, Herron A, Safdar Z, Eissa NT. Critical role for IL-18 in spontaneous lung inflammation caused by autophagy deficiency. J Immunol. 2015;194(11):5407-16. doi:10.4049/jimmunol.1402277.

147. Lee J, Kim HR, Quinley C, Kim J, Gonzalez-Navajas J, Xavier R et al. Autophagy suppresses interleukin-1beta (IL-1beta) signaling by activation of p62 degradation via lysosomal and proteasomal pathways. J Biol Chem. 2012;287(6):4033-40. doi:10.1074/jbc.M111.280065.

148. Shimizu Y, Dobashi K, Nagase H, Ohta K, Sano T, Matsuzaki S et al. Co-localization of iron binding on silica with p62/sequestosome1 (SQSTM1) in lung

granulomas of mice with acute silicosis. J Clin Biochem Nutr. 2015;56(1):74-83. doi:10.3164/jcbn.14-44.

149. Singh R, Kaushik S, Wang Y, Xiang Y, Novak I, Komatsu M et al. Autophagy regulates lipid metabolism. Nature. 2009;458(7242):1131-5. doi:10.1038/nature07976.

150. Razani B, Feng C, Coleman T, Emanuel R, Wen H, Hwang S et al. Autophagy links inflammasomes to atherosclerotic progression. Cell Metab. 2012;15(4):534-44. doi:10.1016/j.cmet.2012.02.011.

151. Romero F, Shah D, Duong M, Penn RB, Fessler MB, Madenspacher J et al. A pneumocyte-macrophage paracrine lipid axis drives the lung toward fibrosis. Am J Respir Cell Mol Biol. 2015;53(1):74-86. doi:10.1165/rcmb.2014-0343OC.

152. Andersson U, Tracey KJ. HMGB1 is a therapeutic target for sterile inflammation and infection. Annu Rev Immunol. 2011;29:139-62. doi:10.1146/annurev-immunol-030409-101323.

153. Orlowski GM, Colbert JD, Sharma S, Bogyo M, Robertson SA, Rock KL. Multiple Cathepsins Promote Pro-IL-1beta Synthesis and NLRP3-Mediated IL-1beta Activation. J Immunol. 2015;195(4):1685-97. doi:10.4049/jimmunol.1500509.

154. Pyo JO, Yoo SM, Ahn HH, Nah J, Hong SH, Kam TI et al. Overexpression of Atg5 in mice activates autophagy and extends lifespan. Nat Commun. 2013;4:2300. doi:10.1038/ncomms3300.

155. Maejima I, Takahashi A, Omori H, Kimura T, Takabatake Y, Saitoh T et al. Autophagy sequesters damaged lysosomes to control lysosomal biogenesis and kidney injury. The EMBO journal. 2013;32(17):2336-47. doi:10.1038/emboj.2013.171.